Search for supersymmetry in events with large missing transverse momentum, jets, and at least one tau lepton in $20\,\mathrm{fb}^{-1}$ of $\sqrt{s} = 8\,\mathrm{TeV}$ proton-proton collision data with the ATLAS detector

The ATLAS collaboration

E-mail: atlas.publications@cern.ch

ABSTRACT: A search for supersymmetry (SUSY) in events with large missing transverse momentum, jets, at least one hadronically decaying tau lepton and zero or one additional light leptons (electron/muon), has been performed using $20.3\,\mathrm{fb}^{-1}$ of proton-proton collision data at $\sqrt{s} = 8\,\mathrm{TeV}$ recorded with the ATLAS detector at the Large Hadron Collider. No excess above the Standard Model background expectation is observed in the various signal regions and 95% confidence level upper limits on the visible cross section for new phenomena are set. The results of the analysis are interpreted in several SUSY scenarios, significantly extending previous limits obtained in the same final states. In the framework of minimal gauge-mediated SUSY breaking models, values of the SUSY breaking scale Λ below $63\,\mathrm{TeV}$ are excluded, independently of $\tan\beta$. Exclusion limits are also derived for an mSUGRA/CMSSM model, in both the R-parity-conserving and R-parity-violating case. A further interpretation is presented in a framework of natural gauge mediation, in which the gluino is assumed to be the only light coloured sparticle and gluino masses below $1090\,\mathrm{GeV}$ are excluded.

Contents

1   Introduction

Supersymmetry (SUSY) [1–5] introduces a symmetry between fermions and bosons, result-
ing in a SUSY partner (sparticle) for each Standard Model (SM) particle, with identical
mass and quantum numbers except a difference of half a unit of spin. As none of these
sparticles have been observed with the same mass as their SM partners, SUSY must be a
broken symmetry if realized in nature. Assuming R-parity conservation [6–10], sparticles
are produced in pairs and then decay through cascades involving other sparticles until the
lightest SUSY particle (LSP), which is stable, is produced. In many SUSY models tau lep-
tons can provide an important signature for new physics. Naturalness arguments [11, 12]
suggest that the lightest third-generation sparticles should have masses of a few hundred
GeV to protect the Higgs boson mass from quadratically divergent quantum corrections.
Light sleptons could play a role in the co-annihilation of neutralinos in the early universe,

and, in particular, models with light tau sleptons (staus) are consistent with dark matter searches [13]. If squarks and gluinos, superpartners of quarks and gluons,[1] are in the LHC reach, their production rate may be dominant among SUSY processes. They could then decay in cascades involving tau leptons, high transverse momentum jets and missing transverse momentum from the LSP, which escapes undetected. More details about the various SUSY models considered in this paper are given in section 2. Furthermore, should SUSY or any other theory of physics Beyond the Standard Model (BSM) be discovered, independent studies of all three lepton flavours are necessary to investigate the coupling structure of the new physics, especially with regard to lepton universality.

This paper reports on an inclusive search for SUSY particles produced via the strong interaction in events with large missing transverse momentum, jets and at least one hadronically decaying tau lepton. Four distinct topologies are studied: one tau lepton ("1τ") or two or more tau leptons ("2τ") in the final state, with no additional light leptons (e/μ); or one or more tau leptons with exactly one electron ("$\tau+e$") or muon ("$\tau+\mu$"). These orthogonal channels have been optimized separately, and, where relevant, are statistically combined to increase the analysis sensitivity. The analysis is performed using $20.3\,\mathrm{fb}^{-1}$ of proton-proton (pp) collision data at $\sqrt{s} = 8\,\mathrm{TeV}$ recorded with the ATLAS detector at the Large Hadron Collider (LHC) in the 2012 run. The results are interpreted in several different models, which are described in more detail in section 2: a minimal gauge-mediated supersymmetry breaking (GMSB) model [14–19], an mSUGRA/CMSSM [20–25] model, a natural gauge mediation framework (nGM) [26] and a bilinear R-parity-violation (bRPV) [27, 28] model.

Previous searches for direct production of the SUSY partners of the tau lepton in the minimal GMSB model have been reported by the LEP Collaborations ALEPH [29], DELPHI [30] and OPAL [31]. The analysis reported in this paper extends the searches presented in ref. [32]. The CMS Collaboration presented the results of a supersymmetry search in events with tau leptons, jets and missing transverse momentum in $4.98\,\mathrm{fb}^{-1}$ of $7\,\mathrm{TeV}$ data in ref. [33].

2 SUSY scenarios

The search presented in this paper is sensitive to a variety of SUSY scenarios, which are outlined below. In particular, good sensitivity is achieved for SUSY strong production processes due to the requirement of several high-momentum jets.

GMSB model. Minimal GMSB models can be described by six parameters: the SUSY-breaking mass scale in the low-energy sector (Λ), the messenger mass (M_{mess}), the number of SU(5) messenger fields (N_5), the ratio of the vacuum expectation values of the two Higgs doublets ($\tan\beta$), the Higgs sector mass parameter (μ) and the scale factor for the gravitino mass (C_{grav}). For the analysis presented here, Λ and $\tan\beta$ are treated as free parameters, and the other parameters are fixed to the values used in ref. [32]: $M_{\mathrm{mess}} = 250\,\mathrm{TeV}$, $N_5 = 3$,

---

[1]In addition to squarks and gluinos, charged sleptons and sneutrinos are superpartners of charged leptons and neutrinos. The SUSY partners of the gauge and Higgs bosons are called gauginos and higgsinos, respectively. The charged, electroweak gauginos and higgsinos mix to form charginos ($\chi_i^\pm$, $i = 1,2$), and the neutral ones mix to form neutralinos (χ_j^0, $j = 1,2,3,4$). Finally the gravitino is the SUSY partner of the graviton.

$\mu > 0$ and $C_{grav} = 1$. With this choice of parameters, the production of squark and/or gluino pairs is expected to dominate over other SUSY processes at the LHC.

These sparticles decay into the next-to-lightest SUSY particle (NLSP), which subsequently decays to the LSP. In gauge-mediated models, the LSP is always a very light gravitino ($\tilde{G}$). The experimental signatures are largely determined by the nature of the NLSP: this can be either the lightest stau ($\tilde{\tau}_1$), a selectron or a smuon ($\tilde{\ell}_R$), the lightest neutralino ($\tilde{\chi}_1^0$), or a sneutrino ($\tilde{\nu}$), leading to final states usually containing tau leptons, light leptons ($\ell = e, \mu$), photons, or neutrinos, respectively. In most of the GMSB parameter space considered here the $\tilde{\tau}_1$ is the NLSP for large values of $\tan \beta$ ($\tan \beta > 20$), and final states contain between two and four tau leptons. In the region where the mass difference between the $\tilde{\tau}_1$ and the $\tilde{\ell}_R$ is smaller than the sum of the tau and the light lepton masses both the $\tilde{\tau}_1$ and the $\tilde{\ell}_R$ decay directly into the LSP and therefore both define the phenomenology.

mSUGRA/CMSSM model. The mSUGRA/CMSSM scenario is defined by five parameters: the universal scalar mass (m_0), the universal trilinear coupling (A_0) the universal gaugino mass ($m_{1/2}$), $\tan \beta$ and μ. These are chosen such that across a large area of the (m_0, $m_{1/2}$) plane the mSUGRA/CMSSM lightest Higgs boson mass is compatible with the observed mass of the recently discovered Higgs boson at the LHC [34, 35]. Near the low m_0 boundary of this area the difference in mass between the $\tilde{\tau}_1$ and the lightest SUSY particle, the neutralino, is small and allows the two particles to co-annihilate in the early universe [36]. The dark matter relic density is therefore brought down to values compatible with the Planck and WMAP measurements [37, 38]. The consequence of the small difference in mass for the experimental sensitivity is a bias towards very low momenta of at least one tau lepton and consequently towards fewer detectable tau candidates in the final state.

nGM model. A rich phenomenology is obtained in the framework of general gauge mediation (GGM) [39]. Starting from GGM, it is possible to construct a set of natural Gauge Mediated (nGM) models where the phenomenology depends on the nature of the NLSP [26, 40]. Various models assume that the fermion mass hierarchies are generated by the same physics responsible for breaking SUSY (see for example [41] and [42]). Typically in these models the entire third generation of sfermions is lighter than the other two. Coupled with the fact that sleptons only get soft masses through hypercharge interactions in gauge mediation, this leads to a stau NLSP. In the model considered here it is also assumed that the gluino is the only light coloured sparticle. All squark and slepton mass parameters are set to 2.5 TeV except the lightest stau mass, $m_{\tilde{\tau}}$, which is assumed to be smaller to allow a stau NLSP (this has no effect on the fine tuning). The bino and wino masses (M_1 and M_2 respectively) are also set to 2.5 TeV while all trilinear coupling terms are set to zero. It is further assumed that $\mu \ll M_1, M_2$. This leaves the gluino mass M_3 and the stau mass $m_{\tilde{\tau}}$ as the only free parameters, if μ is also fixed. The value of μ is set to 400 GeV to ensure that strong production is the dominant process at the LHC; moreover, this choice of the μ parameter drives the mass of the $\tilde{\chi}_1^\pm$, $\tilde{\chi}_1^0$ and $\tilde{\chi}_2^0$, which are almost mass degenerate.

The only light sparticles in the model are the stau, a light gluino, higgsino-dominated charginos and neutralinos, and a light gravitino, which is the LSP. Several decay modes are possible for the gluino:

1. $\tilde{g} \to g\tilde{\chi}_i^0 \to g\tau\tilde{\tau}_1 \to g\tau\tau\tilde{G}$, with $i = 1, 2$

2. $\tilde{g} \to q\bar{q}\tilde{\chi}_i^0 \to q\bar{q}\tau\tilde{\tau}_1 \to q\bar{q}\tau\tau\tilde{G}$, with $i = 1, 2$

3. $\tilde{g} \to qq'\tilde{\chi}_1^\pm \to qq'\nu_\tau\tilde{\tau}_1 \to qq'\nu_\tau\tau\tilde{G}$

where q and $\bar{q}$ are almost exclusively quarks of heavy flavour (either top or bottom quarks). The first process proceeds through a squark-quark loop, and equal amounts of $\tilde{\chi}_1^0$ and $\tilde{\chi}_2^0$ production are expected. The second and third processes proceed via an off-shell squark, and the relative proportion of the first process to the other two depends on the precise relationship between M_3 and the squark masses. At the lowest values of M_3, the first process dominates entirely. The effect of the last two processes increases with rising gluino mass (with M_3 approaching the squark masses). For $M_3 \gtrsim 1\,\text{TeV}$, the proportion of decays through the first process is at the level of a few percent, and the other two processes are expected to dominate [26]. The branching ratios are approximately constant as a function of M_3 for the signal scenarios considered.

In gauge-mediated SUSY scenarios a variety of mechanisms exist [43–47] to generate a Higgs boson mass compatible with the observed value [34, 35], without changing the phenomenology of the models considered in this search. In the model used in this analysis, the lightest Higgs boson mass is specifically set to $125\,\text{GeV}$.

bRPV model. In the bRPV scenario, bilinear R-parity-violating (RPV) terms are assumed to be present in the superpotential, resulting in an unstable LSP. The RPV couplings are included in the mSUGRA/CMSSM model described above and, for a chosen set of mSUGRA/CMSSM parameters, the bilinear RPV parameters are determined under the tree-level dominance scenario [48] by fitting them to neutrino oscillation data as described in ref. [49]. The neutralino LSP decays promptly through decay modes that include neutrinos [50]. The main LSP decay modes considered are:

1. $\tilde{\chi}_1^0 \to W^{(*)}\mu$ (or τ),

2. $\tilde{\chi}_1^0 \to Z^{(*)}/h^{(*)}\nu$.

These result in final states with several leptons and jets, but a reduced missing transverse momentum compared with the standard R-parity-conserving mSUGRA/CMSSM model.

3 The ATLAS detector and data sample

The ATLAS experiment is described in detail in ref. [51]. It is a multi-purpose detector with a forward-backward symmetric cylindrical geometry and nearly 4π solid angle coverage.[2] The inner tracking detector (ID), covering $|\eta| < 2.5$, consists of a silicon pixel detector, a

---

[2]ATLAS uses a right-handed coordinate system with its origin at the nominal interaction point (IP) in the centre of the detector and the z-axis along the beam pipe. The x-axis points from the IP to the centre of the LHC ring and the y-axis points upward. Cylindrical coordinates (r, ϕ) are used in the transverse plane, ϕ being the azimuthal angle around the beam pipe. The pseudorapidity is defined in terms of the polar angle θ as $\eta = -\ln\tan(\theta/2)$.

semiconductor microstrip detector and a transition radiation tracker. The ID is surrounded by a thin superconducting solenoid providing an axial 2 T magnetic field and by a fine-granularity lead/liquid-argon (LAr) electromagnetic calorimeter (covering $|\eta| < 3.2$). An iron/scintillator-tile calorimeter provides hadronic coverage in the central pseudorapidity range ($|\eta| < 1.7$). The endcap and forward regions ($1.5 < |\eta| < 4.9$) are instrumented with LAr calorimeters, with either steel, copper or tungsten as the absorber material, for both the electromagnetic and hadronic measurements. An extensive muon spectrometer system that incorporates large superconducting toroidal air-core magnets surrounds the calorimeters. Three layers of precision gas chambers provide tracking coverage in the range $|\eta| < 2.7$, while dedicated fast chambers allow triggering in the region $|\eta| < 2.4$.

The data used in this search are pp collisions recorded by the ATLAS detector at a centre-of-mass energy of $\sqrt{s} = 8$ TeV during the period from April 2012 to December 2012. After the application of beam, detector and data-quality requirements, the total integrated luminosity amounts to $(20.3 \pm 0.6)\,\text{fb}^{-1}$. The luminosity measurement is performed using techniques similar to those in ref. [52], and the calibration of the luminosity scale is derived from beam-separation scans performed in November 2012. In the 1τ and 2τ channels, candidate events are triggered by requiring a jet with high transverse momentum (p_T) and high missing transverse momentum (whose magnitude is denoted by E_T^miss) [53]. In the $\tau + e$ channel, candidate events are triggered by requiring the presence of an energy cluster in the electromagnetic calorimeter with a shower shape consistent with that of an electron, and with uncorrected transverse energy (E_T) above 24 GeV. The selection is further refined by matching the cluster to an isolated track in the ID [53]. In order to maximize the efficiency for high-p_T electrons, data selected using a single-electron trigger with $E_\text{T} > 60$ GeV but no isolation requirements are added. In the $\tau + \mu$ channel, events are selected by requiring a muon candidate identified as a single isolated track reconstructed by the ID and the muon spectrometer, with uncorrected transverse momentum above 24 GeV. In addition, events are also selected using a non-isolated muon trigger, with a muon p_T threshold of 36 GeV [53]. The trigger requirements have been optimized to ensure a uniform trigger efficiency for all data-taking periods, which exceeds 98% with respect to the offline selection for all final states considered.

4 Simulated samples

Samples of Monte Carlo (MC) simulated events are used for evaluating the expected SM backgrounds and for estimating the signal efficiencies for the different SUSY models. Samples of W+jets and Z+jets events with up to four jets from matrix elements (ME) are simulated by the SHERPA [54] generator version 1.4.1, where the CT10 [55] set of parton distribution functions (PDFs) is used. To improve the agreement between data and simulation, W/Z+jets events are reweighted based on the p_T of the vector boson using measured Z boson p_T distributions in the data [56]. For the purpose of evaluating generator uncertainties, additional W/Z+jets samples are produced with the ALPGEN 2.14 [57] MC generator, which simulates W and Z/γ^* production with up to five accompanying partons using the CTEQ6L1 [58] set of PDFs. Z/γ^* events with $m_{\ell\ell} < 40$ GeV are referred to in

this paper as "Drell-Yan". In the `ALPGEN` samples fragmentation and hadronization are performed with `HERWIG` 6.520 [59], using `JIMMY` [60] for the underlying event simulation. The `SHERPA` MC generator is used for simulating the production of diboson events (WW, WZ and ZZ). Alternative samples for evaluating systematic uncertainties are generated by `POWHEG` r2129 [61–63] interfaced to `PYTHIA` 8.165 [64].

Top quark pair production is simulated with `POWHEG` r2129 interfaced to `PYTHIA` 6.426 [65], using the `CT10` PDF set. To improve the agreement between data and simulation, $t\bar{t}$ events are reweighted based on the p_T of the $t\bar{t}$ system; the weights are extracted from the ATLAS measurement of the $t\bar{t}$ differential cross section at $\sqrt{s} = 7\,\text{TeV}$ [66]. Alternative samples to evaluate systematic uncertainties are generated with a setting very similar to the one used for W/Z+jets, using `ALPGEN` with up to four additional partons in the ME. The production of single-top events in the s- and Wt-channels is simulated using `MC@NLO` 4.06 [67–69] with `HERWIG` 6.520 showering and the `CT10` PDF set, while for the t-channel `AcerMC` 3.8 [70] with `PYTHIA` 6.426 showering is used with the `CTEQ6L1` PDF set. In all samples a top quark mass of $172.5\,\text{GeV}$ is used consistently.

The SUSY signal samples used in this analysis are generated with `PYTHIA` 6.426 for the bRPV model and `Herwig++` 2.5.2 [71] for all other models, with the `CTEQ6L1` PDF set in all cases. For all signal models the signal cross sections are calculated to next-to-leading order in the strong coupling constant, adding the resummation of soft gluon emission at next-to-leading-logarithmic accuracy (NLO+NLL) [72–76]. The nominal cross section and the uncertainty are taken from an envelope of cross-section predictions using different PDF sets and factorization and renormalization scales, as described in ref. [77].

The decays of tau leptons are simulated directly in the generators in the case of event samples produced with `SHERPA`, `Herwig++` 2.5.2 and `PYTHIA` 8.165, while in all other cases `TAUOLA` 2.4 [78, 79] is used. For the underlying event model the ATLAS AUET2B tune [80] is used for all samples except for those generated with `Herwig++` 2.5.2 (UEEE tune [81]), with `PYTHIA` 8.165 (AU2 tune [82]), with `SHERPA` (which use the built-in `SHERPA` tune) and the $t\bar{t}$ sample generated with `POWHEG` (Perugia 2011C tune [83]). All samples are processed either through the GEANT4-based simulation of the ATLAS detector [84, 85] or a fast simulation framework where showers in the calorimeters are simulated with a parameterized description [86] and the rest of the detector is simulated with GEANT4. The fast simulation framework is used only for top quark pair production with `POWHEG` and the low-p_T W/Z+jets samples simulated with `SHERPA`. The fast simulation was validated against full GEANT4 simulation on the $t\bar{t}$ sample, where a fraction of the events were simulated in both frameworks. In all cases, a realistic treatment of the variation of the number of pp interactions in the same and neighbouring bunch crossings (pile-up) is included, with an average of around 20 interactions per bunch crossing.

For the initial comparison with data, all SM background cross sections are normalized to the results of higher-order calculations when available. The theoretical cross sections for W and Z production are calculated with DYNNLO [87] with the MSTW 2008 NNLO [88] PDF set. The same ratio of the next-to-next-leading-order (NNLO) to leading-order cross sections is applied to the production of W/Z in association with heavy-flavour jets. The inclusive $t\bar{t}$ cross section is calculated at NNLO, including resummation of next-to-next-to-

leading logarithmic (NNLL) soft gluon terms, with Top++2.0 [89, 90] using MSTW 2008 NNLO PDFs. Approximate NLO+NNLL calculations are used for single-top production cross sections [91–93]. For the diboson sample, the cross section is calculated at NLO with MCFM [94], using MSTW 2008 PDFs.

5 Event reconstruction

Vertices consistent with the interaction region and with at least five associated tracks with $p_T > 400\,\mathrm{MeV}$ are selected; the primary vertex (PV) is then identified by choosing the vertex with the largest summed $|p_T|^2$ of the associated tracks [95].

Jets are reconstructed from three dimensional calorimeter energy clusters using the anti-k_t jet clustering algorithm [96] with distance parameter $R = 0.4$. Jet momenta are constructed by performing a four-vector sum over clusters of calorimeter cells, treating each as an $(E, \vec{p})$ four-vector with zero mass. The jets are corrected for energy from additional pile-up collisions using the method suggested in ref. [97], which estimates the pile-up activity in any given event as well as the sensitivity of any given jet to pile-up. Clusters are classified as originating from electromagnetic or hadronic showers by using the local cluster weighting calibration method [98]. Based on this classification, specific energy corrections from a combination of MC simulation and data [99] are applied. A further calibration (jet energy scale) is applied to calibrate on average the energies of jets to the scale of their constituent particles [99]. In this analysis jets are selected within an acceptance of $|\eta| < 2.8$ and are required to have $p_T > 20\,\mathrm{GeV}$.

Jets containing b-quarks are used in the analysis to define specific regions where the contribution of background events from W/Z+jets or $t\bar{t}$ processes are estimated. They are identified using a neural-network algorithm [100, 101] and a working point corresponding to 60% (< 0.5%) tagging efficiency for b-jets (light-flavour or gluon jets) is used, where the tagging efficiency was studied on simulated $t\bar{t}$ events.

Reconstruction of hadronically decaying tau leptons starts from jets with $p_T > 10\,\mathrm{GeV}$ [102], and an η- and p_T-dependent energy calibration to the tau energy scale for hadronic decays is applied [103]. Discriminating variables based on observables sensitive to the transverse and longitudinal shapes of the energy deposits of tau candidates in the calorimeter are combined with tracking information as inputs to a boosted decision tree (BDT) discriminator. Measurements from the transition radiation tracker and calorimeter information are used to veto electrons misidentified as taus. Suitable tau lepton candidates must have one or three associated tracks (one or three "prongs"), with a charge sum of ± 1, and satisfy $p_T > 20\,\mathrm{GeV}$ and $|\eta| < 2.5$. A sample of $Z \to \tau\tau$ events is used to measure the efficiency of the BDT tau identification. The "loose" ("medium") working points in ref. [102] are used herein and correspond to an efficiency of approximately 70% (60%), independent of p_T, with a rejection factor of 10 (20) against jets misidentified as tau candidates (referred to as "fake" taus).

Muon candidates are identified by matching one or more track segments in the muon spectrometer [104] with an extrapolated inner detector track. They are required to have $p_T > 10\,\mathrm{GeV}$ and $|\eta| < 2.4$. Electron candidates must satisfy $p_T > 20\,\mathrm{GeV}$, $|\eta| < 2.47$

and satisfy the "Medium++" identification criteria described in ref. [105], re-optimized for 2012 conditions. Muons and electrons satisfying these identification criteria are referred to as "baseline" leptons.

The missing transverse momentum vector $\vec{p}_{\mathrm{T}}^{\,\mathrm{miss}}$ and its magnitude, $E_{\mathrm{T}}^{\mathrm{miss}}$, are measured from the transverse momenta of identified jets, electrons, muons and all calorimeter clusters with $|\eta| < 4.5$ not associated with such objects [106]. In the $E_{\mathrm{T}}^{\mathrm{miss}}$ measurement tau leptons are not distinguished from jets and it was checked that this does not introduce a bias in any kinematic variables used in the analysis.

Following object reconstruction, ambiguities between candidate jets, taus and light leptons are resolved and further criteria are applied to select "signal" objects. Muons are required to have $p_{\mathrm{T}} > 25\,\mathrm{GeV}$ and to be isolated. The scalar sum of the transverse momenta of tracks within a cone of size $\Delta R \equiv \sqrt{(\Delta\eta)^2 + (\Delta\phi)^2} = 0.2$ around the muon candidate, excluding the muon candidate track itself, is required to be less than $1.8\,\mathrm{GeV}$. Electrons are required to have $p_{\mathrm{T}} > 25\,\mathrm{GeV}$ and pass the "Tight++" selection [105]. The sum of all transverse components of deposits in the calorimeter around the electron candidate in a cone of size $\Delta R = 0.2$ is required to be less than 10% of the electron candidate p_{T}. Finally the electron trajectory is required to deviate not more than $1\,\mathrm{mm}$ in the transverse plane and $2\,\mathrm{mm}$ in the longitudinal direction from the reconstructed PV. Signal jets are required to have $p_{\mathrm{T}} > 30\,\mathrm{GeV}$ and to be within the acceptance of the inner detector ($|\eta| < 2.5$). Soft central jets ($p_{\mathrm{T}} < 50\,\mathrm{GeV}$, $|\eta| < 2.4$) originating from pile-up collisions are removed by requiring a jet vertex fraction (JVF) above 0.5, where the JVF is defined as the ratio of the sum of the transverse momentum of jet-matched tracks that originate from the PV to the sum of transverse momentum of all tracks associated with the jet.

6 Event selection

For the 1τ channel, events with only one hadronically decaying medium tau lepton candidate with $p_{\mathrm{T}} > 30\,\mathrm{GeV}$, no additional loose tau candidates, and no candidate muons or electrons are selected; in the 2τ channel, events are selected with two or more loose tau leptons with $p_{\mathrm{T}} > 20\,\mathrm{GeV}$ and no candidate muons or electrons; events in the $\tau{+}e$ and $\tau{+}\mu$ channels have one or more loose tau candidates with $p_{\mathrm{T}} > 20\,\mathrm{GeV}$ and one additional signal electron or muon, respectively.

All events have to fulfil a common initial set of requirements, in the following referred to as the "preselection". Events are required to have a reconstructed PV, to have no jets or muons that show signs of problematic reconstruction, to have no jets failing to satisfy quality criteria, and to have no muons that are likely to have originated from cosmic rays.

After the preselection, several requirements are applied to define various signal regions (SRs) in each final state. The individual SRs have been optimized for specific signal models and are combined in the final results for the respective signal scenarios. Two SRs (1τ "Loose" and 2τ "Inclusive") are designed with relaxed selections to maintain sensitivity for other BSM scenarios and to provide model independent limits.

The following variables are used to suppress the main background processes (W+jets, Z+jets and top, including $t\bar{t}$ and single-top events) in each final state:

	1τ Loose SR	1τ Tight SR
Trigger selection	$p_{\mathrm{T}}^{\mathrm{jet1}} > 130\,\mathrm{GeV}$, $p_{\mathrm{T}}^{\mathrm{jet2}} > 30\,\mathrm{GeV}$ $E_{\mathrm{T}}^{\mathrm{miss}} > 150\,\mathrm{GeV}$	
Taus	$N_{\tau}^{\mathrm{medium}} = 1$ $p_{\mathrm{T}} > 30\,\mathrm{GeV}$	
Light leptons	$N_{\ell}^{\mathrm{baseline}} = 0$	
Multijet rejection	$\Delta\phi(\mathrm{jet}_{1,2}, p_{\mathrm{T}}^{\mathrm{miss}}) > 0.4$, $\Delta\phi(\tau, p_{\mathrm{T}}^{\mathrm{miss}}) > 0.2$	
Signal selections	$m_{\mathrm{T}}^{\tau} > 140\,\mathrm{GeV}$	
	$E_{\mathrm{T}}^{\mathrm{miss}} > 200\,\mathrm{GeV}$ $H_{\mathrm{T}} > 800\,\mathrm{GeV}$	$E_{\mathrm{T}}^{\mathrm{miss}} > 300\,\mathrm{GeV}$ $H_{\mathrm{T}} > 1000\,\mathrm{GeV}$

	2τ Inclusive SR	2τ GMSB SR	2τ nGM SR	2τ bRPV SR
Trigger selection	$p_{\mathrm{T}}^{\mathrm{jet1}} > 130\,\mathrm{GeV}$, $p_{\mathrm{T}}^{\mathrm{jet2}} > 30\,\mathrm{GeV}$ $E_{\mathrm{T}}^{\mathrm{miss}} > 150\,\mathrm{GeV}$			
Taus	$N_{\tau}^{\mathrm{loose}} \geq 2$ $p_{\mathrm{T}} > 20\,\mathrm{GeV}$			
Light leptons	$N_{\ell}^{\mathrm{baseline}} = 0$			
Multijet rejection	$\Delta\phi(\mathrm{jet}_{1,2}, p_{\mathrm{T}}^{\mathrm{miss}}) \geq 0.3$			
Signal selections	$m_{\mathrm{T}}^{\tau_1} + m_{\mathrm{T}}^{\tau_2} \geq 150\,\mathrm{GeV}$	$m_{\mathrm{T}}^{\tau_1} + m_{\mathrm{T}}^{\tau_2} \geq 250\,\mathrm{GeV}$		$m_{\mathrm{T}}^{\tau_1} + m_{\mathrm{T}}^{\tau_2} \geq 150\,\mathrm{GeV}$
	$H_{\mathrm{T}}^{\mathrm{2j}} > 1000\,\mathrm{GeV}$	$H_{\mathrm{T}}^{\mathrm{2j}} > 1000\,\mathrm{GeV}$ $N_{\mathrm{jet}} \geq 4$	$H_{\mathrm{T}}^{\mathrm{2j}} > 600\,\mathrm{GeV}$ $N_{\mathrm{jet}} \geq 4$	$H_{\mathrm{T}}^{\mathrm{2j}} > 1000\,\mathrm{GeV}$ $N_{\mathrm{jet}} \geq 4$

	$\tau+\ell$ GMSB SR	$\tau+\ell$ nGM SR	$\tau+\ell$ bRPV SR	$\tau+\ell$ mSUGRA SR
Trigger selection	$p_{\mathrm{T}}^{\ell} > 25\,\mathrm{GeV}$			
Taus	$N_{\tau}^{\mathrm{loose}} \geq 1$ $p_{\mathrm{T}} > 20\,\mathrm{GeV}$			
Light leptons	$N_{\ell}^{\mathrm{signal}} = 1$, $\quad N_{\mathrm{other\ lep}}^{\mathrm{baseline}} = 0$			
Multijet rejection	$m_{\mathrm{T}}^{\ell} > 100\,\mathrm{GeV}$			
Signal selections	$m_{\mathrm{eff}} > 1700\,\mathrm{GeV}$	$E_{\mathrm{T}}^{\mathrm{miss}} > 350\,\mathrm{GeV}$ $N_{\mathrm{jet}} \geq 3$	$m_{\mathrm{eff}} > 1300\,\mathrm{GeV}$ $N_{\mathrm{jet}} \geq 4$	$E_{\mathrm{T}}^{\mathrm{miss}} > 300\,\mathrm{GeV}$ $N_{\mathrm{jet}} \geq 3$

Table 1. Signal region selection criteria for the different channels presented in this paper.

- m_{T}^{τ}, the transverse mass formed by $E_{\mathrm{T}}^{\mathrm{miss}}$ and the p_{T} of the tau lepton in the 1τ channel $m_{\mathrm{T}}^{\tau} = \sqrt{2p_{\mathrm{T}}^{\tau} E_{\mathrm{T}}^{\mathrm{miss}}(1 - \cos(\Delta\phi(\tau, p_{\mathrm{T}}^{\mathrm{miss}})))}$. In addition the variable $m_{\mathrm{T}}^{\tau_1} + m_{\mathrm{T}}^{\tau_2}$ is used as a discriminating variable in the 2τ channel;

- m_{T}^{ℓ}, the transverse mass formed by $E_{\mathrm{T}}^{\mathrm{miss}}$ and the p_{T} of the light leptons $m_{\mathrm{T}}^{\ell} = \sqrt{2p_{\mathrm{T}}^{\ell} E_{\mathrm{T}}^{\mathrm{miss}}(1 - \cos(\Delta\phi(\ell, p_{\mathrm{T}}^{\mathrm{miss}})))}$;

- H_{T}, the scalar sum of the transverse momenta of the tau, light lepton and signal jet ($p_{\mathrm{T}} > 30\,\mathrm{GeV}$) candidates in the event: $H_{\mathrm{T}} = \sum_{\mathrm{all}\ \ell} p_{\mathrm{T}}^{\ell} + \sum_{\mathrm{all}\ \tau} p_{\mathrm{T}}^{\tau} + \sum_{\mathrm{all\ jets}} p_{\mathrm{T}}^{\mathrm{jet}}$;

- $H_{\mathrm{T}}^{\mathrm{2j}}$, the scalar sum of the transverse momenta of the tau and light lepton candidates

and the two jets with the largest transverse momenta in the event: $H_{\mathrm{T}}^{2\mathrm{j}} = \sum_{\mathrm{all}\,\ell} p_{\mathrm{T}}^{\ell} + \sum_{\mathrm{all}\,\tau} p_{\mathrm{T}}^{\tau} + \sum_{i=1,2} p_{\mathrm{T}}^{\mathrm{jet}_i}$;

- the magnitude of the missing transverse momentum $E_{\mathrm{T}}^{\mathrm{miss}}$;

- the effective mass $m_{\mathrm{eff}} = H_{\mathrm{T}}^{2\mathrm{j}} + E_{\mathrm{T}}^{\mathrm{miss}}$;

- the number of reconstructed signal jets N_{jet}.

While optimizing the choice of variables, studies showed that there is a correlation between H_{T} and N_{jet}, given that the sum of the jet p_{T} is used in the defintion of H_{T}. In the 2τ and τ+lepton channels, where a selection on N_{jet} is used to define different SRs, the variable $H_{\mathrm{T}}^{2\mathrm{j}}$ is used in order to avoid such correlation.

1τ signal regions

The various selection criteria used to define the two SRs in the 1τ channel are summarized in table 1. A requirement on the azimuthal angle between $\vec{p}_{\mathrm{T}}^{\mathrm{miss}}$ and either of the two leading jets ($\Delta\phi(\mathrm{jet}_{1,2}, p_{\mathrm{T}}^{\mathrm{miss}})$) is used to remove multijet events, where the $E_{\mathrm{T}}^{\mathrm{miss}}$ arises from mismeasured highly energetic jets. To further reduce these events in the SRs, a tighter selection on $E_{\mathrm{T}}^{\mathrm{miss}}$ is also applied. The transverse mass m_{T}^{τ} is used to remove W+jets events, while a requirement on H_{T} is applied in order to reduce the contribution of all remaining backgrounds.

The main SR ("tight SR") applies tight selections on $E_{\mathrm{T}}^{\mathrm{miss}}$ and H_{T} as a result of optimizing the sensitivity in the high-Λ region of the GMSB model parameter space, given that lower mass regions were excluded in earlier analyses. A "loose SR", with looser requirements on $E_{\mathrm{T}}^{\mathrm{miss}}$ and H_{T}, is also defined and used to calculate model-independent limits. In the GMSB model the strong production cross section, for which the analysis has the largest sensitivity, decreases faster with increasing Λ than the cross sections for weak production. Therefore, the selection efficiency with respect to the total SUSY production decreases for large values of Λ. For high $\tan\beta$, the product of acceptance and efficiency is of the order of 0.3%, decreasing to 0.1% for low $\tan\beta$. The tight SR yields the best sensitivity in the high-$m_{1/2}$, low-m_0 region of the mSUGRA and bRPV models and, when combined with the other channels, extends the overall sensitivity range in these models. In the mSUGRA model the product of acceptance and efficiency for the tight signal selection ranges from the permille level to around 4%, with the higher values being observed in the low $m_{1/2}$ region. In the bRPV signal region the product of acceptance and efficiency for the tight SR ranges from the permille level to around 1% (tight SR), with the higher values being observed in the low-m_0, high-$m_{1/2}$ region. The 1τ channel does not contribute to the nGM scenario where by construction each event contains at least two high-p_{T} taus.

2τ signal regions

The criteria used to define the four SRs in the 2τ channel are shown in table 1. Multijet events are rejected by a requirement on $\Delta\phi(\mathrm{jet}_{1,2}, p_{\mathrm{T}}^{\mathrm{miss}})$, while Z+jets events are efficiently removed by a requirement on $m_{\mathrm{T}}^{\tau_1} + m_{\mathrm{T}}^{\tau_2}$. A selection on $H_{\mathrm{T}}^{2\mathrm{j}}$ is then applied in order to

reduce the contribution of all remaining backgrounds. Additional requirements on the number of jets in the event are also used to define SRs that are sensitive in specific signal models.

The GMSB SR was optimized to be sensitive to the high-Λ region of the parameter space. For high $\tan\beta$ the product of acceptance and efficiency is of the order of 0.5%, falling to 0.2% for low $\tan\beta$. The nGM SR was optimized for high gluino masses. Given the topology of the signal events, at least four jets are required and a lower requirement on the value of H_T^{2j} with respect to the GMSB SR is applied. In this model the gluino pair production cross section is primarily a function of $m_{\tilde{g}}$, ranging from 17.2 pb for $m_{\tilde{g}} = 400\,\mathrm{GeV}$ to 7 fb for $m_{\tilde{g}} = 1100\,\mathrm{GeV}$. The product of acceptance and efficiency for this channel in the nGM model is of the order of 4% for high $m_{\tilde{g}}$, independent of $m_{\tilde{\tau}}$, and it falls to $\sim$2% for low $m_{\tilde{g}}$ due to the analysis requirements on the p_T of the leading jet and on $E_\mathrm{T}^{\mathrm{miss}}$. The 2τ channel has extremely small acceptance in the mSUGRA model, due to the requirement of a second high-p_T tau; for this reason no SR optimized for this scenario is defined. In the bRPV SR the selection was optimized to be sensitive in the low-m_0, high-$m_{1/2}$ region of the parameter space, where the branching ratio to events with two real taus is highest. The product of acceptance and efficiency of the dedicated SR is of the order of 1% in the most sensitive regions of the parameter space, decreasing to the permille level in other regions.

τ+lepton signal regions

Events from multijet production and from decays of W bosons into a light lepton and a neutrino, which constitute the largest source of SM background, are suppressed by requiring $m_\mathrm{T}^{\ell} > 100\,\mathrm{GeV}$. Different SRs are then defined by applying further requirements on $E_\mathrm{T}^{\mathrm{miss}}$, m_{eff} and N_{jet} to yield good sensitivity to each of the considered signal models. In the GMSB model, the SR selection was also optimized for the high-Λ region; a tight requirement on m_{eff} is applied to significantly reduce the contribution of all backgrounds. The product of acceptance and efficiency in this SR varies between 0.2% to 0.4% across the $(\Lambda, \tan\beta)$ plane. The nGM SR was optimized for high gluino masses. Since a high jet multiplicity is expected in this scenario, events with at least three signal jets are selected. The remaining background contribution is reduced with a requirement on $E_\mathrm{T}^{\mathrm{miss}}$. The product of acceptance and efficiency of this selection is of the order of 2% for high $m_{\tilde{g}}$, decreasing to 0.2% for lower values of the gluino mass. Requirements similar to those for the nGM SR are applied to define the mSUGRA SR, which was optimized to be sensitive in a low-$m_{1/2}$ and high-m_0 region of the parameter space. The product of acceptance and efficiency in this case ranges from the permille level to 2% across the parameter space. For the bRPV SR the selection optimization is performed in a high-m_0, medium-$m_{1/2}$ region of the parameter space. At least four signal jets are required and the remaining background contribution is reduced with a requirement on m_{eff}. The product of acceptance and efficiency also in this case ranges from the permille level to 2%. The full list of criteria used to define the different SRs in the τ+e and τ+μ channels is given in table 1.

Background	1τ	2τ	τ+lepton
W+jets (true)	matrix inversion	matrix inversion	—
W+jets (fake)	matrix inversion		matrix inversion
Z+jets (true)	with W+jets	matrix inversion	—
Z+jets (fake)	with W+jets	—	—
Top (true)	matrix inversion	matrix inversion	matrix inversion
Top (fake)	matrix inversion		matrix inversion
Multijets	ABCD method	jet-smearing method	matrix method
Dibosons	from simulation	from simulation	from simulation

Table 2. Overview of the various techniques employed for background estimation.

7 Background estimation

The background in this analysis arises predominantly from W+jets, Z+jets, top and multijet events, with contributions from "true" taus and "fake" taus (jets misidentified as taus). The contributions of these backgrounds in the various signal regions are estimated from data. Because of the differences of the topologies in the four final states considered, different techniques are employed to estimate the multijet background. Table 2 gives an overview of all the different methods used for the background estimation in all channels, which are described in the following subsections. The small diboson background contributions are estimated using MC simulations, while the contributions from other backgrounds like low mass Drell-Yan, $t\bar{t}$ +V and $H \to \tau\tau$ were found to be negligible.

7.1 W, Z and top quark backgrounds

The main estimation technique for electroweak and top quark backgrounds is referred to in the following as the "matrix inversion" method. In each signal region, the SM background predicted by MC simulation is scaled by factors obtained from appropriately defined control regions (CRs). This is done to reduce the impact of possible mis-modelling of tau misidentification probabilities and kinematics in the MC simulations. The CRs are chosen such that:

- they are as kinematically close as possible to the final signal regions, without overlapping with them, while having low signal contamination;

- each CR is enriched with a specific background process;

- the tau misidentification probability is, to a good approximation, independent of the kinematic variables used to separate the SR from the CRs.

By doing this, the measured ratio of the data to MC event yields in the CR can be used to compute scaling factors to correct the MC background prediction in the SR. The vector defined by the scaling factors for each background ($\vec{\omega}$) is obtained by inverting the equation $\vec{N}^{\text{data}} = A\vec{\omega}$, where $\vec{N}^{\text{data}}$ is the observed number of data events in each CR, after subtracting the expected number of events from other SM processes, and the matrix A is obtained from the MC expectation for the number of events originating from each of the backgrounds

	$N_{b\text{-jet}} = 0$	$N_{b\text{-jet}} > 0$
$m_{\mathrm{T}}^\tau < 90\,\mathrm{GeV}$ or $\Delta\phi(\tau, p_{\mathrm{T}}^{\mathrm{miss}}) < 1.0$ or $p_{\mathrm{T}}^\tau > 55\,\mathrm{GeV}$	$\mathrm{CR_{WTrue}}$	$\mathrm{CR_{TTrue}}$
$90\,\mathrm{GeV} < m_{\mathrm{T}}^\tau < 140\,\mathrm{GeV}$ and $\Delta\phi(\tau, p_{\mathrm{T}}^{\mathrm{miss}}) > 1.0$ and $p_{\mathrm{T}}^\tau < 55\,\mathrm{GeV}$	$\mathrm{CR_{WFake}}$	$\mathrm{CR_{TFake}}$

(a) Control region selections in the 1τ analysis. A multijet rejection cut $\Delta\phi(\mathrm{jet}_{1,2}, p_{\mathrm{T}}^{\mathrm{miss}}) > 0.4$ is applied in all CRs.

Top CR	W CR	Z CR
$H_{\mathrm{T}}^{2\mathrm{j}} < 550\,\mathrm{GeV}$		
$m_{\mathrm{T}}^{\tau_1} + m_{\mathrm{T}}^{\tau_2} > 150/200\,\mathrm{GeV}$		$m_{\mathrm{T}}^{\tau_1} + m_{\mathrm{T}}^{\tau_2} < 80\,\mathrm{GeV}$
$N_{b\text{-jet}} > 0$	$N_{b\text{-jet}} = 0$	—

(b) Control region selections in the 2τ analysis. A multijet rejection cut $\Delta\phi(\mathrm{jet}_{1,2}, p_{\mathrm{T}}^{\mathrm{miss}}) > 0.3$ is applied in all CRs.

| Top fake-tau CR	Top true-tau CR	W CR
$50\,\mathrm{GeV} < E_{\mathrm{T}}^{\mathrm{miss}} < 130\,\mathrm{GeV}$		
$50\,\mathrm{GeV} < m_{\mathrm{T}}^\ell < 190\,\mathrm{GeV}$		
$m_{\mathrm{eff}} < 1000\,\mathrm{GeV}$		
$N_{b\text{-jet}} \geq 1$		$N_{b\text{-jet}} = 0$
$50\,\mathrm{GeV} < m_{\mathrm{T}}^\ell < 120\,\mathrm{GeV}$	$120\,\mathrm{GeV} < m_{\mathrm{T}}^\ell < 190\,\mathrm{GeV}$	

(c) Control region selections in the τ+lepton analysis.

Table 3. Overview of the various control regions employed for the background estimation of W, Z and top quark backgrounds. Trigger requirements and selected objects are identical to the signal region requirements in the respective channels.

(W, Z and top). The signal contamination in all CRs has been determined from MC simulation and is well below 5%, except for the nGM SR in the 2τ channel where up to 10% contamination is observed.[3] Correlations due to the contribution of each background process in the different CRs are properly taken into account in the matrix A. To obtain the statistical uncertainties on the scaling factors, all contributing parameters are varied within their uncertainties, the procedure is repeated and new scaling factors are obtained. The width of the distribution of the resulting scaling factors is then used as their statistical uncertainty.

1τ channel. The dominant backgrounds to the 1τ SR arise from W+jets, Z+jets and $t\bar{t}$. Events can be divided into those which contain a true tau and those in which a jet is misidentified as a tau. Since the composition of true and fake taus in the control region and signal region may differ, it is necessary to compute separate scaling factors for events

---

[3]It was checked that this contamination has a negligible effect on the limit obtained in this scenario.
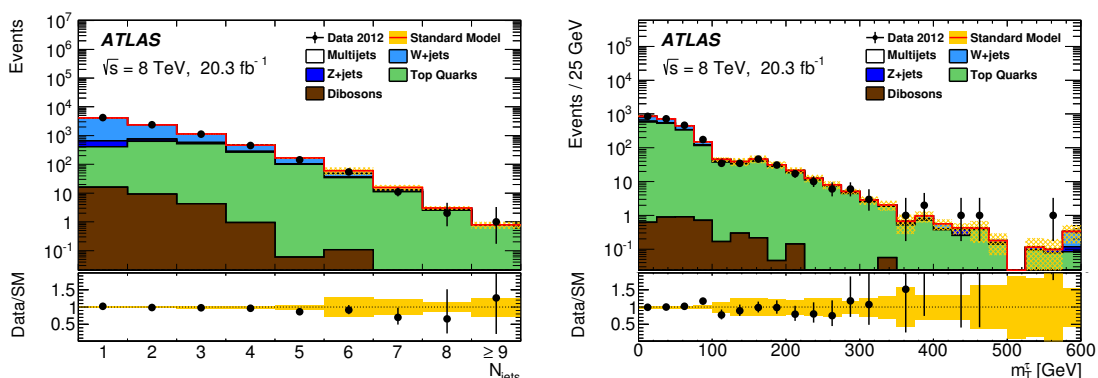
(a) N_{jets} distribution in inclusive W/Z and $t\bar{t}$ region. **(b)** m_{T}^{τ} distribution in the $t\bar{t}$ validation region.

Figure 1. Kinematic distributions in the 1τ channel for events (a) in an inclusive W/Z and $t\bar{t}$ validation region and (b) $t\bar{t}$-enriched validation region. Data are represented by the points. All backgrounds are scaled according to the results of the data-driven background estimates. The shaded band centred around the total background indicates the statistical uncertainty on the background expectation.

with true and fake taus. For this purpose, the CRs are defined by using two variables: the transverse mass, used to separate true and fake taus, and the b-tagging, used to provide a top-enriched ($t\bar{t}$ CR) or top-depleted (W or Z CR) sample. The contribution in these CRs from other backgrounds (e.g. multijet background) is negligible. The full list of selection requirements for these control regions, after the preselection, tau selection and light-lepton veto requirements are applied, is provided in table 3. The matrix A is a 4×4 matrix from which the scale factors for W events with a true tau candidate, W/Z events with a fake tau candidate, and top events with either a true or a fake tau candidate are obtained. In Z+jets events, the background is dominated by Z decays to neutrinos, and therefore the tau candidate is typically a misidentified jet. For this reason, the scaling factor is obtained from the CR defined for W+jets (fake) events.

Typical scaling factors obtained for the various MC samples are $\sim$0.6 for W+jets, Z+jets and $\sim$1.0 for $t\bar{t}$ with fake taus, while they are $\sim$1.1 for W+jets and $\sim$1.0 for $t\bar{t}$ with true taus. The comparatively large scale factor for W+jets and Z+jets with fake tau candidates reflects the insufficient description in MC simulation of narrow jets, which in these events are predominantly initiated by colour-connected light quarks, as opposed to the fake tau candidates in ttbar events. The associated statistical uncertainties on these scaling factors are in the range of 5–50%, depending on the CR. Good agreement between data and scaled MC events is observed in the relevant kinematic distributions in the CRs. Figure 1(a) shows the jet multiplicity distribution (an independent variable not used for background separation) on an inclusive data sample made from the four CRs, extending the kinematic range up to (but excluding) the SR. A $t\bar{t}$-enriched validation region is formed from the inclusive sample by means of b-tagging, and the corresponding m_{T}^{τ} distribution is shown in figure 1(b). It shows good agreement in the true-tau-dominated low-m_{T}^{τ} range as well as for $m_{\text{T}}^{\tau} > 140\,\text{GeV}$ (beyond the CR), where events with either a true or a fake tau candidate contribute with similar amounts.

(a) Tau p_T distribution in combined W and $t\bar{t}$ CR.

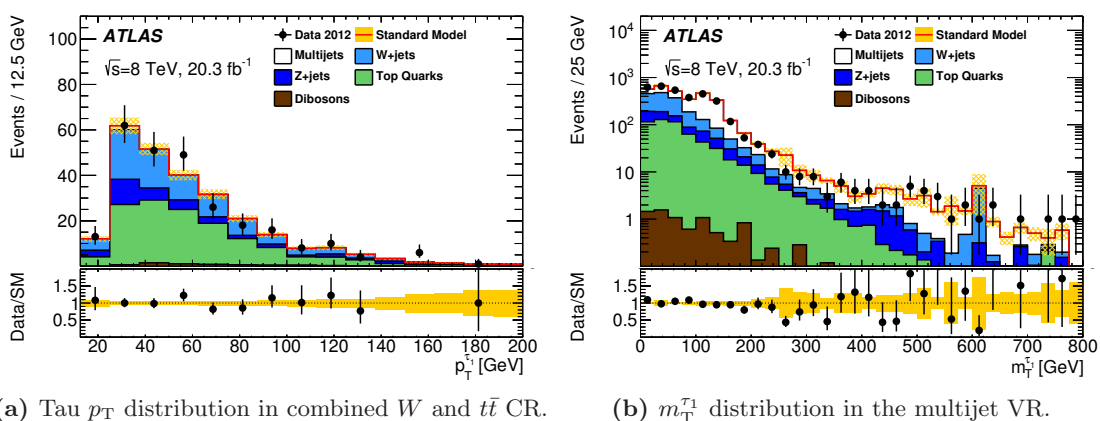**(b)** $m_T^{\tau_1}$ distribution in the multijet VR.

Figure 2. Kinematic distributions for events (a) in the 2τ W and $t\bar{t}$ control region and (b) in the multijet validation region. Data are represented by the points. All backgrounds are scaled according to the results of the data-driven background estimates. The shaded band centred around the total background indicates the statistical uncertainty on the background expectation.

2τ channel. In the 2τ analysis, the backgrounds from W+jets and $t\bar{t}$ are dominated by events in which one tau candidate is a true tau and the other is a jet misidentified as a tau. The contributions from Z+jets events are dominated by final states with $Z \to \tau\tau$ decays. The definitions of the 2τ control regions are given in table 3. Three CRs are defined, for W+jets, Z+jets and $t\bar{t}$ events. All CRs have a negligible contamination from multijet events due to the requirement on $\Delta\phi(\mathrm{jet}_{1,2}, p_T^{\mathrm{miss}})$. Given that the ratio of true to fake tau candidates in the CR and SR is the same, as confirmed by generator-level MC studies, there is no need to separate the CRs for fake tau and true tau backgrounds. The matrix A in this case is a 3×3 matrix from which the scale factors for W, Z and top events are obtained. The selection criteria $m_T^{\tau_1} + m_T^{\tau_2} > 150\,\mathrm{GeV}$ (for the Inclusive and bRPV SR) or $m_T^{\tau_1} + m_T^{\tau_2} > 200\,\mathrm{GeV}$ (for the GMSB and nGM SR) are applied to reproduce the signal region kinematics.

Typical scaling factors obtained for various MC samples are ~ 0.6 for the W+jets, ~ 1.4 for the Z+jets and ~ 0.9 for $t\bar{t}$, with associated statistical uncertainties in the range of 10–30%. Good agreement between data and scaled MC events in the relevant kinematic distributions is observed in the CRs. An example can be seen in figure 2(a), where the distribution of the transverse momentum of the leading tau candidate in data and scaled MC is compared in an inclusive CR defined by combining the W and $t\bar{t}$ CRs discussed in this section.

τ+lepton channel. In the τ+lepton analysis the ratio of real to fake taus depends on the background process. For W decays, due to the high efficiency and purity of the electron and muon reconstruction, the light lepton is always a real lepton from the W decay, while the tau is faked by a recoiling hadronic object. For $t\bar{t}$ the light lepton originates from the decay chain of one of the top quarks, while the tau can either be a real tau from the decay of the other top or a fake tau from a jet in the event. Z decays do not contribute a significant amount to the background and are estimated from simulation.
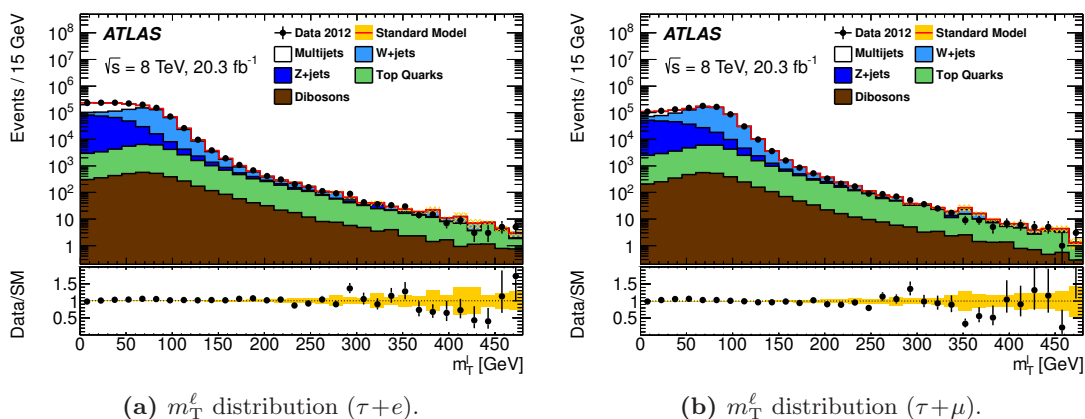
(a) m_T^ℓ distribution ($\tau{+}e$).   **(b)** m_T^ℓ distribution ($\tau{+}\mu$).

Figure 3. Kinematic distributions in the $\tau{+}$lepton combined W and $t\bar{t}$ control regions. Data are represented by the points. All backgrounds are scaled according to the results of the data-driven background estimates and the multijet background is estimated as described in section 7.2. The shaded band centred around the total background indicates the statistical uncertainty on the background expectation.

Three control regions are defined for W, $t\bar{t}$ with fake taus and $t\bar{t}$ with true taus. Events with true or fake taus are separated by using a requirement on the m_T^ℓ of the event, as summarized in table 3. The matrix A in this case is a 3×3 matrix from which the scale factors for W, top with true taus and top with fake taus are obtained.

Typical scaling factors obtained are $\sim$0.7 for the $W{+}$jets, $\sim$0.9 for the $t\bar{t}$ with a fake tau and $\sim$0.8 for $t\bar{t}$ with a true tau. The associated statistical uncertainties are of the order of 20%. An example of the very good agreement in the CRs between data and scaled MC is shown in figure 3, which presents the m_T^ℓ distribution for the $\tau{+}e$ and $\tau{+}\mu$ channels in a combined W and $t\bar{t}$ CR defined as the CR selection apart from the cut on the variable plotted.

7.2 Multijet backgrounds

To estimate the multijet background contribution in the signal regions, different methods are employed for each of the three channels.

1τ channel. For the 1τ channel, the contribution arising from multijet background processes due to fake taus is estimated from data using the so-called "ABCD" method. Four exclusive regions, labelled A, B, C and D, are defined in a two-dimensional plane specified by two discriminating variables that are uncorrelated for background events: the tau identification tightness and a combination of $E_\mathrm{T}^\mathrm{miss}$ and its angular separation in ϕ to either of the leading and sub-leading jets (table 4). To increase the number of events in regions A and C, very loose tau candidates are defined by taking the nominal (medium) tau selection and relaxing the criteria on the BDT discriminant. Region D is defined to be similar to the SR, except for the fact that the requirement on $E_\mathrm{T}^\mathrm{miss}$ is inverted and there is no requirement on H_T. Multijet events in region D may be estimated because the ratio of the numbers of events in regions A and B is equal to the ratio of numbers of events in regions

	Very loose tau	Nominal tau
$\Delta\phi(\text{jet}_{1,2}, p_\mathrm{T}^\mathrm{miss}) < 0.4$ no cut on $E_\mathrm{T}^\mathrm{miss}$	Control region A	Control region B
$\Delta\phi(\text{jet}_{1,2}, p_\mathrm{T}^\mathrm{miss}) > 0.4$ $E_\mathrm{T}^\mathrm{miss} < 200/300\,\text{GeV}$	Control region C	Region D

(a) Regions used in the ABCD method for the 1τ analysis. The requirement on H_T is not applied in the definition of these control regions.

Multijet CR	Multijet VR
$p_\mathrm{T}^{\text{jet1}} > 130\,\text{GeV},\ p_\mathrm{T}^{\text{jet2}} > 30\,\text{GeV}$	
$E_\mathrm{T}^\mathrm{miss} > 150\,\text{GeV}$	
$N_\ell^\text{baseline} = 0$	
$\Delta\phi(\text{jet}_{1,2}, p_\mathrm{T}^\mathrm{miss}) < 0.3$	
$E_\mathrm{T}^\mathrm{miss}/m_\text{eff} < 0.4$	
$N_\tau^\text{loose} = 0$	$N_\tau^\text{loose} = 1$

(b) Regions used for normalization and validation of the multijet pseudo-data in the 2τ analysis. The $E_\mathrm{T}^\mathrm{miss}$ object in the selection is defined by the jet-smearing method.

Table 4. Definitions of control regions used in the estimates of the multijet backgrounds.

C and D. Therefore, the number of events in region D (N_D) is $N_\mathrm{D} = c \times N_\mathrm{B}$, where N_B is the number of events in region B and $c = \frac{N_\mathrm{C}}{N_\mathrm{A}}$ is the "correction factor". In order to estimate the total yield from multijet events in the final SR, the number of events obtained in region D is scaled by the fraction of events passing the final requirements on H_T and $E_\mathrm{T}^\mathrm{miss}$. This fraction is derived in region A, after checking that it has little dependence on the requirements used to define the different multijet regions. In each region, the non-multijet contribution is estimated using MC events scaled according to the procedure detailed in the previous section, and is subtracted from the data.

2τ channel. Background events from multijet production contain both fake $E_\mathrm{T}^\mathrm{miss}$ from instrumental effects in the jet energy measurements and fake taus. Since both effects are difficult to simulate reliably and the large cross section would require very large simulation samples, the multijet background expectation for the 2τ final state is computed using a sample from data with the "Jet Smearing" technique [107]. Using this method a sample of events with artificial $E_\mathrm{T}^\mathrm{miss}$ is obtained, where all other particles, including fake taus, are taken from data. This sample is then used in the analysis to estimate the background from multijet events. Events with low $E_\mathrm{T}^\mathrm{miss}$ are selected from data requiring that they pass a single-jet trigger and have an $E_\mathrm{T}^\mathrm{miss}$ significance $S = E_\mathrm{T}^\mathrm{miss}/\sqrt{\sum E_\mathrm{T}} < 0.6\,\text{GeV}^{\frac{1}{2}}$, where $\sum E_\mathrm{T}$ includes the same reconstructed objects used for computing $E_\mathrm{T}^\mathrm{miss}$, as detailed in section 5. A pseudo-data sample with fake $E_\mathrm{T}^\mathrm{miss}$ is then obtained by applying jet energy resolution smearing to all jets in these events. After subtracting the small contribution ($< 7\%$) from other backgrounds using scaled MC simulations, this sample is normalized in

a multijet-enriched CR defined by the criteria in table 4, which include the presence of two or more jets with the same p_T requirements as the SR.

The performance of the method is assessed in a validation region (VR) which has identical kinematic requirements to the normalization region but where one tau is required (table 4). All relevant kinematic properties, including those of the fake taus, are found to be well described by the normalized multijet template, as shown in figure 2(b) for one of the kinematic variables considered in the analysis.

τ+lepton channel. In the τ+lepton channels the background contribution due to events with fake leptons is dominated by multijet events. Hence the multijet background contribution can be obtained from data by estimating the number of fake lepton events. For this purpose, the "matrix method" described in ref. [108] is used, which exploits the difference in the isolation of the lepton candidates in events with true and fake leptons. The estimated contribution is found to be negligible.

8   Systematic uncertainties on the background

Various systematic uncertainties were studied and the effect on the number of expected background events in each of the SRs was calculated. Because of the normalization procedure in the CRs, these estimates are not affected by theoretical errors on absolute cross sections, but only by generator dependencies when extrapolating from the CRs to the SRs.

The difference in the estimated number of background events from two different generators is used to define the uncertainty due to the choice of MC generator for the $t\bar{t}$, W+jets, Z+jets and diboson samples (see section 4). Moreover, the uncertainties on initial- and final-state radiation modelling and renormalization and factorization scales, which are found to be relatively small, are fully covered by the difference in generators. For all samples, the statistical uncertainty on the prediction obtained from the alternative MC generator is also included in the estimate of the generator uncertainty.

The experimental systematic uncertainties on the SM background estimates arise from the jet energy scale and resolution [99], the tau energy scale [103] and tau identification [102]. The relative difference between the number of expected background events obtained with the nominal MC simulation and that obtained after applying the uncertainty variations on the corresponding objects is taken to be the systematic uncertainty on the background estimate. The uncertainties from the jet and tau energy scales are the largest experimental uncertainties and are treated as uncorrelated, given that they are calibrated by different methods. The systematic uncertainty associated with the simulation of pile-up is taken into account by recomputing the event weights in all MC samples such that the resulting variation in the average interactions per bunch crossing corresponds to the observed uncertainty. The uncertainty on the integrated luminosity is 2.8%, as detailed in ref. [52]. This uncertainty affects only the normalization of the diboson background, which is estimated entirely from simulation.

Additional uncertainties due to the methods used to estimate the background from multijet events are also considered. In the 1τ channel, a 100% uncertainty is obtained by

Source of uncertainty	1τ Loose	1τ Tight	2τ Incl.	2τ GMSB	2τ nGM	2τ bRPV
Generator uncertainties	19%	30%	22%	78%	27%	33%
Jet energy resolution	2.8%	9.7%	2.1%	4.7%	2.1%	9.4%
Jet energy scale	3.6%	4.0%	5.3%	2.4%	4.9%	8.0%
Tau energy scale	3.6%	1.3%	2.3%	8.6%	3.0%	2.8%
Pile-up re-weighting	1.0%	1.0%	1.4%	1.5%	1.6%	1.3%
Multijet estimate	10.5%	9.6%	2.0%	7.5%	0.8%	3.8%
Total syst.	24%	35%	24%	79%	30%	36%

Source of uncertainty	$\tau+e$ GMSB	$\tau+e$ nGM	$\tau+e$ bRPV	$\tau+e$ mSUG.	$\tau+\mu$ GMSB	$\tau+\mu$ nGM	$\tau+\mu$ bRPV	$\tau+\mu$ mSUG.
Generator uncertainties	51%	46%	19%	28%	28%	30%	39%	32%
Jet energy resolution	4%	5%	9%	3%	5%	6%	8%	3%
Jet energy scale	7%	9%	7%	12%	7%	13%	10%	13%
Tau energy scale	7%	2%	8%	1%	8%	8%	4%	4%
Pile-up re-weighting	3%	2%	1%	0%	2%	3%	1%	1%
Total syst.	60%	48%	32%	30%	36%	34%	41%	33%

Table 5. Overview of the major systematic uncertainties on the total expected background in each signal region for the background estimates in the channels presented in this paper. The total systematic error also includes some minor systematic uncertainties, not detailed in the text or in the table.

taking into account possible correlations between the variables used in the ABCD method, as well as the uncertainties on the scaling factors of the non-multijet samples that are subtracted from the data. In the 2τ channel, uncertainties of the Jet Smearing method are evaluated by varying the jet response function used within the smearing process. This reflects the uncertainty on the ability to constrain the jet response to data in special multijet control regions when measuring the optimal jet response [107]. In the $\tau+$lepton channels, given that only an upper limit on the estimate of the multijet background is obtained, a conservative 100% uncertainty on the multijet background is assumed.

The total systematic uncertainty related to the background estimation and its breakdown into the main contributions are shown in table 5 for each signal region.

The total experimental systematic uncertainty on the signal selection efficiency from the various sources discussed in this section varies for each channel and for each signal model considered. In the GMSB scenario this uncertainty is 5–10% for the 1τ channel, rising to 20% for high values of Λ; 20–30% for most of the parameter space in the 2τ channel, increasing to as high as 45% in the region of highest Λ and low $\tan\beta$; 5–15% for the $\tau+$lepton channel. In the mSUGRA model the signal systematic uncertainty is at the level of 10% across most of the $(m_0, m_{1/2})$ plane for all channels. The total experimental uncertainty on the signal selection efficiency in the nGM scenario is 10–20% for the 2τ channel; in the $\tau+$lepton channels it is of the order of 15–20% for lower masses and decreases to an average level of 5–10% for high $m_{\tilde{g}}$. In the $(m_0, m_{1/2})$ plane of the bRPV model the total systematic uncertainty on the signal selection efficiency is at the level of 10% across
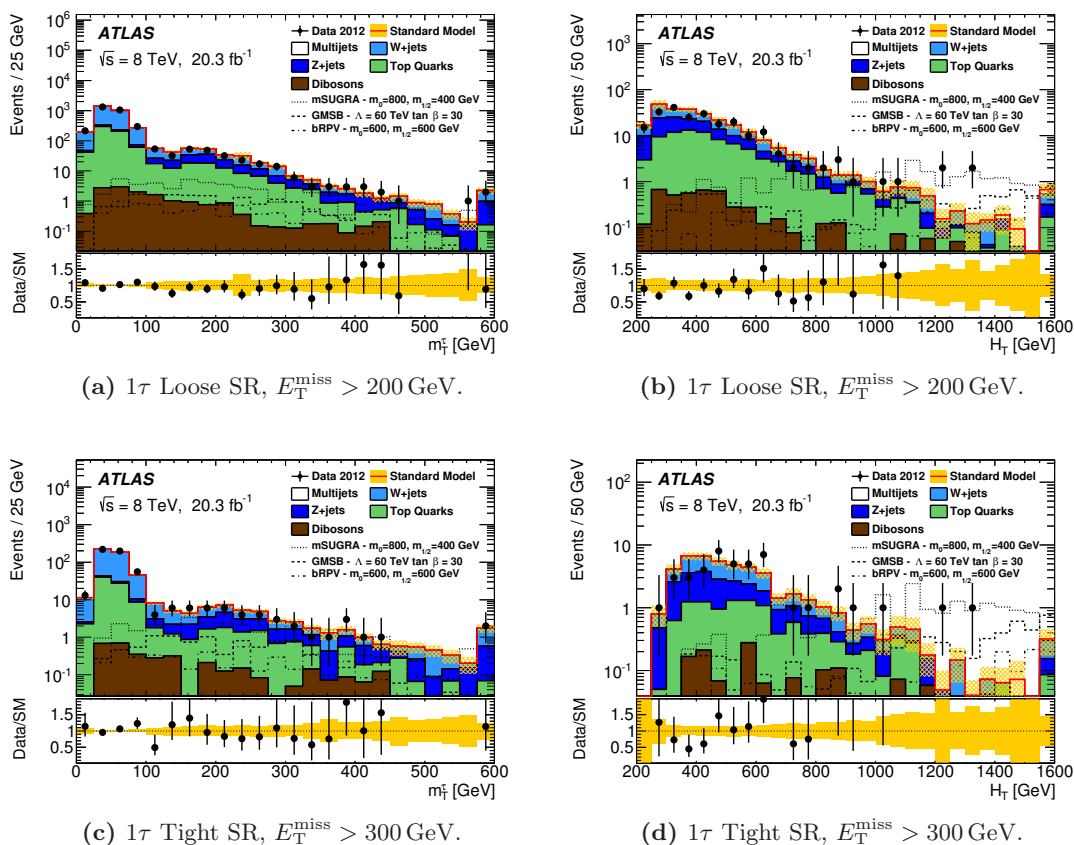
(a) 1τ Loose SR, $E_{\mathrm{T}}^{\mathrm{miss}} > 200\,\mathrm{GeV}$.

(b) 1τ Loose SR, $E_{\mathrm{T}}^{\mathrm{miss}} > 200\,\mathrm{GeV}$.

(c) 1τ Tight SR, $E_{\mathrm{T}}^{\mathrm{miss}} > 300\,\mathrm{GeV}$.

(d) 1τ Tight SR, $E_{\mathrm{T}}^{\mathrm{miss}} > 300\,\mathrm{GeV}$.

Figure 4. Distribution of m_{T}^{τ} after all analysis requirements but the requirement on m_{T}^{τ} and the final requirement on H_{T}, and of H_{T} after the m_{T}^{τ} requirement for (a, b) the 1τ "Loose" and (c, d) "Tight" SRs. Data are represented by the points. The SM prediction includes the data-driven corrections discussed in the text. The shaded band centred around the total SM background indicates the statistical uncertainty on the background expectation. MC events are normalized to data in the CRs corresponding to m_{T}^{τ} below 130 GeV. Also shown is the expected signal from typical mSUGRA, GMSB and bRPV samples. The last bin in the expected background distribution is an overflow bin.

most of the plane for all channels, rising to 50% at the lowest $m_{1/2}$ region studied and to 80% for individual signal samples generated at the highest $m_{1/2}$ values.

9 Results

Observed data and expected background events in the signal regions

Data and scaled background simulation were compared for different kinematic quantities. Figure 4 shows the m_{T}^{τ} distribution after all the requirements of the analysis except the ones on m_{T}^{τ} and H_{T}, as well as the H_{T} distribution after the requirement on m_{T}^{τ} for the 1τ channel. "Loose" and "Tight" SR plots are displayed individually with the corresponding requirement on $E_{\mathrm{T}}^{\mathrm{miss}}$ applied. Figure 5 shows the $m_{\mathrm{T}}^{\tau_1} + m_{\mathrm{T}}^{\tau_2}$, $H_{\mathrm{T}}^{2\mathrm{j}}$ and N_{jet} distributions after all the requirements of the analysis except the final selection on $m_{\mathrm{T}}^{\tau_1} + m_{\mathrm{T}}^{\tau_2}$ and $H_{\mathrm{T}}^{2\mathrm{j}}$ for the 2τ
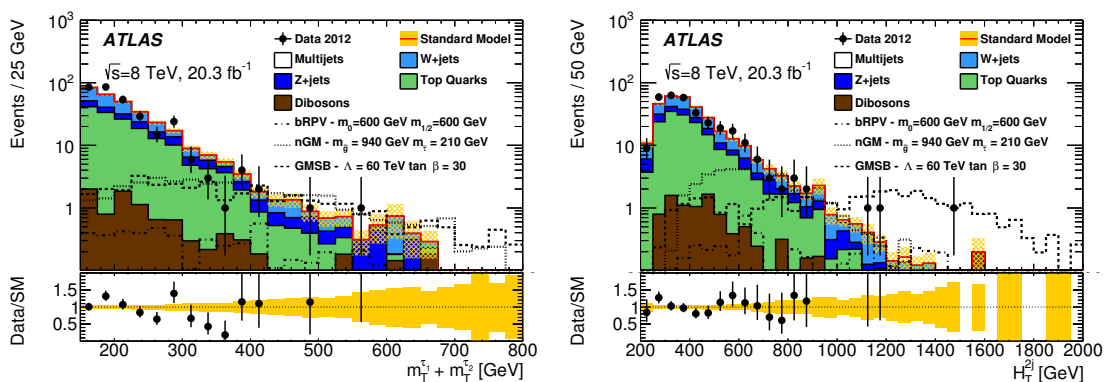
(a) 2τ $m_{\mathrm{T}}^{\tau_1} + m_{\mathrm{T}}^{\tau_2}$ distribution.

(b) 2τ $H_{\mathrm{T}}^{2\mathrm{j}}$ distribution.
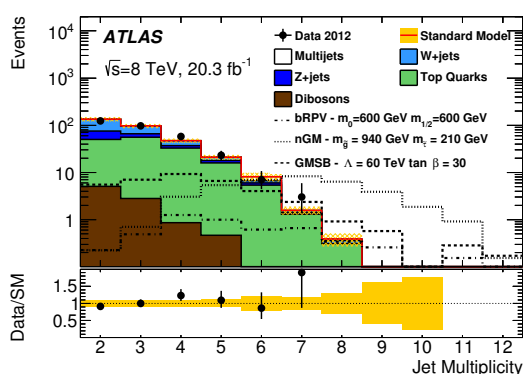
(c) 2τ N_{jet} distribution.

Figure 5. Distribution of $m_{\mathrm{T}}^{\tau_1} + m_{\mathrm{T}}^{\tau_2}$, $H_{\mathrm{T}}^{2\mathrm{j}}$ and N_{jet} in the 2τ channel after all analysis requirements but the final SR requirements on $m_{\mathrm{T}}^{\tau_1} + m_{\mathrm{T}}^{\tau_2}$ and $H_{\mathrm{T}}^{2\mathrm{j}}$. To reduce the contributions from events with Z bosons decaying into tau leptons, the requirement $m_{\mathrm{T}}^{\tau_1} + m_{\mathrm{T}}^{\tau_2} > 150\,\mathrm{GeV}$ is applied to all distributions. Data are represented by the points. The SM prediction includes the data-driven corrections discussed in the text. The shaded band centred around the total SM background indicates the statistical uncertainty on the background expectation. MC events are normalized to data in the CRs corresponding to $H_{\mathrm{T}}^{2\mathrm{j}}$ below $550\,\mathrm{GeV}$. Also shown is the expected signal from typical bRPV, nGM and GMSB samples. There are no data events in the overflow bin after all analysis requirements are applied.

channel. The $m_{\mathrm{T}}^{\tau_1} + m_{\mathrm{T}}^{\tau_2} > 150\,\mathrm{GeV}$ requirement common to all SRs is applied to reduce contributions from events with Z bosons decaying into tau leptons. Figures 6 and 7 show the m_{eff} and $E_{\mathrm{T}}^{\mathrm{miss}}$ distributions for each of the SRs in the τ+lepton channels. All common requirements and the jet multiplicity selection corresponding to the respective SR are applied.

Good agreement between data and SM expectations is observed for all distributions after applying all corrections and data-driven background estimation techniques.

Tables 6–9 summarize the number of observed events in the four channels in data and the number of expected background events. No significant excess over the Standard Model background estimate is observed. Upper limits at 95% confidence level (CL) on the number of signal events for each SR independent of any specific SUSY model are derived using the
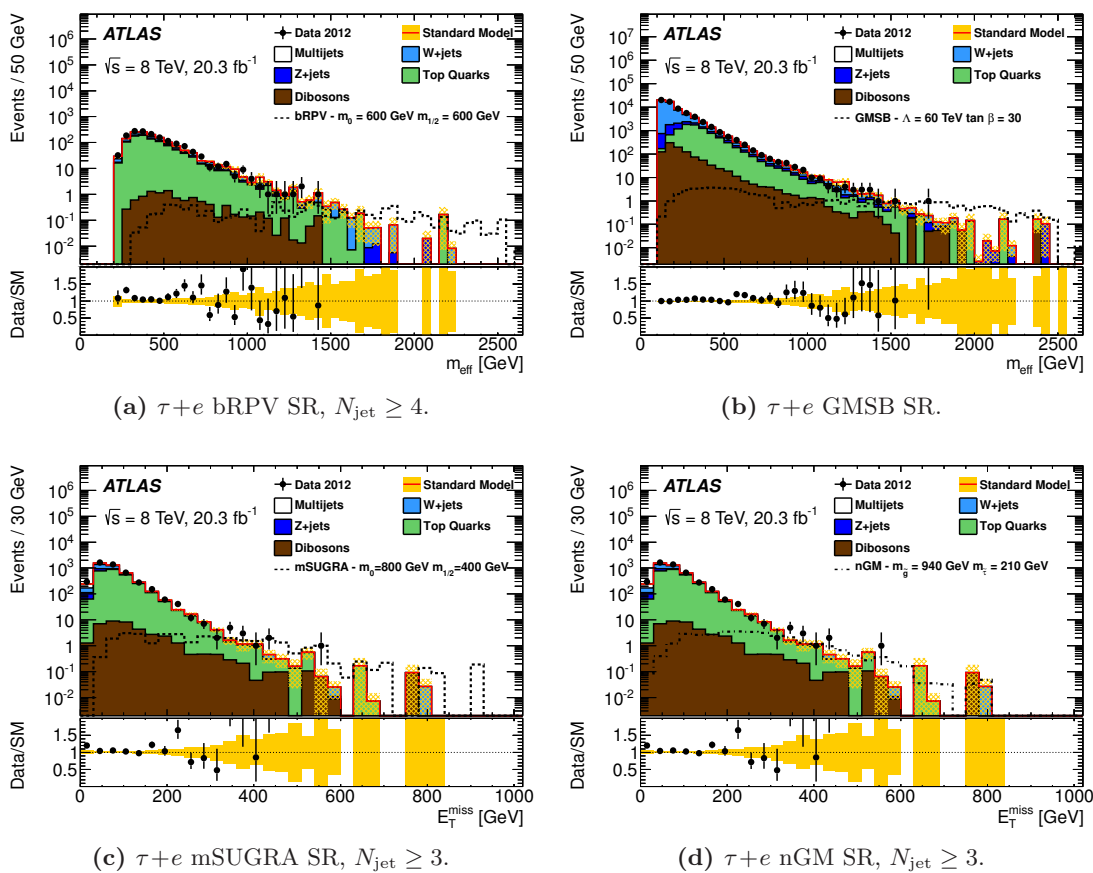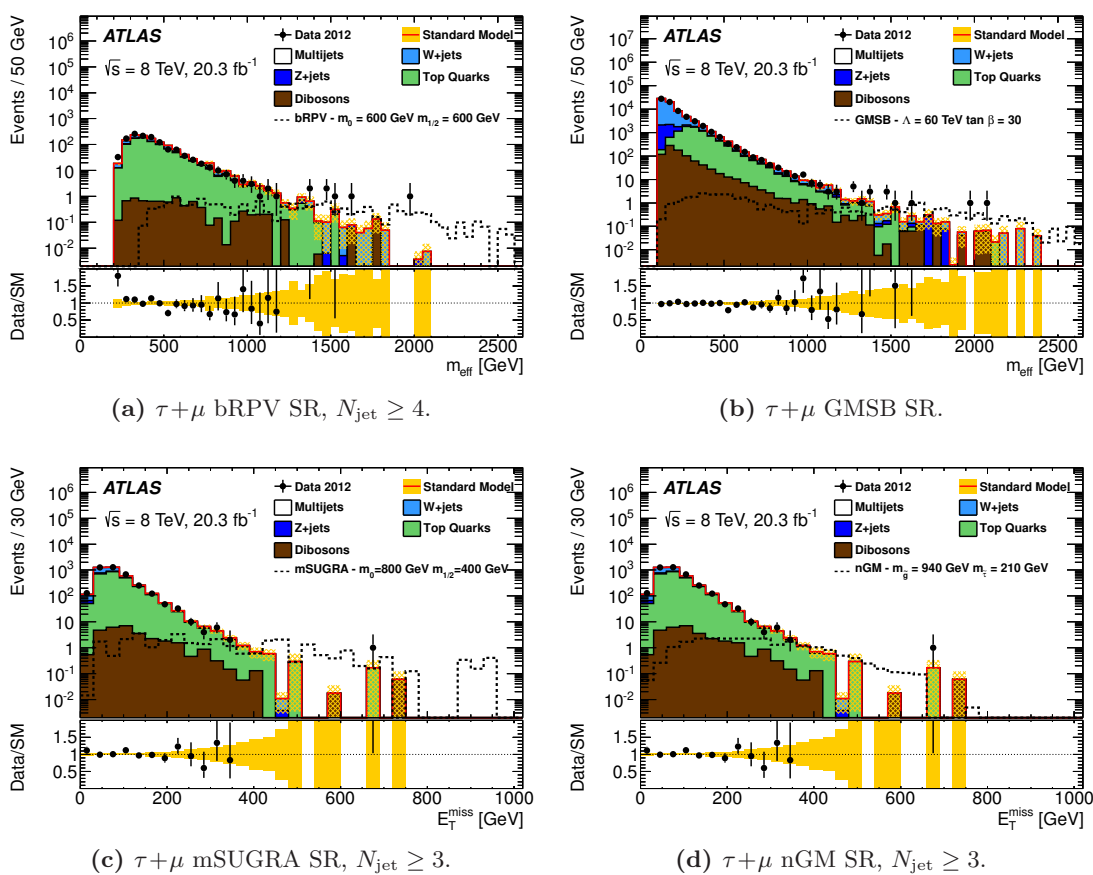
Figure 6. Distribution of the final kinematic variables in the $\tau + e$ channel after all analysis requirements but the final SR selections on m_{eff} and $E_{\mathrm{T}}^{\mathrm{miss}}$. Data are represented by the points. The SM prediction includes the data-driven corrections discussed in the text. The shaded band centred around the total SM background indicates the statistical uncertainty on the background expectation. MC events are normalized to data in the CRs described in the text. Also shown is the expected signal from typical bRPV, GMSB, mSUGRA and nGM signal samples. The last bin in the expected background distribution is an overflow bin. There are no data events in the overflow bin after all analysis requirements are applied.

CLs prescription [109]. The profile likelihood ratio is used as a test statistic [110] and all systematic uncertainties on the background estimate are treated as nuisance parameters, neglecting any possible signal contamination in the control regions. The limits are computed by randomly generating a large number of pseudo-datasets and repeating the CLs procedure. This calculation was compared to an asymptotic approximation [110], which is used for the model-dependent limits, and was found to be in good agreement. These limits are then translated into upper limits on the visible signal cross section, σ_{vis}, by normalizing them to the total integrated luminosity in data. The visible cross section is defined as the product of acceptance, selection efficiency and production cross section. These results are also given in tables 6–9 for all channels.

JHEP09(2014)103

Figure 7. Distribution of the final kinematic variables in the $\tau+\mu$ channel after all analysis requirements but the final SR selections on m_{eff} and E_T^{miss}. Data are represented by the points. The SM prediction includes the data-driven corrections discussed in the text. The shaded band centred around the total SM background indicates the statistical uncertainty on the background expectation. MC events are normalized to data in the CRs described in the text. Also shown is the expected signal from typical bRPV, GMSB, mSUGRA and nGM signal samples. The last bin in the expected background distribution is an overflow bin. There are no data events in the overflow bin after all analysis requirements are applied.

Interpretation

A statistical combination of SRs is performed to produce 95% CL limits on the model parameters for all signal models. For each scenario the combination of SRs from each channel that gives the best expected sensitivity is chosen (see table 10). In setting the limits the full likelihood function that represents the outcome of the combination is used. The combination profits from the fact that all channels considered in the analysis are statistically independent. The limits are calculated using an asymptotic approximation and including all experimental uncertainties on the background and signal expectations, as well as theoretical uncertainties on the background, as nuisance parameters, neglecting any possible signal contamination in the control regions. Correlations between signal and background uncertainties are taken into account.

	1τ Loose	1τ Tight
Multijet	$1.12 \pm 0.49\,^{+1.27}_{-1.12}$	$0.23 \pm 0.10 \pm 0.24$
W + jets	$3.13 \pm 0.57 \pm 1.10$	$0.73 \pm 0.20 \pm 0.69$
Z + jets	$1.89 \pm 0.56 \pm 1.58$	$0.42 \pm 0.15 \pm 0.14$
Top	$3.87 \pm 0.99 \pm 1.62$	$0.82 \pm 0.34 \pm 0.46$
Diboson	$0.47 \pm 0.18 \pm 0.16$	$0.16 \pm 0.10 \pm 0.09$
Total background	$10.5 \pm 1.4 \pm 2.6$	$2.4 \pm 0.4 \pm 0.8$
Data	12	3
Signal MC Events		
GMSB 60/30	—	$6.4 \pm 0.7 \pm 0.4$
nGM 940/210	—	—
bRPV 600/600	—	$2.8 \pm 0.4 \pm 0.4$
mSUGRA 800/400	—	$15.7 \pm 2.2 \pm 1.1$
Obs (exp) limit on signal events	$11.7\ (10.1^{+3.6}_{-2.6})$	$5.9\ (5.3^{+1.8}_{-1.3})$
Obs (exp) limit on vis. cross section (fb)	$0.58\ (0.50)$	$0.29\ (0.26)$
Discovery p-value $p(s=0)$	0.37	0.37

Table 6. Number of expected background events and data yields in the 1τ final state. Where possible, the uncertainties on the number of expected events are separated into statistical (first) and systematic (second) components. The statistical uncertainty comprises the limited number of simulated events in both the SR and the CRs as well as the limited number of data events in the CRs. The SM prediction is computed taking into account correlations between the different uncertainties. Also shown are the number of expected signal events for one selected benchmark point for each signal model studied. For GMSB the chosen point has the parameters $\Lambda = 60\,\mathrm{TeV}$ / $\tan\beta = 30$, for nGM $m_{\tilde{g}} = 940\,\mathrm{GeV}$ / $m_{\tilde{\tau}_1} = 210\,\mathrm{GeV}$, for bRPV $m_0 = 600\,\mathrm{GeV}$ / $m_{1/2} = 600\,\mathrm{GeV}$ and for mSUGRA $m_0 = 800\,\mathrm{GeV}$ / $m_{1/2} = 400\,\mathrm{GeV}$. The resulting 95% CL limit on the number of observed (expected) signal events and on the visible cross sections from any new-physics scenario for each of the final states is shown, taking into account the observed events in data and the background expectations. Discovery p-values are capped at 0.5 in cases where the expected number of events exceeds the observed number.

The resulting observed and expected limits in the GMSB scenario for the combination of all final states considered are shown in figure 8. The yellow band around the expected exclusion limit represents the 1σ statistical and systematic uncertainty on the expected background, as well as the experimental uncertainty on the signal. The dashed red lines around the observed limit indicate the effect of the theoretical uncertainties on the signal cross section. The limits quoted in the following correspond to the assumption that the signal cross section is reduced by 1σ. A lower limit on the SUSY breaking scale Λ of $63\,\mathrm{TeV}$ is determined, independent of the value of $\tan\beta$. The limit on Λ increases to $73\,\mathrm{TeV}$ for large $\tan\beta$ ($\tan\beta > 20$). This corresponds to excluding gluino masses lower than about $1600\,\mathrm{GeV}$. These are the strongest available limits on GMSB-like SUSY with tau lepton signatures.

—	2τ Inclusive	2τ GMSB	2τ nGM	2τ bRPV
Multijet	$0.12 \pm 0.05 \pm 0.06$	$0.062 \pm 0.045 \pm 0.021$	$0.066 \pm 0.045 \pm 0.032$	$0.11 \pm 0.05 \pm 0.04$
W + jets	$1.26 \pm 0.33 \pm 0.54$	$0.14 \pm 0.07 \pm 0.18$	$0.78 \pm 0.31 \pm 0.47$	$0.48 \pm 0.15 \pm 0.31$
Z + jets	$0.54 \pm 0.15 \pm 0.64$	$0.037 \pm 0.020 \pm 0.042$	$0.65 \pm 0.28 \pm 0.94$	$0.18 \pm 0.07 \pm 0.21$
Top	$0.57 \pm 0.14 \pm 0.32$	$0.050 \pm 0.031 \pm 0.053$	$1.65 \pm 0.38 \pm 0.65$	$0.32 \pm 0.10 \pm 0.19$
Diboson	$0.39 \pm 0.19 \pm 0.30$	0 ± 0	0 ± 0	0 ± 0
Total background	$2.9 \pm 0.4 \pm 0.7$	$0.28 \pm 0.10 \pm 0.22$	$3.1 \pm 0.5 \pm 0.9$	$1.09 \pm 0.19 \pm 0.39$
Data	3	0	1	1
Signal MC Events				
GMSB 60/30	—	$9.7 \pm 0.8 \pm 0.6$	—	—
nGM 940/210	—	—	$17.7 \pm 0.8 \pm 1.1$	—
bRPV 600/600	—	—	—	$1.9 \pm 0.3 \pm 0.2$
mSUGRA 800/400	—	—	—	—
Obs (exp) limit on signal events	$5.7\ (5.4^{+1.7}_{-1.4})$	$3.4\ (3.4^{+0.6}_{-0.2})$	$3.8\ (5.4^{+1.8}_{-1.5})$	$4.1\ (4.0^{+1.5}_{-0.3})$
Obs (exp) limit on vis. cross section (fb)	$0.28\ (0.26)$	$0.17\ (0.17)$	$0.18\ (0.27)$	$0.20\ (0.20)$
Discovery p-value $p(s=0)$	0.47	0.50	0.50	0.50

Table 7. Number of expected background events and data yields in the 2τ final state. Further details can be found in table 6.

—	$\tau+e$ GMSB	$\tau+e$ nGM	$\tau+e$ bRPV	$\tau+e$ mSUGRA
Multijet	< 0.2	< 0.1	< 0.3	< 0.4
W + jets	$0.25 \pm 0.11 \pm 0.31$	$0.45 \pm 0.14 \pm 0.28$	$1.61 \pm 0.54 \pm 0.58$	$0.96 \pm 0.22 \pm 0.46$
Z + jets	$0.28 \pm 0.12 \pm 0.29$	$0.11 \pm 0.06 \pm 0.11$	$0.20 \pm 0.09 \pm 0.81$	$0.15 \pm 0.07 \pm 0.16$
Top	$0.52 \pm 0.26 \pm 0.54$	$2.98 \pm 0.82 \pm 1.93$	$1.99 \pm 0.59 \pm 0.81$	$7.43 \pm 1.31 \pm 2.52$
Diboson	$0.29 \pm 0.13 \pm 0.28$	$0.73 \pm 0.21 \pm 0.21$	$0.22 \pm 0.12 \pm 0.12$	$1.47 \pm 0.30 \pm 0.32$
Total background	$1.34 \pm 0.33 \pm 0.80$	$4.3 \pm 0.9 \pm 2.0$	$4.0 \pm 0.8 \pm 1.3$	$10.0 \pm 1.4 \pm 3.0$
Data	1	8	3	14
Signal MC Events				
GMSB 60/30	$8.1 \pm 0.5 \pm 1.0$	—	—	—
nGM 940/210	—	$6.4 \pm 0.5 \pm 0.5$	—	—
bRPV 600/600	—	—	$4.03 \pm 0.48 \pm 0.18$	—
mSUGRA 800/400	—	—	—	$14.1 \pm 1.9 \pm 0.8$
Obs (exp) limit on signal events	$4.1\ (4.2^{+1.7}_{-0.4})$	$11.4\ (8.3^{+2.8}_{-2.0})$	$5.3\ (6.0^{+2.2}_{-1.1})$	$14.6\ (11.7^{+4.1}_{-3.2})$
Obs (exp) limit on vis. cross section (fb)	$0.20\ (0.21)$	$0.56\ (0.41)$	$0.26\ (0.30)$	$0.72\ (0.58)$
Discovery p-value $p(s=0)$	0.50	0.15	0.50	0.24

Table 8. Number of expected background events and data yields in the $\tau+e$ final state. Further details can be found in table 6.

—	$\tau+\mu$ GMSB	$\tau+\mu$ nGM	$\tau+\mu$ bRPV	$\tau+\mu$ mSUGRA
Multijet	< 0.01	< 0.04	< 0.04	< 0.01
W + jets	$0.32 \pm 0.13 \pm 0.08$	$0.39 \pm 0.15 \pm 0.42$	$0.82 \pm 0.32 \pm 0.70$	$0.75 \pm 0.20 \pm 0.38$
Z + jets	$0.33 \pm 0.24 \pm 0.5$	$0.06 \pm 0.03 \pm 0.07$	$0.29 \pm 0.13 \pm 0.16$	$0.07 \pm 0.03 \pm 0.07$
Top	$0.02 \pm 0.02 \pm 0.01$	$2.80 \pm 0.83 \pm 0.97$	$1.22 \pm 0.46 \pm 0.57$	$8.36 \pm 1.40 \pm 2.90$
Diboson	$0.29 \pm 0.13 \pm 0.16$	$0.32 \pm 0.14 \pm 0.28$	$0.22 \pm 0.12 \pm 0.10$	$0.72 \pm 0.21 \pm 0.55$
Total background	$0.98 \pm 0.31 \pm 0.35$	$3.6 \pm 0.9 \pm 1.2$	$2.5 \pm 0.6 \pm 1.0$	$9.9 \pm 1.5 \pm 3.3$
Data	2	2	7	9
Signal MC Events				
GMSB 60/30	$4.34 \pm 0.48 \pm 0.26$	—	—	—
nGM 940/210	—	$5.2 \pm 0.4 \pm 0.4$	—	—
bRPV 600/600	—	—	$5.55 \pm 0.52 \pm 0.24$	—
mSUGRA 800/400	—	—	—	$13.6 \pm 2.0 \pm 0.5$
Obs (exp) limit on signal events	$5.3\ (4.0^{+1.6}_{-0.2})$	$4.6\ (5.6^{+2.1}_{-1.5})$	$10.6\ (6.1^{+2.6}_{-1.0})$	$9.9\ (10.0^{+3.6}_{-2.7})$
Obs (exp) limit on vis. cross section (fb)	$0.26\ (0.20)$	$0.23\ (0.28)$	$0.52\ (0.30)$	$0.49\ (0.49)$
Discovery p-value $p(s=0)$	0.22	0.50	0.04	0.50

Table 9. Number of expected background events and data yields in the $\tau+\mu$ final state. Further details can be found in table 6.

Signal scenario	1τ SR	2τ SR	τ+lepton SR
GMSB	Tight	GMSB	GMSB
nGM	—	nGM	nGM
bRPV	Tight	bRPV	bRPV
mSUGRA	Tight	—	mSUGRA

Table 10. Overview of the signal regions used from each channel for the combined limit setting.

Figure 9 shows the expected and observed exclusion limits obtained when interpreting the 1τ and τ+lepton analysis results in the mSUGRA/CMSSM model plane. Values of $m_{1/2}$ up to 640 GeV for low m_0 and 300 GeV for larger m_0 ($m_0 > 2000$ GeV) are excluded.

Figure 10 shows the expected and observed nGM exclusion limit obtained using the dedicated SRs of the 2τ and the τ+lepton channels for this scenario. Exclusion limits on the mass of the gluino are set at 1090 GeV, independent of the $\tilde{\tau}_1$ mass.

Figure 11 shows the expected and observed exclusion limit in the bRPV scenario for the combination of all final states considered. Values of $m_{1/2}$ up to 680 GeV are excluded for low m_0, while the exclusion along the m_0 axis reaches a maximum of 920 GeV for $m_{1/2} = 360$ GeV.
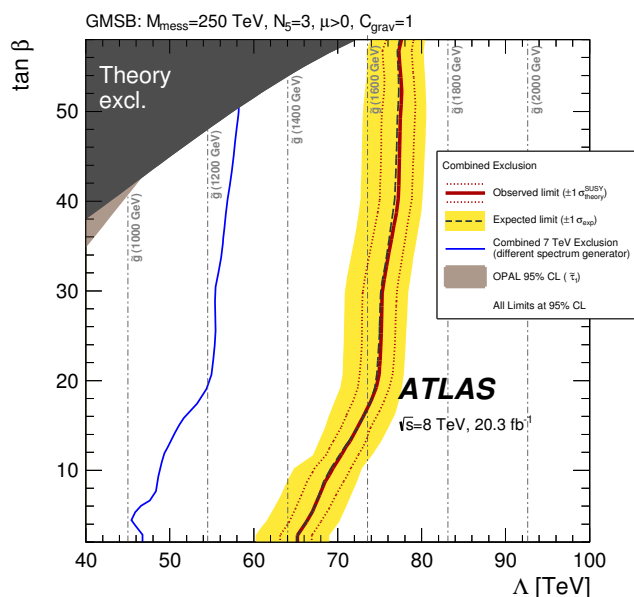
Figure 8. Expected and observed 95% CL lower limits on the minimal GMSB model parameters Λ and $\tan\beta$ using a combination of all channels. The result is obtained using $20.3\,\text{fb}^{-1}$ of $\sqrt{s} = 8\,\text{TeV}$ ATLAS data. The dark grey area indicates the region which is theoretically excluded due to unphysical sparticle mass values. Additional model parameters are $M_{\text{mess}} = 250\,\text{TeV}$, $N_5 = 3$, $\mu > 0$ and $C_{\text{grav}} = 1$. The OPAL limits on the $\tilde{\tau}_1$ mass [31] and the previous ATLAS [32] limits are shown. For the latter, a different mass spectrum generator was employed.
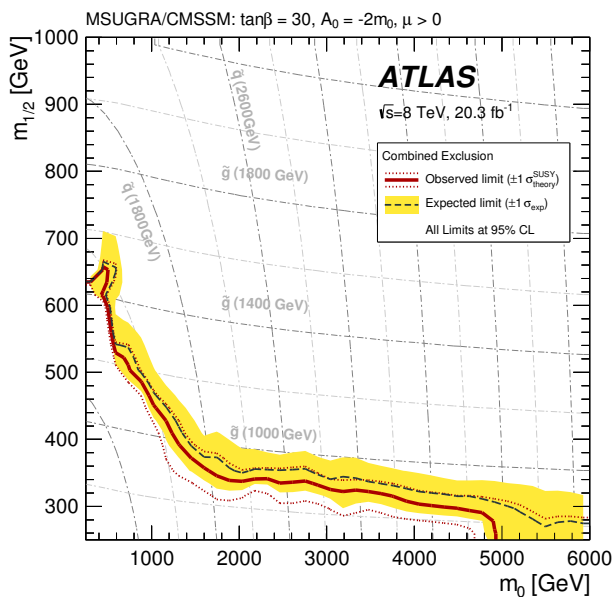
Figure 9. Expected and observed 95% CL lower limits on the mSUGRA/CMSSM model parameters m_0 and $m_{1/2}$ for the combination of the 1τ, $\tau+e$ and $\tau+\mu$ channels. Additional model parameters are $A_0 = -2m_0$, $\tan\beta = 30$ and $\text{sign}(\mu) = +1$.
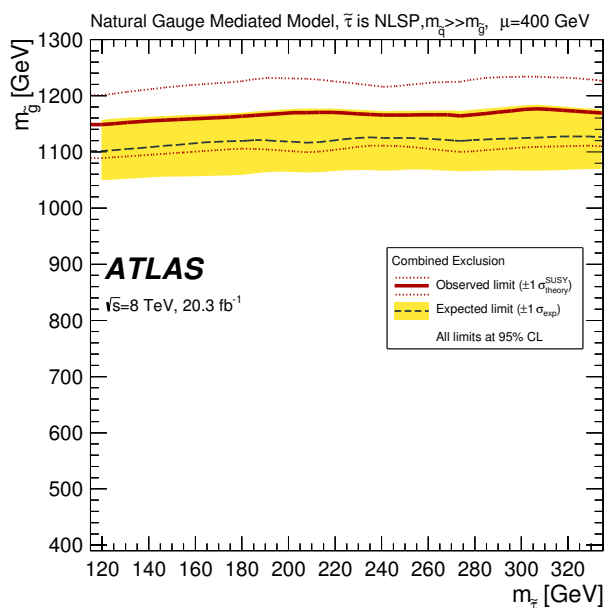
Figure 10. Expected and observed 95% CL lower limits on the simplified nGM model parameters $m_{\tilde{\tau}}$ and $m_{\tilde{g}}$ for the combination of the 2τ, $\tau+e$ and $\tau+\mu$ channels. Additional squark and slepton mass parameters are set to 2.5 TeV, $M_1 = M_2 = 2.5$ TeV, and all trilinear coupling terms are set to zero. Also, the parameter μ is fixed to $\mu = 400$ GeV.
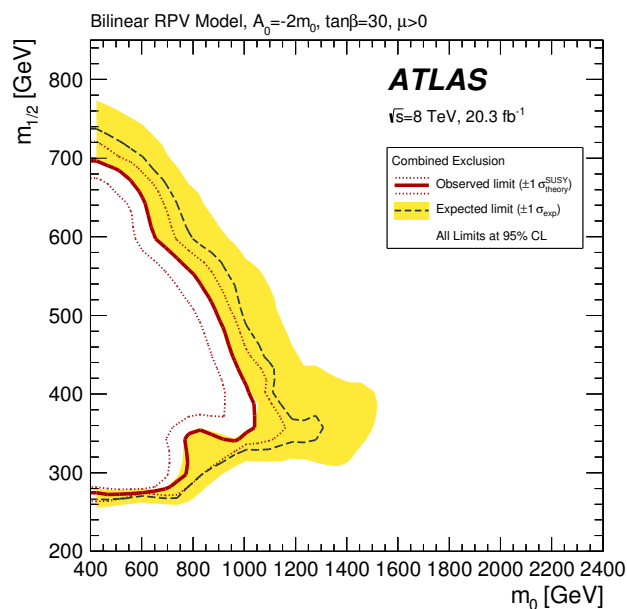
Figure 11. Expected and observed 95% CL lower limits on the bRPV model parameters m_0 and $m_{1/2}$ for the combination of all channels. Additional model parameters are $A_0 = -2m_0$, $\tan\beta = 30$ and $\text{sign}(\mu) = +1$.

10 Conclusions

A search for supersymmetry in final states with jets, $E_{\mathrm{T}}^{\mathrm{miss}}$ and one or more hadronically decaying tau leptons is performed using $20.3\,\mathrm{fb}^{-1}$ of $\sqrt{s} = 8\,\mathrm{TeV}$ pp collision data recorded with the ATLAS detector at the LHC. No excess over the expected Standard Model background is observed. The results are used to set model-independent 95% CL upper limits on the number of signal events from new phenomena and corresponding upper limits on the visible cross sections.

A limit on the SUSY breaking scale Λ of $63\,\mathrm{TeV}$ is obtained, independent of the value of $\tan\beta$, for a minimal GMSB model. The limit on Λ increases to $73\,\mathrm{TeV}$ for high $\tan\beta$ ($\tan\beta > 20$). In a natural Gauge Mediation model, a limit on the gluino mass of $1090\,\mathrm{GeV}$ independent of the $\tilde{\tau}_1$ mass (provided the $\tilde{\tau}_1$ is the NLSP) is obtained from the combination of the 2τ and τ+lepton channels. The results of the analysis in the 1τ and the τ+lepton channels are interpreted in the mSUGRA/CMSSM model and stringent limits in the $(m_0, m_{1/2})$ plane are obtained. In the bilinear R-parity-violating scenario, values of $m_{1/2}$ up to $680\,\mathrm{GeV}$ are excluded for low m_0. Moreover, values of m_0 up to $920\,\mathrm{GeV}$ are excluded, for $m_{1/2} = 360\,\mathrm{GeV}$.

References

[1] Y. Golfand and E.P. Likhtman, *Extension of the algebra of Poincaré group generators and violation of p invariance*, *JETP Lett.* **13** (1971) 323 [*Pisma Zh. Eksp. Teor. Fiz.* **13** (1971) 452] [INSPIRE].

[2] A. Neveu and J.H. Schwarz, *Factorizable dual model of pions*, *Nucl. Phys.* **B 31** (1971) 86 [INSPIRE].

[3] P. Ramond, *Dual theory for free fermions*, *Phys. Rev.* **D 3** (1971) 2415 [INSPIRE].

[4] D.V. Volkov and V.P. Akulov, *Is the neutrino a Goldstone particle?*, *Phys. Lett.* **B 46** (1973) 109 [INSPIRE].

[5] J. Wess and B. Zumino, *Supergauge transformations in four-dimensions*, *Nucl. Phys.* **B 70** (1974) 39 [INSPIRE].

[6] P. Fayet, *Supersymmetry and weak, electromagnetic and strong interactions*, *Phys. Lett.* **B 64** (1976) 159 [INSPIRE].

[7] P. Fayet, *Spontaneously broken supersymmetric theories of weak, electromagnetic and strong interactions*, *Phys. Lett.* **B 69** (1977) 489 [INSPIRE].

[8] G.R. Farrar and P. Fayet, *Phenomenology of the production, decay and detection of new hadronic states associated with supersymmetry*, *Phys. Lett.* **B 76** (1978) 575 [INSPIRE].

[9] P. Fayet, *Relations between the masses of the superpartners of leptons and quarks, the Goldstino couplings and the neutral currents*, *Phys. Lett.* **B 84** (1979) 416 [INSPIRE].

[10] S. Dimopoulos and H. Georgi, *Softly broken supersymmetry and* SU(5), *Nucl. Phys.* **B 193** (1981) 150 [INSPIRE].

[11] R. Barbieri and G.F. Giudice, *Upper bounds on supersymmetric particle masses*, *Nucl. Phys.* **B 306** (1988) 63 [INSPIRE].

[12] B. de Carlos and J.A. Casas, *One loop analysis of the electroweak breaking in supersymmetric models and the fine tuning problem*, *Phys. Lett.* **B 309** (1993) 320 [hep-ph/9303291] [INSPIRE].

[13] D. Albornoz Vásquez, G. Bélanger and C. Boehm, *Revisiting light neutralino scenarios in the MSSM*, *Phys. Rev.* **D 84** (2011) 095015 [arXiv:1108.1338] [INSPIRE].

[14] M. Dine and W. Fischler, *A phenomenological model of particle physics based on supersymmetry*, *Phys. Lett.* **B 110** (1982) 227 [INSPIRE].

[15] L. Álvarez-Gaumé, M. Claudson and M.B. Wise, *Low-energy supersymmetry*, *Nucl. Phys.* **B 207** (1982) 96 [INSPIRE].

[16] C.R. Nappi and B.A. Ovrut, *Supersymmetric extension of the* SU(3) × SU(2) × U(1) *model*, *Phys. Lett.* **B 113** (1982) 175 [INSPIRE].

[17] M. Dine and A.E. Nelson, *Dynamical supersymmetry breaking at low-energies*, *Phys. Rev.* **D 48** (1993) 1277 [hep-ph/9303230] [INSPIRE].

[18] M. Dine, A.E. Nelson and Y. Shirman, *Low-energy dynamical supersymmetry breaking simplified*, *Phys. Rev.* **D 51** (1995) 1362 [`hep-ph/9408384`] [ɪɴSPIRE].

[19] M. Dine, A.E. Nelson, Y. Nir and Y. Shirman, *New tools for low-energy dynamical supersymmetry breaking*, *Phys. Rev.* **D 53** (1996) 2658 [`hep-ph/9507378`] [ɪɴSPIRE].

[20] A.H. Chamseddine, R.L. Arnowitt and P. Nath, *Locally supersymmetric grand unification*, *Phys. Rev. Lett.* **49** (1982) 970 [ɪɴSPIRE].

[21] R. Barbieri, S. Ferrara and C.A. Savoy, *Gauge models with spontaneously broken local supersymmetry*, *Phys. Lett.* **B 119** (1982) 343 [ɪɴSPIRE].

[22] L.E. Ibáñez, *Locally supersymmetric* SU(5) *grand unification*, *Phys. Lett.* **B 118** (1982) 73 [ɪɴSPIRE].

[23] L.J. Hall, J.D. Lykken and S. Weinberg, *Supergravity as the messenger of supersymmetry breaking*, *Phys. Rev.* **D 27** (1983) 2359 [ɪɴSPIRE].

[24] N. Ohta, *Grand unified theories based on local supersymmetry*, *Prog. Theor. Phys.* **70** (1983) 542 [ɪɴSPIRE].

[25] G.L. Kane, C.F. Kolda, L. Roszkowski and J.D. Wells, *Study of constrained minimal supersymmetry*, *Phys. Rev.* **D 49** (1994) 6173 [`hep-ph/9312272`] [ɪɴSPIRE].

[26] J. Barnard, B. Farmer, T. Gherghetta and M. White, *Natural gauge mediation with a bino NLSP at the LHC*, *Phys. Rev. Lett.* **109** (2012) 241801 [`arXiv:1208.6062`] [ɪɴSPIRE].

[27] M. Hirsch, M.A. Diaz, W. Porod, J.C. Romao and J.W.F. Valle, *Neutrino masses and mixings from supersymmetry with bilinear R-parity violation: a theory for solar and atmospheric neutrino oscillations*, *Phys. Rev.* **D 62** (2000) 113008 [*Erratum ibid.* **D 65** (2002) 119901] [`hep-ph/0004115`] [ɪɴSPIRE].

[28] F. de Campos et al., *Probing bilinear R-parity violating supergravity at the LHC*, *JHEP* **05** (2008) 048 [`arXiv:0712.2156`] [ɪɴSPIRE].

[29] ALEPH collaboration, A. Heister et al., *Search for gauge mediated SUSY breaking topologies in* e^+e^- *collisions at center-of-mass energies up to* 209 *GeV*, *Eur. Phys. J.* **C 25** (2002) 339 [`hep-ex/0203024`] [ɪɴSPIRE].

[30] DELPHI collaboration, J. Abdallah et al., *Search for supersymmetric particles in light gravitino scenarios and sleptons NLSP*, *Eur. Phys. J.* **C 27** (2003) 153 [`hep-ex/0303025`] [ɪɴSPIRE].

[31] OPAL collaboration, G. Abbiendi et al., *Searches for gauge-mediated supersymmetry breaking topologies in* e^+e^- *collisions at LEP*2, *Eur. Phys. J.* **C 46** (2006) 307 [`hep-ex/0507048`] [ɪɴSPIRE].

[32] ATLAS collaboration, *Search for supersymmetry in events with large missing transverse momentum, jets and at least one* τ *lepton in* 7 *TeV proton-proton collision data with the ATLAS detector*, *Eur. Phys. J.* **C 72** (2012) 2215 [`arXiv:1210.1314`] [ɪɴSPIRE].

[33] CMS collaboration, *Search for physics beyond the standard model in events with* τ *leptons, jets and large transverse momentum imbalance in pp collisions at* $\sqrt{s} = 7$ *TeV*, *Eur. Phys. J.* **C 73** (2013) 2493 [`arXiv:1301.3792`] [ɪɴSPIRE].

[34] ATLAS collaboration, *Observation of a new particle in the search for the standard model Higgs boson with the ATLAS detector at the LHC*, *Phys. Lett.* **B 716** (2012) 1 [`arXiv:1207.7214`] [ɪɴSPIRE].

[35] CMS collaboration, *Observation of a new boson at a mass of* 125 *GeV with the CMS experiment at the LHC*, *Phys. Lett.* **B 716** (2012) 30 [arXiv:1207.7235] [inSPIRE].

[36] J.R. Ellis, T. Falk, K.A. Olive and M. Srednicki, *Calculations of neutralino-stau coannihilation channels and the cosmologically relevant region of MSSM parameter space*, *Astropart. Phys.* **13** (2000) 181 [*Erratum ibid.* **15** (2001) 413] [hep-ph/9905481] [inSPIRE].

[37] PLANCK collaboration, P.A.R. Ade et al., *Planck* 2013 *results. XVI. Cosmological parameters*, *Astron. Astrophys.* (2014) [arXiv:1303.5076] [inSPIRE].

[38] WMAP collaboration, G. Hinshaw et al., *Nine-year Wilkinson Microwave Anisotropy Probe (WMAP) observations: cosmological parameter results*, *Astrophys. J. Suppl.* **208** (2013) 19 [arXiv:1212.5226] [inSPIRE].

[39] M. Buican, P. Meade, N. Seiberg and D. Shih, *Exploring general gauge mediation*, *JHEP* **03** (2009) 016 [arXiv:0812.3668] [inSPIRE].

[40] M. Asano, H.D. Kim, R. Kitano and Y. Shimizu, *Natural supersymmetry at the LHC*, *JHEP* **12** (2010) 019 [arXiv:1010.0692] [inSPIRE].

[41] M. Gabella, T. Gherghetta and J. Giedt, *A gravity dual and LHC study of single-sector supersymmetry breaking*, *Phys. Rev.* **D 76** (2007) 055001 [arXiv:0704.3571] [inSPIRE].

[42] N. Craig, M. McCullough and J. Thaler, *Flavor mediation delivers natural SUSY*, *JHEP* **06** (2012) 046 [arXiv:1203.1622] [inSPIRE].

[43] N. Craig, D. Green and A. Katz, *(De)constructing a natural and flavorful supersymmetric standard model*, *JHEP* **07** (2011) 045 [arXiv:1103.3708] [inSPIRE].

[44] R. Auzzi, A. Giveon and S.B. Gudnason, *Flavor of quiver-like realizations of effective supersymmetry*, *JHEP* **02** (2012) 069 [arXiv:1112.6261] [inSPIRE].

[45] C. Csáki, L. Randall and J. Terning, *Light stops from Seiberg duality*, *Phys. Rev.* **D 86** (2012) 075009 [arXiv:1201.1293] [inSPIRE].

[46] G. Larsen, Y. Nomura and H.L.L. Roberts, *Supersymmetry with light stops*, *JHEP* **06** (2012) 032 [arXiv:1202.6339] [inSPIRE].

[47] N. Craig, S. Dimopoulos and T. Gherghetta, *Split families unified*, *JHEP* **04** (2012) 116 [arXiv:1203.0572] [inSPIRE].

[48] Y. Grossman and S. Rakshit, *Neutrino masses in R-parity violating supersymmetric models*, *Phys. Rev.* **D 69** (2004) 093002 [hep-ph/0311310] [inSPIRE].

[49] D.F. Carvalho, M.E. Gomez and J.C. Romao, *Charged lepton flavor violation in supersymmetry with bilinear R-parity violation*, *Phys. Rev.* **D 65** (2002) 093013 [hep-ph/0202054] [inSPIRE].

[50] W. Porod, M. Hirsch, J. Romao and J.W.F. Valle, *Testing neutrino mixing at future collider experiments*, *Phys. Rev.* **D 63** (2001) 115004 [hep-ph/0011248] [inSPIRE].

[51] ATLAS collaboration, *The ATLAS experiment at the CERN Large Hadron Collider*, 2008 *JINST* **3** S08003 [inSPIRE].

[52] ATLAS collaboration, *Improved luminosity determination in pp collisions at* $\sqrt{s} = 7$ *TeV using the ATLAS detector at the LHC*, *Eur. Phys. J.* **C 73** (2013) 2518 [arXiv:1302.4393] [inSPIRE].

[53] ATLAS collaboration, *Performance of the ATLAS trigger system in* 2010, *Eur. Phys. J.* **C 72** (2012) 1849 [arXiv:1110.1530] [inSPIRE].

[54] T. Gleisberg et al., *Event generation with SHERPA* 1.1, *JHEP* **02** (2009) 007 [arXiv:0811.4622] [INSPIRE].

[55] H.-L. Lai et al., *New parton distributions for collider physics*, *Phys. Rev.* **D 82** (2010) 074024 [arXiv:1007.2241] [INSPIRE].

[56] ATLAS collaboration, *Search for pair-produced third-generation squarks decaying via charm quarks or in compressed supersymmetric scenarios in pp collisions at $\sqrt{s} = 8$ TeV with the ATLAS detector*, submitted to *Phys. Rev.* **D** [arXiv:1407.0608] [INSPIRE].

[57] M.L. Mangano, M. Moretti, F. Piccinini, R. Pittau and A.D. Polosa, *ALPGEN, a generator for hard multiparton processes in hadronic collisions*, *JHEP* **07** (2003) 001 [hep-ph/0206293] [INSPIRE].

[58] J. Pumplin et al., *New generation of parton distributions with uncertainties from global QCD analysis*, *JHEP* **07** (2002) 012 [hep-ph/0201195] [INSPIRE].

[59] G. Corcella et al., *HERWIG* 6: *an event generator for hadron emission reactions with interfering gluons (including supersymmetric processes)*, *JHEP* **01** (2001) 010 [hep-ph/0011363] [INSPIRE].

[60] J.M. Butterworth, J.R. Forshaw and M.H. Seymour, *Multiparton interactions in photoproduction at HERA*, *Z. Phys.* **C 72** (1996) 637 [hep-ph/9601371] [INSPIRE].

[61] P. Nason, *A new method for combining NLO QCD with shower Monte Carlo algorithms*, *JHEP* **11** (2004) 040 [hep-ph/0409146] [INSPIRE].

[62] S. Frixione, P. Nason and C. Oleari, *Matching NLO QCD computations with parton shower simulations: the POWHEG method*, *JHEP* **11** (2007) 070 [arXiv:0709.2092] [INSPIRE].

[63] S. Alioli, P. Nason, C. Oleari and E. Re, *A general framework for implementing NLO calculations in shower Monte Carlo programs: the POWHEG BOX*, *JHEP* **06** (2010) 043 [arXiv:1002.2581] [INSPIRE].

[64] T. Sjöstrand, S. Mrenna and P.Z. Skands, *A brief introduction to PYTHIA* 8.1, *Comput. Phys. Commun.* **178** (2008) 852 [arXiv:0710.3820] [INSPIRE].

[65] T. Sjöstrand, S. Mrenna and P.Z. Skands, *PYTHIA* 6.4 *physics and manual*, *JHEP* **05** (2006) 026 [hep-ph/0603175] [INSPIRE].

[66] ATLAS collaboration, *Measurements of normalized differential cross-sections for $t\bar{t}$ production in pp collisions at $\sqrt{s} = 7$ TeV using the ATLAS detector*, submitted to *Phys. Rev.* **D** [arXiv:1407.0371] [INSPIRE].

[67] S. Frixione and B.R. Webber, *Matching NLO QCD computations and parton shower simulations*, *JHEP* **06** (2002) 029 [hep-ph/0204244] [INSPIRE].

[68] S. Frixione, P. Nason and B.R. Webber, *Matching NLO QCD and parton showers in heavy flavor production*, *JHEP* **08** (2003) 007 [hep-ph/0305252] [INSPIRE].

[69] S. Frixione, E. Laenen, P. Motylinski and B.R. Webber, *Single-top production in MC@NLO*, *JHEP* **03** (2006) 092 [hep-ph/0512250] [INSPIRE].

[70] B.P. Kersevan and E. Richter-Was, *The Monte Carlo event generator AcerMC versions* 2.0 *to* 3.8 *with interfaces to PYTHIA* 6.4, *HERWIG* 6.5 *and ARIADNE* 4.1, *Comput. Phys. Commun.* **184** (2013) 919 [hep-ph/0405247] [INSPIRE].

[71] M. Bähr et al., *HERWIG++ physics and manual*, *Eur. Phys. J.* **C 58** (2008) 639 [arXiv:0803.0883] [INSPIRE].

[72] W. Beenakker, R. Hopker, M. Spira and P.M. Zerwas, *Squark and gluino production at hadron colliders*, *Nucl. Phys.* **B 492** (1997) 51 [hep-ph/9610490] [INSPIRE].

[73] A. Kulesza and L. Motyka, *Threshold resummation for squark-antisquark and gluino-pair production at the LHC*, *Phys. Rev. Lett.* **102** (2009) 111802 [arXiv:0807.2405] [INSPIRE].

[74] A. Kulesza and L. Motyka, *Soft gluon resummation for the production of gluino-gluino and squark-antisquark pairs at the LHC*, *Phys. Rev.* **D 80** (2009) 095004 [arXiv:0905.4749] [INSPIRE].

[75] W. Beenakker et al., *Soft-gluon resummation for squark and gluino hadroproduction*, *JHEP* **12** (2009) 041 [arXiv:0909.4418] [INSPIRE].

[76] W. Beenakker et al., *Squark and gluino hadroproduction*, *Int. J. Mod. Phys.* **A 26** (2011) 2637 [arXiv:1105.1110] [INSPIRE].

[77] M. Krämer et al., *Supersymmetry production cross sections in pp collisions at $\sqrt{s} = 7\ TeV$*, arXiv:1206.2892 [INSPIRE].

[78] S. Jadach, Z. Was, R. Decker and J.H. Kuhn, *The τ decay library TAUOLA: version* 2.4, *Comput. Phys. Commun.* **76** (1993) 361 [INSPIRE].

[79] P. Golonka et al., *The Tauola photos F environment for the TAUOLA and PHOTOS packages: release.* 2, *Comput. Phys. Commun.* **174** (2006) 818 [hep-ph/0312240] [INSPIRE].

[80] ATLAS collaboration, *ATLAS tunes of PYTHIA 6 and PYTHIA 8 for MC11*, ATL-PHYS-PUB-2011-009, CERN, Geneva Switzerland (2011).

[81] P.M. Nadolsky et al., *Implications of CTEQ global analysis for collider observables*, *Phys. Rev.* **D 78** (2008) 013004 [arXiv:0802.0007] [INSPIRE].

[82] ATLAS collaboration, *Summary of ATLAS PYTHIA 8 tunes*, ATL-PHYS-PUB-2012-003, CERN, Geneva Switzerland (2012).

[83] P.Z. Skands, *Tuning Monte Carlo generators: the Perugia tunes*, *Phys. Rev.* **D 82** (2010) 074018 [arXiv:1005.3457] [INSPIRE].

[84] GEANT4 collaboration, S. Agostinelli et al., *GEANT4: a simulation toolkit*, *Nucl. Instrum. Meth.* **A 506** (2003) 250 [INSPIRE].

[85] ATLAS collaboration, *The ATLAS simulation infrastructure*, *Eur. Phys. J.* **C 70** (2010) 823 [arXiv:1005.4568] [INSPIRE].

[86] ATLAS collaboration, *The simulation principle and performance of the ATLAS fast calorimeter simulation FastCaloSim*, ATL-PHYS-PUB-2010-013, CERN, Geneva Switzerland (2010).

[87] S. Catani, L. Cieri, G. Ferrera, D. de Florian and M. Grazzini, *Vector boson production at hadron colliders: a fully exclusive QCD calculation at NNLO*, *Phys. Rev. Lett.* **103** (2009) 082001 [arXiv:0903.2120] [INSPIRE].

[88] A.D. Martin, W.J. Stirling, R.S. Thorne and G. Watt, *Parton distributions for the LHC*, *Eur. Phys. J.* **C 63** (2009) 189 [arXiv:0901.0002] [INSPIRE].

[89] M. Cacciari, M. Czakon, M. Mangano, A. Mitov and P. Nason, *Top-pair production at hadron colliders with next-to-next-to-leading logarithmic soft-gluon resummation*, *Phys. Lett.* **B 710** (2012) 612 [arXiv:1111.5869] [INSPIRE].

[90] M. Czakon and A. Mitov, *Top++: a program for the calculation of the top-pair cross-section at hadron colliders*, *Comput. Phys. Commun.* **185** (2014) 2930 [arXiv:1112.5675] [INSPIRE].

[91] N. Kidonakis, *NNLL resummation for s-channel single top quark production*, *Phys. Rev.* **D 81** (2010) 054028 [arXiv:1001.5034] [INSPIRE].

[92] N. Kidonakis, *Two-loop soft anomalous dimensions for single top quark associated production with a W^- or H^-*, *Phys. Rev.* **D 82** (2010) 054018 [arXiv:1005.4451] [INSPIRE].

[93] N. Kidonakis, *Next-to-next-to-leading-order collinear and soft gluon corrections for t-channel single top quark production*, *Phys. Rev.* **D 83** (2011) 091503 [arXiv:1103.2792] [INSPIRE].

[94] J.M. Campbell, R.K. Ellis and C. Williams, *Vector boson pair production at the LHC*, *JHEP* **07** (2011) 018 [arXiv:1105.0020] [INSPIRE].

[95] ATLAS collaboration, *Performance of primary vertex reconstruction in proton-proton collisions at $\sqrt{s} = 7$ TeV in the ATLAS experiment*, ATLAS-CONF-2010-069, CERN, Geneva Switzerland (2010).

[96] M. Cacciari, G.P. Salam and G. Soyez, *The anti-k_t jet clustering algorithm*, *JHEP* **04** (2008) 063 [arXiv:0802.1189] [INSPIRE].

[97] M. Cacciari and G.P. Salam, *Pileup subtraction using jet areas*, *Phys. Lett.* **B 659** (2008) 119 [arXiv:0707.1378] [INSPIRE].

[98] C. Issever, K. Borras and D. Wegener, *An improved weighting algorithm to achieve software compensation in a fine grained LAr calorimeter*, *Nucl. Instrum. Meth.* **A 545** (2005) 803 [physics/0408129] [INSPIRE].

[99] ATLAS collaboration, *Jet energy measurement and its systematic uncertainty in proton-proton collisions at $\sqrt{s} = 7$ TeV with the ATLAS detector*, submitted to *Eur. Phys. J.* **C** (2014) [arXiv:1406.0076] [INSPIRE].

[100] ATLAS collaboration, *Commissioning of the ATLAS high-performance b-tagging algorithms in the 7 TeV collision data*, ATLAS-CONF-2011-102, CERN, Geneva Switzerland (2011).

[101] ATLAS collaboration, *Measurement of the b-tag efficiency in a sample of jets containing muons with $5\,\text{fb}^{-1}$ of data from the ATLAS detector*, ATLAS-CONF-2012-043, CERN, Geneva Switzerland (2012).

[102] ATLAS collaboration, *Identification of the hadronic decays of τ leptons in 2012 data with the ATLAS detector*, ATLAS-CONF-2013-064, CERN, Geneva Switzerland (2013).

[103] ATLAS collaboration, *Determination of the τ energy scale and the associated systematic uncertainty in proton-proton collisions at $\sqrt{s} = 8$ TeV with the ATLAS detector at the LHC in 2012*, ATLAS-CONF-2013-044, CERN, Geneva Switzerland (2013).

[104] ATLAS collaboration, *Muon reconstruction efficiency and momentum resolution of the ATLAS experiment in proton-proton collisions at $\sqrt{s} = 7$ TeV in 2010*, *Eur. Phys. J.* **C 74** (2014) 3034 [arXiv:1404.4562] [INSPIRE].

[105] ATLAS collaboration, *Electron reconstruction and identification efficiency measurements with the ATLAS detector using the 2011 LHC proton-proton collision data*, *Eur. Phys. J.* **C 74** (2014) 2941 [arXiv:1404.2240] [INSPIRE].

[106] ATLAS collaboration, *Performance of missing transverse momentum reconstruction in proton-proton collisions at 7 TeV with ATLAS*, *Eur. Phys. J.* **C 72** (2012) 1844 [arXiv:1108.5602] [INSPIRE].

[107] ATLAS collaboration, *Search for squarks and gluinos with the ATLAS detector in final states with jets and missing transverse momentum using* $4.7 \, \text{fb}^{-1}$ *of* $\sqrt{s} = 7 \, TeV$ *proton-proton collision data*, *Phys. Rev.* **D 87** (2013) 012008 [arXiv:1208.0949] [INSPIRE].

[108] ATLAS collaboration, *Further search for supersymmetry at* $\sqrt{s} = 7 \, TeV$ *in final states with jets, missing transverse momentum and isolated leptons with the ATLAS detector*, *Phys. Rev.* **D 86** (2012) 092002 [arXiv:1208.4688] [INSPIRE].

[109] A.L. Read, *Presentation of search results: the* CL_s *technique*, *J. Phys.* **G 28** (2002) 2693 [INSPIRE].

[110] G. Cowan, K. Cranmer, E. Gross and O. Vitells, *Asymptotic formulae for likelihood-based tests of new physics*, *Eur. Phys. J.* **C 71** (2011) 1554 [arXiv:1007.1727] [INSPIRE].

The ATLAS collaboration

G. Aad[84], B. Abbott[112], J. Abdallah[152], S. Abdel Khalek[116], O. Abdinov[11], R. Aben[106],
B. Abi[113], M. Abolins[89], O.S. AbouZeid[159], H. Abramowicz[154], H. Abreu[153], R. Abreu[30],
Y. Abulaiti[147a,147b], B.S. Acharya[165a,165b,a], L. Adamczyk[38a], D.L. Adams[25], J. Adelman[177],
S. Adomeit[99], T. Adye[130], T. Agatonovic-Jovin[13a], J.A. Aguilar-Saavedra[125a,125f], M. Agustoni[17],
S.P. Ahlen[22], F. Ahmadov[64,b], G. Aielli[134a,134b], H. Akerstedt[147a,147b], T.P.A. Åkesson[80],
G. Akimoto[156], A.V. Akimov[95], G.L. Alberghi[20a,20b], J. Albert[170], S. Albrand[55],
M.J. Alconada Verzini[70], M. Aleksa[30], I.N. Aleksandrov[64], C. Alexa[26a], G. Alexander[154],
G. Alexandre[49], T. Alexopoulos[10], M. Alhroob[165a,165c], G. Alimonti[90a], L. Alio[84], J. Alison[31],
B.M.M. Allbrooke[18], L.J. Allison[71], P.P. Allport[73], J. Almond[83], A. Aloisio[103a,103b], A. Alonso[36],
F. Alonso[70], C. Alpigiani[75], A. Altheimer[35], B. Alvarez Gonzalez[89], M.G. Alviggi[103a,103b],
K. Amako[65], Y. Amaral Coutinho[24a], C. Amelung[23], D. Amidei[88], S.P. Amor Dos Santos[125a,125c],
A. Amorim[125a,125b], S. Amoroso[48], N. Amram[154], G. Amundsen[23], C. Anastopoulos[140],
L.S. Ancu[49], N. Andari[30], T. Andeen[35], C.F. Anders[58b], G. Anders[30], K.J. Anderson[31],
A. Andreazza[90a,90b], V. Andrei[58a], X.S. Anduaga[70], S. Angelidakis[9], I. Angelozzi[106], P. Anger[44],
A. Angerami[35], F. Anghinolfi[30], A.V. Anisenkov[108], N. Anjos[125a], A. Annovi[47], A. Antonaki[9],
M. Antonelli[47], A. Antonov[97], J. Antos[145b], F. Anulli[133a], M. Aoki[65], L. Aperio Bella[18],
R. Apolle[119,c], G. Arabidze[89], I. Aracena[144], Y. Arai[65], J.P. Araque[125a], A.T.H. Arce[45],
J-F. Arguin[94], S. Argyropoulos[42], M. Arik[19a], A.J. Armbruster[30], O. Arnaez[30], V. Arnal[81],
H. Arnold[48], M. Arratia[28], O. Arslan[21], A. Artamonov[96], G. Artoni[23], S. Asai[156], N. Asbah[42],
A. Ashkenazi[154], B. Åsman[147a,147b], L. Asquith[6], K. Assamagan[25], R. Astalos[145a],
M. Atkinson[166], N.B. Atlay[142], B. Auerbach[6], K. Augsten[127], M. Aurousseau[146b], G. Avolio[30],
G. Azuelos[94,d], Y. Azuma[156], M.A. Baak[30], A. Baas[58a], C. Bacci[135a,135b], H. Bachacou[137],
K. Bachas[155], M. Backes[30], M. Backhaus[30], J. Backus Mayes[144], E. Badescu[26a],
P. Bagiacchi[133a,133b], P. Bagnaia[133a,133b], Y. Bai[33a], T. Bain[35], J.T. Baines[130], O.K. Baker[177],
P. Balek[128], F. Balli[137], E. Banas[39], Sw. Banerjee[174], A.A.E. Bannoura[176], V. Bansal[170],
H.S. Bansil[18], L. Barak[173], S.P. Baranov[95], E.L. Barberio[87], D. Barberis[50a,50b], M. Barbero[84],
T. Barillari[100], M. Barisonzi[176], T. Barklow[144], N. Barlow[28], B.M. Barnett[130], R.M. Barnett[15],
Z. Barnovska[5], A. Baroncelli[135a], G. Barone[49], A.J. Barr[119], F. Barreiro[81],
J. Barreiro Guimarães da Costa[57], R. Bartoldus[144], A.E. Barton[71], P. Bartos[145a], V. Bartsch[150],
A. Bassalat[116], A. Basye[166], R.L. Bates[53], J.R. Batley[28], M. Battaglia[138], M. Battistin[30],
F. Bauer[137], H.S. Bawa[144,e], M.D. Beattie[71], T. Beau[79], P.H. Beauchemin[162],
R. Beccherle[123a,123b], P. Bechtle[21], H.P. Beck[17], K. Becker[176], S. Becker[99], M. Beckingham[171],
C. Becot[116], A.J. Beddall[19c], A. Beddall[19c], S. Bedikian[177], V.A. Bednyakov[64], C.P. Bee[149],
L.J. Beemster[106], T.A. Beermann[176], M. Begel[25], K. Behr[119], C. Belanger-Champagne[86],
P.J. Bell[49], W.H. Bell[49], G. Bella[154], L. Bellagamba[20a], A. Bellerive[29], M. Bellomo[85],
K. Belotskiy[97], O. Beltramello[30], O. Benary[154], D. Benchekroun[136a], K. Bendtz[147a,147b],
N. Benekos[166], Y. Benhammou[154], E. Benhar Noccioli[49], J.A. Benitez Garcia[160b],
D.P. Benjamin[45], J.R. Bensinger[23], K. Benslama[131], S. Bentvelsen[106], D. Berge[106],
E. Bergeaas Kuutmann[16], N. Berger[5], F. Berghaus[170], J. Beringer[15], C. Bernard[22], P. Bernat[77],
C. Bernius[78], F.U. Bernlochner[170], T. Berry[76], P. Berta[128], C. Bertella[84], G. Bertoli[147a,147b],
F. Bertolucci[123a,123b], C. Bertsche[112], D. Bertsche[112], M.I. Besana[90a], G.J. Besjes[105],
O. Bessidskaia[147a,147b], M. Bessner[42], N. Besson[137], C. Betancourt[48], S. Bethke[100], W. Bhimji[46],
R.M. Bianchi[124], L. Bianchini[23], M. Bianco[30], O. Biebel[99], S.P. Bieniek[77], K. Bierwagen[54],
J. Biesiada[15], M. Biglietti[135a], J. Bilbao De Mendizabal[49], H. Bilokon[47], M. Bindi[54], S. Binet[116],
A. Bingul[19c], C. Bini[133a,133b], C.W. Black[151], J.E. Black[144], K.M. Black[22], D. Blackburn[139],
R.E. Blair[6], J.-B. Blanchard[137], T. Blazek[145a], I. Bloch[42], C. Blocker[23], W. Blum[82,*],

U. Blumenschein[54], G.J. Bobbink[106], V.S. Bobrovnikov[108], S.S. Bocchetta[80], A. Bocci[45],
C. Bock[99], C.R. Boddy[119], M. Boehler[48], T.T. Boek[176], J.A. Bogaerts[30], A.G. Bogdanchikov[108],
A. Bogouch[91,*], C. Bohm[147a], J. Bohm[126], V. Boisvert[76], T. Bold[38a], V. Boldea[26a],
A.S. Boldyrev[98], M. Bomben[79], M. Bona[75], M. Boonekamp[137], A. Borisov[129], G. Borissov[71],
M. Borri[83], S. Borroni[42], J. Bortfeldt[99], V. Bortolotto[135a,135b], K. Bos[106], D. Boscherini[20a],
M. Bosman[12], H. Boterenbrood[106], J. Boudreau[124], J. Bouffard[2], E.V. Bouhova-Thacker[71],
D. Boumediene[34], C. Bourdarios[116], N. Bousson[113], S. Boutouil[136d], A. Boveia[31], J. Boyd[30],
I.R. Boyko[64], J. Bracinik[18], A. Brandt[8], G. Brandt[15], O. Brandt[58a], U. Bratzler[157], B. Brau[85],
J.E. Brau[115], H.M. Braun[176,*], S.F. Brazzale[165a,165c], B. Brelier[159], K. Brendlinger[121],
A.J. Brennan[87], R. Brenner[167], S. Bressler[173], K. Bristow[146c], T.M. Bristow[46], D. Britton[53],
F.M. Brochu[28], I. Brock[21], R. Brock[89], C. Bromberg[89], J. Bronner[100], G. Brooijmans[35],
T. Brooks[76], W.K. Brooks[32b], J. Brosamer[15], E. Brost[115], J. Brown[55],
P.A. Bruckman de Renstrom[39], D. Bruncko[145b], R. Bruneliere[48], S. Brunet[60], A. Bruni[20a],
G. Bruni[20a], M. Bruschi[20a], L. Bryngemark[80], T. Buanes[14], Q. Buat[143], F. Bucci[49],
P. Buchholz[142], R.M. Buckingham[119], A.G. Buckley[53], S.I. Buda[26a], I.A. Budagov[64],
F. Buehrer[48], L. Bugge[118], M.K. Bugge[118], O. Bulekov[97], A.C. Bundock[73], H. Burckhart[30],
S. Burdin[73], B. Burghgrave[107], S. Burke[130], I. Burmeister[43], E. Busato[34], D. Büscher[48],
V. Büscher[82], P. Bussey[53], C.P. Buszello[167], B. Butler[57], J.M. Butler[22], A.I. Butt[3],
C.M. Buttar[53], J.M. Butterworth[77], P. Butti[106], W. Buttinger[28], A. Buzatu[53], M. Byszewski[10],
S. Cabrera Urbán[168], D. Caforio[20a,20b], O. Cakir[4a], P. Calafiura[15], A. Calandri[137], G. Calderini[79],
P. Calfayan[99], R. Calkins[107], L.P. Caloba[24a], D. Calvet[34], S. Calvet[34], R. Camacho Toro[49],
S. Camarda[42], D. Cameron[118], L.M. Caminada[15], R. Caminal Armadans[12], S. Campana[30],
M. Campanelli[77], A. Campoverde[149], V. Canale[103a,103b], A. Canepa[160a], M. Cano Bret[75],
J. Cantero[81], R. Cantrill[125a], T. Cao[40], M.D.M. Capeans Garrido[30], I. Caprini[26a], M. Caprini[26a],
M. Capua[37a,37b], R. Caputo[82], R. Cardarelli[134a], T. Carli[30], G. Carlino[103a], L. Carminati[90a,90b],
S. Caron[105], E. Carquin[32a], G.D. Carrillo-Montoya[146c], J.R. Carter[28], J. Carvalho[125a,125c],
D. Casadei[77], M.P. Casado[12], M. Casolino[12], E. Castaneda-Miranda[146b], A. Castelli[106],
V. Castillo Gimenez[168], N.F. Castro[125a], P. Catastini[57], A. Catinaccio[30], J.R. Catmore[118],
A. Cattai[30], G. Cattani[134a,134b], S. Caughron[89], V. Cavaliere[166], D. Cavalli[90a],
M. Cavalli-Sforza[12], V. Cavasinni[123a,123b], F. Ceradini[135a,135b], B. Cerio[45], K. Cerny[128],
A.S. Cerqueira[24b], A. Cerri[150], L. Cerrito[75], F. Cerutti[15], M. Cerv[30], A. Cervelli[17], S.A. Cetin[19b],
A. Chafaq[136a], D. Chakraborty[107], I. Chalupkova[128], P. Chang[166], B. Chapleau[86],
J.D. Chapman[28], D. Charfeddine[116], D.G. Charlton[18], C.C. Chau[159], C.A. Chavez Barajas[150],
S. Cheatham[86], A. Chegwidden[89], S. Chekanov[6], S.V. Chekulaev[160a], G.A. Chelkov[64,f],
M.A. Chelstowska[88], C. Chen[63], H. Chen[25], K. Chen[149], L. Chen[33d,g], S. Chen[33c], X. Chen[146c],
Y. Chen[66], Y. Chen[35], H.C. Cheng[88], Y. Cheng[31], A. Cheplakov[64], R. Cherkaoui El Moursli[136e],
V. Chernyatin[25,*], E. Cheu[7], L. Chevalier[137], V. Chiarella[47], G. Chiefari[103a,103b], J.T. Childers[6],
A. Chilingarov[71], G. Chiodini[72a], A.S. Chisholm[18], R.T. Chislett[77], A. Chitan[26a],
M.V. Chizhov[64], S. Chouridou[9], B.K.B. Chow[99], D. Chromek-Burckhart[30], M.L. Chu[152],
J. Chudoba[126], J.J. Chwastowski[39], L. Chytka[114], G. Ciapetti[133a,133b], A.K. Ciftci[4a], R. Ciftci[4a],
D. Cinca[53], V. Cindro[74], A. Ciocio[15], P. Cirkovic[13b], Z.H. Citron[173], M. Citterio[90a],
M. Ciubancan[26a], A. Clark[49], P.J. Clark[46], R.N. Clarke[15], W. Cleland[124], J.C. Clemens[84],
C. Clement[147a,147b], Y. Coadou[84], M. Cobal[165a,165c], A. Coccaro[139], J. Cochran[63], L. Coffey[23],
J.G. Cogan[144], J. Coggeshall[166], B. Cole[35], S. Cole[107], A.P. Colijn[106], J. Collot[55], T. Colombo[58c],
G. Colon[85], G. Compostella[100], P. Conde Muiño[125a,125b], E. Coniavitis[48], M.C. Conidi[12],
S.H. Connell[146b], I.A. Connelly[76], S.M. Consonni[90a,90b], V. Consorti[48], S. Constantinescu[26a],
C. Conta[120a,120b], G. Conti[57], F. Conventi[103a,h], M. Cooke[15], B.D. Cooper[77],
A.M. Cooper-Sarkar[119], N.J. Cooper-Smith[76], K. Copic[15], T. Cornelissen[176], M. Corradi[20a],

F. Corriveau[86,i], A. Corso-Radu[164], A. Cortes-Gonzalez[12], G. Cortiana[100], G. Costa[90a],
M.J. Costa[168], D. Costanzo[140], D. Côté[8], G. Cottin[28], G. Cowan[76], B.E. Cox[83], K. Cranmer[109],
G. Cree[29], S. Crépé-Renaudin[55], F. Crescioli[79], W.A. Cribbs[147a,147b], M. Crispin Ortuzar[119],
M. Cristinziani[21], V. Croft[105], G. Crosetti[37a,37b], C.-M. Cuciuc[26a], T. Cuhadar Donszelmann[140],
J. Cummings[177], M. Curatolo[47], C. Cuthbert[151], H. Czirr[142], P. Czodrowski[3], Z. Czyczula[177],
S. D'Auria[53], M. D'Onofrio[73], M.J. Da Cunha Sargedas De Sousa[125a,125b], C. Da Via[83],
W. Dabrowski[38a], A. Dafinca[119], T. Dai[88], O. Dale[14], F. Dallaire[94], C. Dallapiccola[85], M. Dam[36],
A.C. Daniells[18], M. Dano Hoffmann[137], V. Dao[48], G. Darbo[50a], S. Darmora[8], J.A. Dassoulas[42],
A. Dattagupta[60], W. Davey[21], C. David[170], T. Davidek[128], E. Davies[119,c], M. Davies[154],
O. Davignon[79], A.R. Davison[77], P. Davison[77], Y. Davygora[58a], E. Dawe[143], I. Dawson[140],
R.K. Daya-Ishmukhametova[85], K. De[8], R. de Asmundis[103a], S. De Castro[20a,20b], S. De Cecco[79],
N. De Groot[105], P. de Jong[106], H. De la Torre[81], F. De Lorenzi[63], L. De Nooij[106], D. De Pedis[133a],
A. De Salvo[133a], U. De Sanctis[165a,165b], A. De Santo[150], J.B. De Vivie De Regie[116],
W.J. Dearnaley[71], R. Debbe[25], C. Debenedetti[138], B. Dechenaux[55], D.V. Dedovich[64],
I. Deigaard[106], J. Del Peso[81], T. Del Prete[123a,123b], F. Deliot[137], C.M. Delitzsch[49],
M. Deliyergiyev[74], A. Dell'Acqua[30], L. Dell'Asta[22], M. Dell'Orso[123a,123b], M. Della Pietra[103a,h],
D. della Volpe[49], M. Delmastro[5], P.A. Delsart[55], C. Deluca[106], S. Demers[177], M. Demichev[64],
A. Demilly[79], S.P. Denisov[129], D. Derendarz[39], J.E. Derkaoui[136d], F. Derue[79], P. Dervan[73],
K. Desch[21], C. Deterre[42], P.O. Deviveiros[106], A. Dewhurst[130], S. Dhaliwal[106],
A. Di Ciaccio[134a,134b], L. Di Ciaccio[5], A. Di Domenico[133a,133b], C. Di Donato[103a,103b],
A. Di Girolamo[30], B. Di Girolamo[30], A. Di Mattia[153], B. Di Micco[135a,135b], R. Di Nardo[47],
A. Di Simone[48], R. Di Sipio[20a,20b], D. Di Valentino[29], F.A. Dias[46], M.A. Diaz[32a], E.B. Diehl[88],
J. Dietrich[42], T.A. Dietzsch[58a], S. Diglio[84], A. Dimitrievska[13a], J. Dingfelder[21],
C. Dionisi[133a,133b], P. Dita[26a], S. Dita[26a], F. Dittus[30], F. Djama[84], T. Djobava[51b],
M.A.B. do Vale[24c], A. Do Valle Wemans[125a,125g], T.K.O. Doan[5], D. Dobos[30], C. Doglioni[49],
T. Doherty[53], T. Dohmae[156], J. Dolejsi[128], Z. Dolezal[128], B.A. Dolgoshein[97,*], M. Donadelli[24d],
S. Donati[123a,123b], P. Dondero[120a,120b], J. Donini[34], J. Dopke[130], A. Doria[103a], M.T. Dova[70],
A.T. Doyle[53], M. Dris[10], J. Dubbert[88], J. Dube[15], E. Dubreuil[34], E. Duchovni[173], G. Duckeck[99],
O.A. Ducu[26a], D. Duda[176], A. Dudarev[30], F. Dudziak[63], L. Duflot[116], L. Duguid[76],
M. Dührssen[30], M. Dunford[58a], H. Duran Yildiz[4a], M. Düren[52], A. Durglishvili[51b],
M. Dwuznik[38a], M. Dyndal[38a], J. Ebke[99], W. Edson[2], N.C. Edwards[46], W. Ehrenfeld[21],
T. Eifert[144], G. Eigen[14], K. Einsweiler[15], T. Ekelof[167], M. El Kacimi[136c], M. Ellert[167], S. Elles[5],
F. Ellinghaus[82], N. Ellis[30], J. Elmsheuser[99], M. Elsing[30], D. Emeliyanov[130], Y. Enari[156],
O.C. Endner[82], M. Endo[117], R. Engelmann[149], J. Erdmann[177], A. Ereditato[17], D. Eriksson[147a],
G. Ernis[176], J. Ernst[2], M. Ernst[25], J. Ernwein[137], D. Errede[166], S. Errede[166], E. Ertel[82],
M. Escalier[116], H. Esch[43], C. Escobar[124], B. Esposito[47], A.I. Etienvre[137], E. Etzion[154],
H. Evans[60], A. Ezhilov[122], L. Fabbri[20a,20b], G. Facini[31], R.M. Fakhrutdinov[129], S. Falciano[133a],
R.J. Falla[77], J. Faltova[128], Y. Fang[33a], M. Fanti[90a,90b], A. Farbin[8], A. Farilla[135a], T. Farooque[12],
S. Farrell[15], S.M. Farrington[171], P. Farthouat[30], F. Fassi[136e], P. Fassnacht[30], D. Fassouliotis[9],
A. Favareto[50a,50b], L. Fayard[116], P. Federic[145a], O.L. Fedin[122,j], W. Fedorko[169],
M. Fehling-Kaschek[48], S. Feigl[30], L. Feligioni[84], C. Feng[33d], E.J. Feng[6], H. Feng[88],
A.B. Fenyuk[129], S. Fernandez Perez[30], S. Ferrag[53], J. Ferrando[53], A. Ferrari[167], P. Ferrari[106],
R. Ferrari[120a], D.E. Ferreira de Lima[53], A. Ferrer[168], D. Ferrere[49], C. Ferretti[88],
A. Ferretto Parodi[50a,50b], M. Fiascaris[31], F. Fiedler[82], A. Filipčič[74], M. Filipuzzi[42], F. Filthaut[105],
M. Fincke-Keeler[170], K.D. Finelli[151], M.C.N. Fiolhais[125a,125c], L. Fiorini[168], A. Firan[40],
A. Fischer[2], J. Fischer[176], W.C. Fisher[89], E.A. Fitzgerald[23], M. Flechl[48], I. Fleck[142],
P. Fleischmann[88], S. Fleischmann[176], G.T. Fletcher[140], G. Fletcher[75], T. Flick[176], A. Floderus[80],
L.R. Flores Castillo[174,k], A.C. Florez Bustos[160b], M.J. Flowerdew[100], A. Formica[137], A. Forti[83],

D. Fortin[160a], D. Fournier[116], H. Fox[71], S. Fracchia[12], P. Francavilla[79], M. Franchini[20a,20b],
S. Franchino[30], D. Francis[30], L. Franconi[118], M. Franklin[57], S. Franz[61], M. Fraternali[120a,120b],
S.T. French[28], C. Friedrich[42], F. Friedrich[44], D. Froidevaux[30], J.A. Frost[28], C. Fukunaga[157],
E. Fullana Torregrosa[82], B.G. Fulsom[144], J. Fuster[168], C. Gabaldon[55], O. Gabizon[173],
A. Gabrielli[20a,20b], A. Gabrielli[133a,133b], S. Gadatsch[106], S. Gadomski[49], G. Gagliardi[50a,50b],
P. Gagnon[60], C. Galea[105], B. Galhardo[125a,125c], E.J. Gallas[119], V. Gallo[17], B.J. Gallop[130],
P. Gallus[127], G. Galster[36], K.K. Gan[110], J. Gao[33b,g], Y.S. Gao[144,e], F.M. Garay Walls[46],
F. Garberson[177], C. García[168], J.E. García Navarro[168], M. Garcia-Sciveres[15], R.W. Gardner[31],
N. Garelli[144], V. Garonne[30], C. Gatti[47], G. Gaudio[120a], B. Gaur[142], L. Gauthier[94],
P. Gauzzi[133a,133b], I.L. Gavrilenko[95], C. Gay[169], G. Gaycken[21], E.N. Gazis[10], P. Ge[33d],
Z. Gecse[169], C.N.P. Gee[130], D.A.A. Geerts[106], Ch. Geich-Gimbel[21], K. Gellerstedt[147a,147b],
C. Gemme[50a], A. Gemmell[53], M.H. Genest[55], S. Gentile[133a,133b], M. George[54], S. George[76],
D. Gerbaudo[164], A. Gershon[154], H. Ghazlane[136b], N. Ghodbane[34], B. Giacobbe[20a],
S. Giagu[133a,133b], V. Giangiobbe[12], P. Giannetti[123a,123b], F. Gianotti[30], B. Gibbard[25],
S.M. Gibson[76], M. Gilchriese[15], T.P.S. Gillam[28], D. Gillberg[30], G. Gilles[34], D.M. Gingrich[3,d],
N. Giokaris[9], M.P. Giordani[165a,165c], R. Giordano[103a,103b], F.M. Giorgi[20a], F.M. Giorgi[16],
P.F. Giraud[137], D. Giugni[90a], C. Giuliani[48], M. Giulini[58b], B.K. Gjelsten[118], S. Gkaitatzis[155],
I. Gkialas[155,l], L.K. Gladilin[98], C. Glasman[81], J. Glatzer[30], P.C.F. Glaysher[46], A. Glazov[42],
G.L. Glonti[64], M. Goblirsch-Kolb[100], J.R. Goddard[75], J. Godfrey[143], J. Godlewski[30],
C. Goeringer[82], S. Goldfarb[88], T. Golling[177], D. Golubkov[129], A. Gomes[125a,125b,125d],
L.S. Gomez Fajardo[42], R. Gonçalo[125a], J. Goncalves Pinto Firmino Da Costa[137], L. Gonella[21],
S. González de la Hoz[168], G. Gonzalez Parra[12], S. Gonzalez-Sevilla[49], L. Goossens[30],
P.A. Gorbounov[96], H.A. Gordon[25], I. Gorelov[104], B. Gorini[30], E. Gorini[72a,72b], A. Gorišek[74],
E. Gornicki[39], A.T. Goshaw[6], C. Gössling[43], M.I. Gostkin[64], M. Gouighri[136a], D. Goujdami[136c],
M.P. Goulette[49], A.G. Goussiou[139], C. Goy[5], S. Gozpinar[23], H.M.X. Grabas[137], L. Graber[54],
I. Grabowska-Bold[38a], P. Grafström[20a,20b], K-J. Grahn[42], J. Gramling[49], E. Gramstad[118],
S. Grancagnolo[16], V. Grassi[149], V. Gratchev[122], H.M. Gray[30], E. Graziani[135a],
O.G. Grebenyuk[122], Z.D. Greenwood[78,m], K. Gregersen[77], I.M. Gregor[42], P. Grenier[144],
J. Griffiths[8], A.A. Grillo[138], K. Grimm[71], S. Grinstein[12,n], Ph. Gris[34], Y.V. Grishkevich[98],
J.-F. Grivaz[116], J.P. Grohs[44], A. Grohsjean[42], E. Gross[173], J. Grosse-Knetter[54],
G.C. Grossi[134a,134b], J. Groth-Jensen[173], Z.J. Grout[150], L. Guan[33b], F. Guescini[49], D. Guest[177],
O. Gueta[154], C. Guicheney[34], E. Guido[50a,50b], T. Guillemin[116], S. Guindon[2], U. Gul[53],
C. Gumpert[44], J. Gunther[127], J. Guo[35], S. Gupta[119], P. Gutierrez[112], N.G. Gutierrez Ortiz[53],
C. Gutschow[77], N. Guttman[154], C. Guyot[137], C. Gwenlan[119], C.B. Gwilliam[73], A. Haas[109],
C. Haber[15], H.K. Hadavand[8], N. Haddad[136e], P. Haefner[21], S. Hageböck[21], Z. Hajduk[39],
H. Hakobyan[178], M. Haleem[42], D. Hall[119], G. Halladjian[89], K. Hamacher[176], P. Hamal[114],
K. Hamano[170], M. Hamer[54], A. Hamilton[146a], S. Hamilton[162], G.N. Hamity[146c], P.G. Hamnett[42],
L. Han[33b], K. Hanagaki[117], K. Hanawa[156], M. Hance[15], P. Hanke[58a], R. Hanna[137], J.B. Hansen[36],
J.D. Hansen[36], P.H. Hansen[36], K. Hara[161], A.S. Hard[174], T. Harenberg[176], F. Hariri[116],
S. Harkusha[91], D. Harper[88], R.D. Harrington[46], O.M. Harris[139], P.F. Harrison[171], F. Hartjes[106],
M. Hasegawa[66], S. Hasegawa[102], Y. Hasegawa[141], A. Hasib[112], S. Hassani[137], S. Haug[17],
M. Hauschild[30], R. Hauser[89], M. Havranek[126], C.M. Hawkes[18], R.J. Hawkings[30], A.D. Hawkins[80],
T. Hayashi[161], D. Hayden[89], C.P. Hays[119], H.S. Hayward[73], S.J. Haywood[130], S.J. Head[18],
T. Heck[82], V. Hedberg[80], L. Heelan[8], S. Heim[121], T. Heim[176], B. Heinemann[15], L. Heinrich[109],
J. Hejbal[126], L. Helary[22], C. Heller[99], M. Heller[30], S. Hellman[147a,147b], D. Hellmich[21],
C. Helsens[30], J. Henderson[119], R.C.W. Henderson[71], Y. Heng[174], C. Hengler[42], A. Henrichs[177],
A.M. Henriques Correia[30], S. Henrot-Versille[116], C. Hensel[54], G.H. Herbert[16],
Y. Hernández Jiménez[168], R. Herrberg-Schubert[16], G. Herten[48], R. Hertenberger[99], L. Hervas[30],

G.G. Hesketh[77], N.P. Hessey[106], R. Hickling[75], E. Higón-Rodriguez[168], E. Hill[170], J.C. Hill[28],
K.H. Hiller[42], S. Hillert[21], S.J. Hillier[18], I. Hinchliffe[15], E. Hines[121], M. Hirose[158],
D. Hirschbuehl[176], J. Hobbs[149], N. Hod[106], M.C. Hodgkinson[140], P. Hodgson[140], A. Hoecker[30],
M.R. Hoeferkamp[104], F. Hoenig[99], J. Hoffman[40], D. Hoffmann[84], J.I. Hofmann[58a], M. Hohlfeld[82],
T.R. Holmes[15], T.M. Hong[121], L. Hooft van Huysduynen[109], Y. Horii[102], J-Y. Hostachy[55],
S. Hou[152], A. Hoummada[136a], J. Howard[119], J. Howarth[42], M. Hrabovsky[114], I. Hristova[16],
J. Hrivnac[116], T. Hryn'ova[5], C. Hsu[146c], P.J. Hsu[82], S.-C. Hsu[139], D. Hu[35], X. Hu[25], Y. Huang[42],
Z. Hubacek[30], F. Hubaut[84], F. Huegging[21], T.B. Huffman[119], E.W. Hughes[35], G. Hughes[71],
M. Huhtinen[30], T.A. Hülsing[82], M. Hurwitz[15], N. Huseynov[64,b], J. Huston[89], J. Huth[57],
G. Iacobucci[49], G. Iakovidis[10], I. Ibragimov[142], L. Iconomidou-Fayard[116], E. Ideal[177], P. Iengo[103a],
O. Igonkina[106], T. Iizawa[172], Y. Ikegami[65], K. Ikematsu[142], M. Ikeno[65], Y. Ilchenko[31,o],
D. Iliadis[155], N. Ilic[159], Y. Inamaru[66], T. Ince[100], P. Ioannou[9], M. Iodice[135a], K. Iordanidou[9],
V. Ippolito[57], A. Irles Quiles[168], C. Isaksson[167], M. Ishino[67], M. Ishitsuka[158],
R. Ishmukhametov[110], C. Issever[119], S. Istin[19a], J.M. Iturbe Ponce[83], R. Iuppa[134a,134b],
J. Ivarsson[80], W. Iwanski[39], H. Iwasaki[65], J.M. Izen[41], V. Izzo[103a], B. Jackson[121], M. Jackson[73],
P. Jackson[1], M.R. Jaekel[30], V. Jain[2], K. Jakobs[48], S. Jakobsen[30], T. Jakoubek[126], J. Jakubek[127],
D.O. Jamin[152], D.K. Jana[78], E. Jansen[77], H. Jansen[30], J. Janssen[21], M. Janus[171], G. Jarlskog[80],
N. Javadov[64,b], T. Javůrek[48], L. Jeanty[15], J. Jejelava[51a,p], G.-Y. Jeng[151], D. Jennens[87],
P. Jenni[48,q], J. Jentzsch[43], C. Jeske[171], S. Jézéquel[5], H. Ji[174], J. Jia[149], Y. Jiang[33b],
M. Jimenez Belenguer[42], S. Jin[33a], A. Jinaru[26a], O. Jinnouchi[158], M.D. Joergensen[36],
K.E. Johansson[147a,147b], P. Johansson[140], K.A. Johns[7], K. Jon-And[147a,147b], G. Jones[171],
R.W.L. Jones[71], T.J. Jones[73], J. Jongmanns[58a], P.M. Jorge[125a,125b], K.D. Joshi[83], J. Jovicevic[148],
X. Ju[174], C.A. Jung[43], R.M. Jungst[30], P. Jussel[61], A. Juste Rozas[12,n], M. Kaci[168],
A. Kaczmarska[39], M. Kado[116], H. Kagan[110], M. Kagan[144], E. Kajomovitz[45], C.W. Kalderon[119],
S. Kama[40], A. Kamenshchikov[129], N. Kanaya[156], M. Kaneda[30], S. Kaneti[28], V.A. Kantserov[97],
J. Kanzaki[65], B. Kaplan[109], A. Kapliy[31], D. Kar[53], K. Karakostas[10], N. Karastathis[10],
M. Karnevskiy[82], S.N. Karpov[64], Z.M. Karpova[64], K. Karthik[109], V. Kartvelishvili[71],
A.N. Karyukhin[129], L. Kashif[174], G. Kasieczka[58b], R.D. Kass[110], A. Kastanas[14], Y. Kataoka[156],
A. Katre[49], J. Katzy[42], V. Kaushik[7], K. Kawagoe[69], T. Kawamoto[156], G. Kawamura[54],
S. Kazama[156], V.F. Kazanin[108], M.Y. Kazarinov[64], R. Keeler[170], R. Kehoe[40], M. Keil[54],
J.S. Keller[42], J.J. Kempster[76], H. Keoshkerian[5], O. Kepka[126], B.P. Kerševan[74], S. Kersten[176],
K. Kessoku[156], J. Keung[159], F. Khalil-zada[11], H. Khandanyan[147a,147b], A. Khanov[113],
A. Khodinov[97], A. Khomich[58a], T.J. Khoo[28], G. Khoriauli[21], A. Khoroshilov[176], V. Khovanskiy[96],
E. Khramov[64], J. Khubua[51b], H.Y. Kim[8], H. Kim[147a,147b], S.H. Kim[161], N. Kimura[172], O. Kind[16],
B.T. King[73], M. King[168], R.S.B. King[119], S.B. King[169], J. Kirk[130], A.E. Kiryunin[100],
T. Kishimoto[66], D. Kisielewska[38a], F. Kiss[48], T. Kittelmann[124], K. Kiuchi[161], E. Kladiva[145b],
M. Klein[73], U. Klein[73], K. Kleinknecht[82], P. Klimek[147a,147b], A. Klimentov[25], R. Klingenberg[43],
J.A. Klinger[83], T. Klioutchnikova[30], P.F. Klok[105], E.-E. Kluge[58a], P. Kluit[106], S. Kluth[100],
E. Kneringer[61], E.B.F.G. Knoops[84], A. Knue[53], D. Kobayashi[158], T. Kobayashi[156], M. Kobel[44],
M. Kocian[144], P. Kodys[128], P. Koevesarki[21], T. Koffas[29], E. Koffeman[106], L.A. Kogan[119],
S. Kohlmann[176], Z. Kohout[127], T. Kohriki[65], T. Koi[144], H. Kolanoski[16], I. Koletsou[5], J. Koll[89],
A.A. Komar[95,*], Y. Komori[156], T. Kondo[65], N. Kondrashova[42], K. Köneke[48], A.C. König[105],
S. König[82], T. Kono[65,r], R. Konoplich[109,s], N. Konstantinidis[77], R. Kopeliansky[153],
S. Koperny[38a], L. Köpke[82], A.K. Kopp[48], K. Korcyl[39], K. Kordas[155], A. Korn[77], A.A. Korol[108,t],
I. Korolkov[12], E.V. Korolkova[140], V.A. Korotkov[129], O. Kortner[100], S. Kortner[100],
V.V. Kostyukhin[21], V.M. Kotov[64], A. Kotwal[45], C. Kourkoumelis[9], V. Kouskoura[155],
A. Koutsman[160a], R. Kowalewski[170], T.Z. Kowalski[38a], W. Kozanecki[137], A.S. Kozhin[129],
V. Kral[127], V.A. Kramarenko[98], G. Kramberger[74], D. Krasnopevtsev[97], M.W. Krasny[79],

A. Krasznahorkay[30], J.K. Kraus[21], A. Kravchenko[25], S. Kreiss[109], M. Kretz[58c], J. Kretzschmar[73], K. Kreutzfeldt[52], P. Krieger[159], K. Kroeninger[54], H. Kroha[100], J. Kroll[121], J. Kroseberg[21], J. Krstic[13a], U. Kruchonak[64], H. Krüger[21], T. Kruker[17], N. Krumnack[63], Z.V. Krumshteyn[64], A. Kruse[174], M.C. Kruse[45], M. Kruskal[22], T. Kubota[87], S. Kuday[4a], S. Kuehn[48], A. Kugel[58c], A. Kuhl[138], T. Kuhl[42], V. Kukhtin[64], Y. Kulchitsky[91], S. Kuleshov[32b], M. Kuna[133a,133b], J. Kunkle[121], A. Kupco[126], H. Kurashige[66], Y.A. Kurochkin[91], R. Kurumida[66], V. Kus[126], E.S. Kuwertz[148], M. Kuze[158], J. Kvita[114], A. La Rosa[49], L. La Rotonda[37a,37b], C. Lacasta[168], F. Lacava[133a,133b], J. Lacey[29], H. Lacker[16], D. Lacour[79], V.R. Lacuesta[168], E. Ladygin[64], R. Lafaye[5], B. Laforge[79], T. Lagouri[177], S. Lai[48], H. Laier[58a], L. Lambourne[77], S. Lammers[60], C.L. Lampen[7], W. Lampl[7], E. Lançon[137], U. Landgraf[48], M.P.J. Landon[75], V.S. Lang[58a], A.J. Lankford[164], F. Lanni[25], K. Lantzsch[30], S. Laplace[79], C. Lapoire[21], J.F. Laporte[137], T. Lari[90a], M. Lassnig[30], P. Laurelli[47], W. Lavrijsen[15], A.T. Law[138], P. Laycock[73], O. Le Dortz[79], E. Le Guirriec[84], E. Le Menedeu[12], T. LeCompte[6], F. Ledroit-Guillon[55], C.A. Lee[152], H. Lee[106], J.S.H. Lee[117], S.C. Lee[152], L. Lee[1], G. Lefebvre[79], M. Lefebvre[170], F. Legger[99], C. Leggett[15], A. Lehan[73], M. Lehmacher[21], G. Lehmann Miotto[30], X. Lei[7], W.A. Leight[29], A. Leisos[155], A.G. Leister[177], M.A.L. Leite[24d], R. Leitner[128], D. Lellouch[173], B. Lemmer[54], K.J.C. Leney[77], T. Lenz[21], G. Lenzen[176], B. Lenzi[30], R. Leone[7], S. Leone[123a,123b], K. Leonhardt[44], C. Leonidopoulos[46], S. Leontsinis[10], C. Leroy[94], C.G. Lester[28], C.M. Lester[121], M. Levchenko[122], J. Levêque[5], D. Levin[88], L.J. Levinson[173], M. Levy[18], A. Lewis[119], G.H. Lewis[109], A.M. Leyko[21], M. Leyton[41], B. Li[33b,u], B. Li[84], H. Li[149], H.L. Li[31], L. Li[45], L. Li[33e], S. Li[45], Y. Li[33c,v], Z. Liang[138], H. Liao[34], B. Liberti[134a], P. Lichard[30], K. Lie[166], J. Liebal[21], W. Liebig[14], C. Limbach[21], A. Limosani[87], S.C. Lin[152,w], T.H. Lin[82], F. Linde[106], B.E. Lindquist[149], J.T. Linnemann[89], E. Lipeles[121], A. Lipniacka[14], M. Lisovyi[42], T.M. Liss[166], D. Lissauer[25], A. Lister[169], A.M. Litke[138], B. Liu[152], D. Liu[152], J.B. Liu[33b], K. Liu[33b,x], L. Liu[88], M. Liu[45], M. Liu[33b], Y. Liu[33b], M. Livan[120a,120b], S.S.A. Livermore[119], A. Lleres[55], J. Llorente Merino[81], S.L. Lloyd[75], F. Lo Sterzo[152], E. Lobodzinska[42], P. Loch[7], W.S. Lockman[138], T. Loddenkoetter[21], F.K. Loebinger[83], A.E. Loevschall-Jensen[36], A. Loginov[177], T. Lohse[16], K. Lohwasser[42], M. Lokajicek[126], V.P. Lombardo[5], B.A. Long[22], J.D. Long[88], R.E. Long[71], L. Lopes[125a], D. Lopez Mateos[57], B. Lopez Paredes[140], I. Lopez Paz[12], J. Lorenz[99], N. Lorenzo Martinez[60], M. Losada[163], P. Loscutoff[15], X. Lou[41], A. Lounis[116], J. Love[6], P.A. Love[71], A.J. Lowe[144,e], F. Lu[33a], N. Lu[88], H.J. Lubatti[139], C. Luci[133a,133b], A. Lucotte[55], F. Luehring[60], W. Lukas[61], L. Luminari[133a], O. Lundberg[147a,147b], B. Lund-Jensen[148], M. Lungwitz[82], D. Lynn[25], R. Lysak[126], E. Lytken[80], H. Ma[25], L.L. Ma[33d], G. Maccarrone[47], A. Macchiolo[100], J. Machado Miguens[125a,125b], D. Macina[30], D. Madaffari[84], R. Madar[48], H.J. Maddocks[71], W.F. Mader[44], A. Madsen[167], M. Maeno[8], T. Maeno[25], E. Magradze[54], K. Mahboubi[48], J. Mahlstedt[106], S. Mahmoud[73], C. Maiani[137], C. Maidantchik[24a], A.A. Maier[100], A. Maio[125a,125b,125d], S. Majewski[115], Y. Makida[65], N. Makovec[116], P. Mal[137,y], B. Malaescu[79], Pa. Malecki[39], V.P. Maleev[122], F. Malek[55], U. Mallik[62], D. Malon[6], C. Malone[144], S. Maltezos[10], V.M. Malyshev[108], S. Malyukov[30], J. Mamuzic[13b], B. Mandelli[30], L. Mandelli[90a], I. Mandić[74], R. Mandrysch[62], J. Maneira[125a,125b], A. Manfredini[100], L. Manhaes de Andrade Filho[24b], J.A. Manjarres Ramos[160b], A. Mann[99], P.M. Manning[138], A. Manousakis-Katsikakis[9], B. Mansoulie[137], R. Mantifel[86], L. Mapelli[30], L. March[168], J.F. Marchand[29], G. Marchiori[79], M. Marcisovsky[126], C.P. Marino[170], M. Marjanovic[13a], C.N. Marques[125a], F. Marroquim[24a], S.P. Marsden[83], Z. Marshall[15], L.F. Marti[17], S. Marti-Garcia[168], B. Martin[30], B. Martin[89], T.A. Martin[171], V.J. Martin[46], B. Martin dit Latour[14], H. Martinez[137], M. Martinez[12,n], S. Martin-Haugh[130], A.C. Martyniuk[77], M. Marx[139], F. Marzano[133a], A. Marzin[30], L. Masetti[82], T. Mashimo[156], R. Mashinistov[95], J. Masik[83], A.L. Maslennikov[108], I. Massa[20a,20b], L. Massa[20a,20b], N. Massol[5], P. Mastrandrea[149], A. Mastroberardino[37a,37b], T. Masubuchi[156],

P. Mättig[176], J. Mattmann[82], J. Maurer[26a], S.J. Maxfield[73], D.A. Maximov[108,t], R. Mazini[152],
L. Mazzaferro[134a,134b], G. Mc Goldrick[159], S.P. Mc Kee[88], A. McCarn[88], R.L. McCarthy[149],
T.G. McCarthy[29], N.A. McCubbin[130], K.W. McFarlane[56,*], J.A. Mcfayden[77], G. Mchedlidze[54],
S.J. McMahon[130], R.A. McPherson[170,i], A. Meade[85], J. Mechnich[106], M. Medinnis[42],
S. Meehan[31], S. Mehlhase[99], A. Mehta[73], K. Meier[58a], C. Meineck[99], B. Meirose[80],
C. Melachrinos[31], B.R. Mellado Garcia[146c], F. Meloni[17], A. Mengarelli[20a,20b], S. Menke[100],
E. Meoni[162], K.M. Mercurio[57], S. Mergelmeyer[21], N. Meric[137], P. Mermod[49], L. Merola[103a,103b],
C. Meroni[90a], F.S. Merritt[31], H. Merritt[110], A. Messina[30,z], J. Metcalfe[25], A.S. Mete[164],
C. Meyer[82], C. Meyer[121], J-P. Meyer[137], J. Meyer[30], R.P. Middleton[130], S. Migas[73], L. Mijović[21],
G. Mikenberg[173], M. Mikestikova[126], M. Mikuž[74], A. Milic[30], D.W. Miller[31], C. Mills[46],
A. Milov[173], D.A. Milstead[147a,147b], D. Milstein[173], A.A. Minaenko[129], I.A. Minashvili[64],
A.I. Mincer[109], B. Mindur[38a], M. Mineev[64], Y. Ming[174], L.M. Mir[12], G. Mirabelli[133a],
T. Mitani[172], J. Mitrevski[99], V.A. Mitsou[168], S. Mitsui[65], A. Miucci[49], P.S. Miyagawa[140],
J.U. Mjörnmark[80], T. Moa[147a,147b], K. Mochizuki[84], S. Mohapatra[35], W. Mohr[48],
S. Molander[147a,147b], R. Moles-Valls[168], K. Mönig[42], C. Monini[55], J. Monk[36], E. Monnier[84],
J. Montejo Berlingen[12], F. Monticelli[70], S. Monzani[133a,133b], R.W. Moore[3], N. Morange[62],
D. Moreno[82], M. Moreno Llácer[54], P. Morettini[50a], M. Morgenstern[44], M. Morii[57], S. Moritz[82],
A.K. Morley[148], G. Mornacchi[30], J.D. Morris[75], L. Morvaj[102], H.G. Moser[100], M. Mosidze[51b],
J. Moss[110], K. Motohashi[158], R. Mount[144], E. Mountricha[25], S.V. Mouraviev[95,*], E.J.W. Moyse[85],
S. Muanza[84], R.D. Mudd[18], F. Mueller[58a], J. Mueller[124], K. Mueller[21], T. Mueller[28],
T. Mueller[82], D. Muenstermann[49], Y. Munwes[154], J.A. Murillo Quijada[18], W.J. Murray[171,130],
H. Musheghyan[54], E. Musto[153], A.G. Myagkov[129,aa], M. Myska[127], O. Nackenhorst[54], J. Nadal[54],
K. Nagai[61], R. Nagai[158], Y. Nagai[84], K. Nagano[65], A. Nagarkar[110], Y. Nagasaka[59], M. Nagel[100],
A.M. Nairz[30], Y. Nakahama[30], K. Nakamura[65], T. Nakamura[156], I. Nakano[111],
H. Namasivayam[41], G. Nanava[21], R. Narayan[58b], T. Nattermann[21], T. Naumann[42],
G. Navarro[163], R. Nayyar[7], H.A. Neal[88], P.Yu. Nechaeva[95], T.J. Neep[83], P.D. Nef[144],
A. Negri[120a,120b], G. Negri[30], M. Negrini[20a], S. Nektarijevic[49], A. Nelson[164], T.K. Nelson[144],
S. Nemecek[126], P. Nemethy[109], A.A. Nepomuceno[24a], M. Nessi[30,ab], M.S. Neubauer[166],
M. Neumann[176], R.M. Neves[109], P. Nevski[25], P.R. Newman[18], D.H. Nguyen[6], R.B. Nickerson[119],
R. Nicolaidou[137], B. Nicquevert[30], J. Nielsen[138], N. Nikiforou[35], A. Nikiforov[16],
V. Nikolaenko[129,aa], I. Nikolic-Audit[79], K. Nikolics[49], K. Nikolopoulos[18], P. Nilsson[8],
Y. Ninomiya[156], A. Nisati[133a], R. Nisius[100], T. Nobe[158], L. Nodulman[6], M. Nomachi[117],
I. Nomidis[29], S. Norberg[112], M. Nordberg[30], O. Novgorodova[44], S. Nowak[100], M. Nozaki[65],
L. Nozka[114], K. Ntekas[10], G. Nunes Hanninger[87], T. Nunnemann[99], E. Nurse[77], F. Nuti[87],
B.J. O'Brien[46], F. O'grady[7], D.C. O'Neil[143], V. O'Shea[53], F.G. Oakham[29,d], H. Oberlack[100],
T. Obermann[21], J. Ocariz[79], A. Ochi[66], M.I. Ochoa[77], S. Oda[69], S. Odaka[65], H. Ogren[60], A. Oh[83],
S.H. Oh[45], C.C. Ohm[15], H. Ohman[167], W. Okamura[117], H. Okawa[25], Y. Okumura[31],
T. Okuyama[156], A. Olariu[26a], A.G. Olchevski[64], S.A. Olivares Pino[46], D. Oliveira Damazio[25],
E. Oliver Garcia[168], A. Olszewski[39], J. Olszowska[39], A. Onofre[125a,125e], P.U.E. Onyisi[31,o],
C.J. Oram[160a], M.J. Oreglia[31], Y. Oren[154], D. Orestano[135a,135b], N. Orlando[72a,72b],
C. Oropeza Barrera[53], R.S. Orr[159], B. Osculati[50a,50b], R. Ospanov[121], G. Otero y Garzon[27],
H. Otono[69], M. Ouchrif[136d], E.A. Ouellette[170], F. Ould-Saada[118], A. Ouraou[137],
K.P. Oussoren[106], Q. Ouyang[33a], A. Ovcharova[15], M. Owen[83], V.E. Ozcan[19a], N. Ozturk[8],
K. Pachal[119], A. Pacheco Pages[12], C. Padilla Aranda[12], M. Pagáčová[48], S. Pagan Griso[15],
E. Paganis[140], C. Pahl[100], F. Paige[25], P. Pais[85], K. Pajchel[118], G. Palacino[160b], S. Palestini[30],
M. Palka[38b], D. Pallin[34], A. Palma[125a,125b], J.D. Palmer[18], Y.B. Pan[174], E. Panagiotopoulou[10],
J.G. Panduro Vazquez[76], P. Pani[106], N. Panikashvili[88], S. Panitkin[25], D. Pantea[26a],
L. Paolozzi[134a,134b], Th.D. Papadopoulou[10], K. Papageorgiou[155,l], A. Paramonov[6],

D. Paredes Hernandez[34], M.A. Parker[28], F. Parodi[50a,50b], J.A. Parsons[35], U. Parzefall[48],
E. Pasqualucci[133a], S. Passaggio[50a], A. Passeri[135a], F. Pastore[135a,135b,*], Fr. Pastore[76],
G. Pásztor[29], S. Pataraia[176], N.D. Patel[151], J.R. Pater[83], S. Patricelli[103a,103b], T. Pauly[30],
J. Pearce[170], L.E. Pedersen[36], M. Pedersen[118], S. Pedraza Lopez[168], R. Pedro[125a,125b],
S.V. Peleganchuk[108], D. Pelikan[167], H. Peng[33b], B. Penning[31], J. Penwell[60], D.V. Perepelitsa[25],
E. Perez Codina[160a], M.T. Pérez García-Estañ[168], V. Perez Reale[35], L. Perini[90a,90b],
H. Pernegger[30], R. Perrino[72a], R. Peschke[42], V.D. Peshekhonov[64], K. Peters[30], R.F.Y. Peters[83],
B.A. Petersen[30], T.C. Petersen[36], E. Petit[42], A. Petridis[147a,147b], C. Petridou[155], E. Petrolo[133a],
F. Petrucci[135a,135b], N.E. Pettersson[158], R. Pezoa[32b], P.W. Phillips[130], G. Piacquadio[144],
E. Pianori[171], A. Picazio[49], E. Piccaro[75], M. Piccinini[20a,20b], R. Piegaia[27], D.T. Pignotti[110],
J.E. Pilcher[31], A.D. Pilkington[77], J. Pina[125a,125b,125d], M. Pinamonti[165a,165c,ac], A. Pinder[119],
J.L. Pinfold[3], A. Pingel[36], B. Pinto[125a], S. Pires[79], M. Pitt[173], C. Pizio[90a,90b], L. Plazak[145a],
M.-A. Pleier[25], V. Pleskot[128], E. Plotnikova[64], P. Plucinski[147a,147b], S. Poddar[58a], F. Podlyski[34],
R. Poettgen[82], L. Poggioli[116], D. Pohl[21], M. Pohl[49], G. Polesello[120a], A. Policicchio[37a,37b],
R. Polifka[159], A. Polini[20a], C.S. Pollard[45], V. Polychronakos[25], K. Pommès[30], L. Pontecorvo[133a],
B.G. Pope[89], G.A. Popeneciu[26b], D.S. Popovic[13a], A. Poppleton[30], X. Portell Bueso[12],
S. Pospisil[127], K. Potamianos[15], I.N. Potrap[64], C.J. Potter[150], C.T. Potter[115], G. Poulard[30],
J. Poveda[60], V. Pozdnyakov[64], P. Pralavorio[84], A. Pranko[15], S. Prasad[30], R. Pravahan[8],
S. Prell[63], D. Price[83], J. Price[73], L.E. Price[6], D. Prieur[124], M. Primavera[72a], M. Proissl[46],
K. Prokofiev[47], F. Prokoshin[32b], E. Protopapadaki[137], S. Protopopescu[25], J. Proudfoot[6],
M. Przybycien[38a], H. Przysiezniak[5], E. Ptacek[115], D. Puddu[135a,135b], E. Pueschel[85], D. Puldon[149],
M. Purohit[25,ad], P. Puzo[116], J. Qian[88], G. Qin[53], Y. Qin[83], A. Quadt[54], D.R. Quarrie[15],
W.B. Quayle[165a,165b], M. Queitsch-Maitland[83], D. Quilty[53], A. Qureshi[160b], V. Radeka[25],
V. Radescu[42], S.K. Radhakrishnan[149], P. Radloff[115], P. Rados[87], F. Ragusa[90a,90b], G. Rahal[179],
S. Rajagopalan[25], M. Rammensee[30], A.S. Randle-Conde[40], C. Rangel-Smith[167], K. Rao[164],
F. Rauscher[99], T.C. Rave[48], T. Ravenscroft[53], M. Raymond[30], A.L. Read[118], N.P. Readioff[73],
D.M. Rebuzzi[120a,120b], A. Redelbach[175], G. Redlinger[25], R. Reece[138], K. Reeves[41], L. Rehnisch[16],
H. Reisin[27], M. Relich[164], C. Rembser[30], H. Ren[33a], Z.L. Ren[152], A. Renaud[116], M. Rescigno[133a],
S. Resconi[90a], O.L. Rezanova[108,t], P. Reznicek[128], R. Rezvani[94], R. Richter[100], M. Ridel[79],
P. Rieck[16], J. Rieger[54], M. Rijssenbeek[149], A. Rimoldi[120a,120b], L. Rinaldi[20a], E. Ritsch[61], I. Riu[12],
F. Rizatdinova[113], E. Rizvi[75], S.H. Robertson[86,i], A. Robichaud-Veronneau[86], D. Robinson[28],
J.E.M. Robinson[83], A. Robson[53], C. Roda[123a,123b], L. Rodrigues[30], S. Roe[30], O. Røhne[118],
S. Rolli[162], A. Romaniouk[97], M. Romano[20a,20b], E. Romero Adam[168], N. Rompotis[139],
M. Ronzani[48], L. Roos[79], E. Ros[168], S. Rosati[133a], K. Rosbach[49], M. Rose[76], P. Rose[138],
P.L. Rosendahl[14], O. Rosenthal[142], V. Rossetti[147a,147b], E. Rossi[103a,103b], L.P. Rossi[50a],
R. Rosten[139], M. Rotaru[26a], I. Roth[173], J. Rothberg[139], D. Rousseau[116], C.R. Royon[137],
A. Rozanov[84], Y. Rozen[153], X. Ruan[146c], F. Rubbo[12], I. Rubinskiy[42], V.I. Rud[98], C. Rudolph[44],
M.S. Rudolph[159], F. Rühr[48], A. Ruiz-Martinez[30], Z. Rurikova[48], N.A. Rusakovich[64],
A. Ruschke[99], J.P. Rutherfoord[7], N. Ruthmann[48], Y.F. Ryabov[122], M. Rybar[128], G. Rybkin[116],
N.C. Ryder[119], A.F. Saavedra[151], S. Sacerdoti[27], A. Saddique[3], I. Sadeh[154],
H.F-W. Sadrozinski[138], R. Sadykov[64], F. Safai Tehrani[133a], H. Sakamoto[156], Y. Sakurai[172],
G. Salamanna[135a,135b], A. Salamon[134a], M. Saleem[112], D. Salek[106], P.H. Sales De Bruin[139],
D. Salihagic[100], A. Salnikov[144], J. Salt[168], D. Salvatore[37a,37b], F. Salvatore[150], A. Salvucci[105],
A. Salzburger[30], D. Sampsonidis[155], A. Sanchez[103a,103b], J. Sánchez[168], V. Sanchez Martinez[168],
H. Sandaker[14], R.L. Sandbach[75], H.G. Sander[82], M.P. Sanders[99], M. Sandhoff[176], T. Sandoval[28],
C. Sandoval[163], R. Sandstroem[100], D.P.C. Sankey[130], A. Sansoni[47], C. Santoni[34],
R. Santonico[134a,134b], H. Santos[125a], I. Santoyo Castillo[150], K. Sapp[124], A. Sapronov[64],
J.G. Saraiva[125a,125d], B. Sarrazin[21], G. Sartisohn[176], O. Sasaki[65], Y. Sasaki[156], G. Sauvage[5,*],

E. Sauvan[5], P. Savard[159,d], D.O. Savu[30], C. Sawyer[119], L. Sawyer[78,m], D.H. Saxon[53], J. Saxon[121],
C. Sbarra[20a], A. Sbrizzi[3], T. Scanlon[77], D.A. Scannicchio[164], M. Scarcella[151], V. Scarfone[37a,37b],
J. Schaarschmidt[173], P. Schacht[100], D. Schaefer[30], R. Schaefer[42], S. Schaepe[21], S. Schaetzel[58b],
U. Schäfer[82], A.C. Schaffer[116], D. Schaile[99], R.D. Schamberger[149], V. Scharf[58a],
V.A. Schegelsky[122], D. Scheirich[128], M. Schernau[164], M.I. Scherzer[35], C. Schiavi[50a,50b],
J. Schieck[99], C. Schillo[48], M. Schioppa[37a,37b], S. Schlenker[30], E. Schmidt[48], K. Schmieden[30],
C. Schmitt[82], S. Schmitt[58b], B. Schneider[17], Y.J. Schnellbach[73], U. Schnoor[44], L. Schoeffel[137],
A. Schoening[58b], B.D. Schoenrock[89], A.L.S. Schorlemmer[54], M. Schott[82], D. Schouten[160a],
J. Schovancova[25], S. Schramm[159], M. Schreyer[175], C. Schroeder[82], N. Schuh[82], M.J. Schultens[21],
H.-C. Schultz-Coulon[58a], H. Schulz[16], M. Schumacher[48], B.A. Schumm[138], Ph. Schune[137],
C. Schwanenberger[83], A. Schwartzman[144], Ph. Schwegler[100], Ph. Schwemling[137],
R. Schwienhorst[89], J. Schwindling[137], T. Schwindt[21], M. Schwoerer[5], F.G. Sciacca[17], E. Scifo[116],
G. Sciolla[23], W.G. Scott[130], F. Scuri[123a,123b], F. Scutti[21], J. Searcy[88], G. Sedov[42], E. Sedykh[122],
S.C. Seidel[104], A. Seiden[138], F. Seifert[127], J.M. Seixas[24a], G. Sekhniaidze[103a], S.J. Sekula[40],
K.E. Selbach[46], D.M. Seliverstov[122,*], G. Sellers[73], N. Semprini-Cesari[20a,20b], C. Serfon[30],
L. Serin[116], L. Serkin[54], T. Serre[84], R. Seuster[160a], H. Severini[112], T. Sfiligoj[74], F. Sforza[100],
A. Sfyrla[30], E. Shabalina[54], M. Shamim[115], L.Y. Shan[33a], R. Shang[166], J.T. Shank[22],
M. Shapiro[15], P.B. Shatalov[96], K. Shaw[165a,165b], C.Y. Shehu[150], P. Sherwood[77], L. Shi[152,ae],
S. Shimizu[66], C.O. Shimmin[164], M. Shimojima[101], M. Shiyakova[64], A. Shmeleva[95],
M.J. Shochet[31], D. Short[119], S. Shrestha[63], E. Shulga[97], M.A. Shupe[7], S. Shushkevich[42],
P. Sicho[126], O. Sidiropoulou[155], D. Sidorov[113], A. Sidoti[133a], F. Siegert[44], Dj. Sijacki[13a],
J. Silva[125a,125d], Y. Silver[154], D. Silverstein[144], S.B. Silverstein[147a], V. Simak[127], O. Simard[5],
Lj. Simic[13a], S. Simion[116], E. Simioni[82], B. Simmons[77], R. Simoniello[90a,90b], M. Simonyan[36],
P. Sinervo[159], N.B. Sinev[115], V. Sipica[142], G. Siragusa[175], A. Sircar[78], A.N. Sisakyan[64,*],
S.Yu. Sivoklokov[98], J. Sjölin[147a,147b], T.B. Sjursen[14], H.P. Skottowe[57], K.Yu. Skovpen[108],
P. Skubic[112], M. Slater[18], T. Slavicek[127], K. Sliwa[162], V. Smakhtin[173], B.H. Smart[46],
L. Smestad[14], S.Yu. Smirnov[97], Y. Smirnov[97], L.N. Smirnova[98,af], O. Smirnova[80], K.M. Smith[53],
M. Smizanska[71], K. Smolek[127], A.A. Snesarev[95], G. Snidero[75], S. Snyder[25], R. Sobie[170,i],
F. Socher[44], A. Soffer[154], D.A. Soh[152,ae], C.A. Solans[30], M. Solar[127], J. Solc[127], E.Yu. Soldatov[97],
U. Soldevila[168], A.A. Solodkov[129], A. Soloshenko[64], O.V. Solovyanov[129], V. Solovyev[122],
P. Sommer[48], H.Y. Song[33b], N. Soni[1], A. Sood[15], A. Sopczak[127], B. Sopko[127], V. Sopko[127],
V. Sorin[12], M. Sosebee[8], R. Soualah[165a,165c], P. Soueid[94], A.M. Soukharev[108], D. South[42],
S. Spagnolo[72a,72b], F. Spanò[76], W.R. Spearman[57], F. Spettel[100], R. Spighi[20a], G. Spigo[30],
L.A. Spiller[87], M. Spousta[128], T. Spreitzer[159], B. Spurlock[8], R.D. St. Denis[53,*], S. Staerz[44],
J. Stahlman[121], R. Stamen[58a], S. Stamm[16], E. Stanecka[39], R.W. Stanek[6], C. Stanescu[135a],
M. Stanescu-Bellu[42], M.M. Stanitzki[42], S. Stapnes[118], E.A. Starchenko[129], J. Stark[55],
P. Staroba[126], P. Starovoitov[42], R. Staszewski[39], P. Stavina[145a,*], P. Steinberg[25], B. Stelzer[143],
H.J. Stelzer[30], O. Stelzer-Chilton[160a], H. Stenzel[52], S. Stern[100], G.A. Stewart[53], J.A. Stillings[21],
M.C. Stockton[86], M. Stoebe[86], G. Stoicea[26a], P. Stolte[54], S. Stonjek[100], A.R. Stradling[8],
A. Straessner[44], M.E. Stramaglia[17], J. Strandberg[148], S. Strandberg[147a,147b], A. Strandlie[118],
E. Strauss[144], M. Strauss[112], P. Strizenec[145b], R. Ströhmer[175], D.M. Strom[115], R. Stroynowski[40],
A. Struebig[105], S.A. Stucci[17], B. Stugu[14], N.A. Styles[42], D. Su[144], J. Su[124], R. Subramaniam[78],
A. Succurro[12], Y. Sugaya[117], C. Suhr[107], M. Suk[127], V.V. Sulin[95], S. Sultansoy[4c], T. Sumida[67],
S. Sun[57], X. Sun[33a], J.E. Sundermann[48], K. Suruliz[140], G. Susinno[37a,37b], M.R. Sutton[150],
Y. Suzuki[65], M. Svatos[126], S. Swedish[169], M. Swiatlowski[144], I. Sykora[145a], T. Sykora[128], D. Ta[89],
C. Taccini[135a,135b], K. Tackmann[42], J. Taenzer[159], A. Taffard[164], R. Tafirout[160a], N. Taiblum[154],
H. Takai[25], R. Takashima[68], H. Takeda[66], T. Takeshita[141], Y. Takubo[65], M. Talby[84],
A.A. Talyshev[108,t], J.Y.C. Tam[175], K.G. Tan[87], J. Tanaka[156], R. Tanaka[116], S. Tanaka[132],

S. Tanaka[65], A.J. Tanasijczuk[143], B.B. Tannenwald[110], N. Tannoury[21], S. Tapprogge[82],
S. Tarem[153], F. Tarrade[29], G.F. Tartarelli[90a], P. Tas[128], M. Tasevsky[126], T. Tashiro[67],
E. Tassi[37a,37b], A. Tavares Delgado[125a,125b], Y. Tayalati[136d], F.E. Taylor[93], G.N. Taylor[87],
W. Taylor[160b], F.A. Teischinger[30], M. Teixeira Dias Castanheira[75], P. Teixeira-Dias[76],
K.K. Temming[48], H. Ten Kate[30], P.K. Teng[152], J.J. Teoh[117], S. Terada[65], K. Terashi[156],
J. Terron[81], S. Terzo[100], M. Testa[47], R.J. Teuscher[159,i], J. Therhaag[21], T. Theveneaux-Pelzer[34],
J.P. Thomas[18], J. Thomas-Wilsker[76], E.N. Thompson[35], P.D. Thompson[18], P.D. Thompson[159],
R.J. Thompson[83], A.S. Thompson[53], L.A. Thomsen[36], E. Thomson[121], M. Thomson[28],
W.M. Thong[87], R.P. Thun[88,*], F. Tian[35], M.J. Tibbetts[15], V.O. Tikhomirov[95,ag],
Yu.A. Tikhonov[108,t], S. Timoshenko[97], E. Tiouchichine[84], P. Tipton[177], S. Tisserant[84],
T. Todorov[5], S. Todorova-Nova[128], B. Toggerson[7], J. Tojo[69], S. Tokár[145a], K. Tokushuku[65],
K. Tollefson[89], L. Tomlinson[83], M. Tomoto[102], L. Tompkins[31], K. Toms[104], N.D. Topilin[64],
E. Torrence[115], H. Torres[143], E. Torró Pastor[168], J. Toth[84,ah], F. Touchard[84], D.R. Tovey[140],
H.L. Tran[116], T. Trefzger[175], L. Tremblet[30], A. Tricoli[30], I.M. Trigger[160a], S. Trincaz-Duvoid[79],
M.F. Tripiana[12], W. Trischuk[159], B. Trocmé[55], C. Troncon[90a], M. Trottier-McDonald[143],
M. Trovatelli[135a,135b], P. True[89], M. Trzebinski[39], A. Trzupek[39], C. Tsarouchas[30],
J.C-L. Tseng[119], P.V. Tsiareshka[91], D. Tsionou[137], G. Tsipolitis[10], N. Tsirintanis[9],
S. Tsiskaridze[12], V. Tsiskaridze[48], E.G. Tskhadadze[51a], I.I. Tsukerman[96], V. Tsulaia[15],
S. Tsuno[65], D. Tsybychev[149], A. Tudorache[26a], V. Tudorache[26a], A.N. Tuna[121],
S.A. Tupputi[20a,20b], S. Turchikhin[98,af], D. Turecek[127], I. Turk Cakir[4d], R. Turra[90a,90b],
P.M. Tuts[35], A. Tykhonov[49], M. Tylmad[147a,147b], M. Tyndel[130], K. Uchida[21], I. Ueda[156],
R. Ueno[29], M. Ughetto[84], M. Ugland[14], M. Uhlenbrock[21], F. Ukegawa[161], G. Unal[30], A. Undrus[25],
G. Unel[164], F.C. Ungaro[48], Y. Unno[65], C. Unverdorben[99], D. Urbaniec[35], P. Urquijo[87], G. Usai[8],
A. Usanova[61], L. Vacavant[84], V. Vacek[127], B. Vachon[86], N. Valencic[106], S. Valentinetti[20a,20b],
A. Valero[168], L. Valery[34], S. Valkar[128], E. Valladolid Gallego[168], S. Vallecorsa[49],
J.A. Valls Ferrer[168], W. Van Den Wollenberg[106], P.C. Van Der Deijl[106], R. van der Geer[106],
H. van der Graaf[106], R. Van Der Leeuw[106], D. van der Ster[30], N. van Eldik[30], P. van Gemmeren[6],
J. Van Nieuwkoop[143], I. van Vulpen[106], M.C. van Woerden[30], M. Vanadia[133a,133b], W. Vandelli[30],
R. Vanguri[121], A. Vaniachine[6], P. Vankov[42], F. Vannucci[79], G. Vardanyan[178], R. Vari[133a],
E.W. Varnes[7], T. Varol[85], D. Varouchas[79], A. Vartapetian[8], K.E. Varvell[151], F. Vazeille[34],
T. Vazquez Schroeder[54], J. Veatch[7], F. Veloso[125a,125c], S. Veneziano[133a], A. Ventura[72a,72b],
D. Ventura[85], M. Venturi[170], N. Venturi[159], A. Venturini[23], V. Vercesi[120a], M. Verducci[133a,133b],
W. Verkerke[106], J.C. Vermeulen[106], A. Vest[44], M.C. Vetterli[143,d], O. Viazlo[80], I. Vichou[166],
T. Vickey[146c,ai], O.E. Vickey Boeriu[146c], G.H.A. Viehhauser[119], S. Viel[169], R. Vigne[30],
M. Villa[20a,20b], M. Villaplana Perez[90a,90b], E. Vilucchi[47], M.G. Vincter[29], V.B. Vinogradov[64],
J. Virzi[15], I. Vivarelli[150], F. Vives Vaque[3], S. Vlachos[10], D. Vladoiu[99], M. Vlasak[127], A. Vogel[21],
M. Vogel[32a], P. Vokac[127], G. Volpi[123a,123b], M. Volpi[87], H. von der Schmitt[100],
H. von Radziewski[48], E. von Toerne[21], V. Vorobel[128], K. Vorobev[97], M. Vos[168], R. Voss[30],
J.H. Vossebeld[73], N. Vranjes[137], M. Vranjes Milosavljevic[13a], V. Vrba[126], M. Vreeswijk[106],
T. Vu Anh[48], R. Vuillermet[30], I. Vukotic[31], Z. Vykydal[127], P. Wagner[21], W. Wagner[176],
H. Wahlberg[70], S. Wahrmund[44], J. Wakabayashi[102], J. Walder[71], R. Walker[99], W. Walkowiak[142],
R. Wall[177], P. Waller[73], B. Walsh[177], C. Wang[152,aj], C. Wang[45], F. Wang[174], H. Wang[15],
H. Wang[40], J. Wang[42], J. Wang[33a], K. Wang[86], R. Wang[104], S.M. Wang[152], T. Wang[21],
X. Wang[177], C. Wanotayaroj[115], A. Warburton[86], C.P. Ward[28], D.R. Wardrope[77],
M. Warsinsky[48], A. Washbrook[46], C. Wasicki[42], P.M. Watkins[18], A.T. Watson[18], I.J. Watson[151],
M.F. Watson[18], G. Watts[139], S. Watts[83], B.M. Waugh[77], S. Webb[83], M.S. Weber[17],
S.W. Weber[175], J.S. Webster[31], A.R. Weidberg[119], P. Weigell[100], B. Weinert[60], J. Weingarten[54],
C. Weiser[48], H. Weits[106], P.S. Wells[30], T. Wenaus[25], D. Wendland[16], Z. Weng[152,ae], T. Wengler[30],

S. Wenig[30], N. Wermes[21], M. Werner[48], P. Werner[30], M. Wessels[58a], J. Wetter[162], K. Whalen[29], A. White[8], M.J. White[1], R. White[32b], S. White[123a,123b], D. Whiteson[164], D. Wicke[176], F.J. Wickens[130], W. Wiedenmann[174], M. Wielers[130], P. Wienemann[21], C. Wiglesworth[36], L.A.M. Wiik-Fuchs[21], P.A. Wijeratne[77], A. Wildauer[100], M.A. Wildt[42,ak], H.G. Wilkens[30], J.Z. Will[99], H.H. Williams[121], S. Williams[28], C. Willis[89], S. Willocq[85], A. Wilson[88], J.A. Wilson[18], I. Wingerter-Seez[5], F. Winklmeier[115], B.T. Winter[21], M. Wittgen[144], T. Wittig[43], J. Wittkowski[99], S.J. Wollstadt[82], M.W. Wolter[39], H. Wolters[125a,125c], B.K. Wosiek[39], J. Wotschack[30], M.J. Woudstra[83], K.W. Wozniak[39], M. Wright[53], M. Wu[55], S.L. Wu[174], X. Wu[49], Y. Wu[88], E. Wulf[35], T.R. Wyatt[83], B.M. Wynne[46], S. Xella[36], M. Xiao[137], D. Xu[33a], L. Xu[33b,al], B. Yabsley[151], S. Yacoob[146b,am], R. Yakabe[66], M. Yamada[65], H. Yamaguchi[156], Y. Yamaguchi[117], A. Yamamoto[65], K. Yamamoto[63], S. Yamamoto[156], T. Yamamura[156], T. Yamanaka[156], K. Yamauchi[102], Y. Yamazaki[66], Z. Yan[22], H. Yang[33e], H. Yang[174], U.K. Yang[83], Y. Yang[110], S. Yanush[92], L. Yao[33a], W-M. Yao[15], Y. Yasu[65], E. Yatsenko[42], K.H. Yau Wong[21], J. Ye[40], S. Ye[25], I. Yeletskikh[64], A.L. Yen[57], E. Yildirim[42], M. Yilmaz[4b], R. Yoosoofmiya[124], K. Yorita[172], R. Yoshida[6], K. Yoshihara[156], C. Young[144], C.J.S. Young[30], S. Youssef[22], D.R. Yu[15], J. Yu[8], J.M. Yu[88], J. Yu[113], L. Yuan[66], A. Yurkewicz[107], I. Yusuff[28,an], B. Zabinski[39], R. Zaidan[62], A.M. Zaitsev[129,aa], A. Zaman[149], S. Zambito[23], L. Zanello[133a,133b], D. Zanzi[100], C. Zeitnitz[176], M. Zeman[127], A. Zemla[38a], K. Zengel[23], O. Zenin[129], T. Ženiš[145a], D. Zerwas[116], G. Zevi della Porta[57], D. Zhang[88], F. Zhang[174], H. Zhang[89], J. Zhang[6], L. Zhang[152], X. Zhang[33d], Z. Zhang[116], Z. Zhao[33b], A. Zhemchugov[64], J. Zhong[119], B. Zhou[88], L. Zhou[35], N. Zhou[164], C.G. Zhu[33d], H. Zhu[33a], J. Zhu[88], Y. Zhu[33b], X. Zhuang[33a], K. Zhukov[95], A. Zibell[175], D. Zieminska[60], N.I. Zimine[64], C. Zimmermann[82], R. Zimmermann[21], S. Zimmermann[21], S. Zimmermann[48], Z. Zinonos[54], M. Ziolkowski[142], G. Zobernig[174], A. Zoccoli[20a,20b], M. zur Nedden[16], G. Zurzolo[103a,103b], V. Zutshi[107] and L. Zwalinski[30].

1   Department of Physics, University of Adelaide, Adelaide, Australia
2   Physics Department, SUNY Albany, Albany NY, United States of America
3   Department of Physics, University of Alberta, Edmonton AB, Canada
4   [(a)] Department of Physics, Ankara University, Ankara; [(b)] Department of Physics, Gazi University, Ankara; [(c)] Division of Physics, TOBB University of Economics and Technology, Ankara; [(d)] Turkish Atomic Energy Authority, Ankara, Turkey
5   LAPP, CNRS/IN2P3 and Université de Savoie, Annecy-le-Vieux, France
6   High Energy Physics Division, Argonne National Laboratory, Argonne IL, United States of America
7   Department of Physics, University of Arizona, Tucson AZ, United States of America
8   Department of Physics, The University of Texas at Arlington, Arlington TX, United States of America
9   Physics Department, University of Athens, Athens, Greece
10 Physics Department, National Technical University of Athens, Zografou, Greece
11 Institute of Physics, Azerbaijan Academy of Sciences, Baku, Azerbaijan
12 Institut de Física d'Altes Energies and Departament de Física de la Universitat Autònoma de Barcelona, Barcelona, Spain
13 [(a)] Institute of Physics, University of Belgrade, Belgrade; [(b)] Vinca Institute of Nuclear Sciences, University of Belgrade, Belgrade, Serbia
14 Department for Physics and Technology, University of Bergen, Bergen, Norway
15 Physics Division, Lawrence Berkeley National Laboratory and University of California, Berkeley CA, United States of America
16 Department of Physics, Humboldt University, Berlin, Germany
17 Albert Einstein Center for Fundamental Physics and Laboratory for High Energy Physics, University of Bern, Bern, Switzerland
18 School of Physics and Astronomy, University of Birmingham, Birmingham, United Kingdom

19 [a] *Department of Physics, Bogazici University, Istanbul;* [b] *Department of Physics, Dogus University, Istanbul;* [c] *Department of Physics Engineering, Gaziantep University, Gaziantep, Turkey*

20 [a] *INFN Sezione di Bologna;* [b] *Dipartimento di Fisica e Astronomia, Università di Bologna, Bologna, Italy*

21 *Physikalisches Institut, University of Bonn, Bonn, Germany*

22 *Department of Physics, Boston University, Boston MA, United States of America*

23 *Department of Physics, Brandeis University, Waltham MA, United States of America*

24 [a] *Universidade Federal do Rio De Janeiro COPPE/EE/IF, Rio de Janeiro;* [b] *Federal University of Juiz de Fora (UFJF), Juiz de Fora;* [c] *Federal University of Sao Joao del Rei (UFSJ), Sao Joao del Rei;* [d] *Instituto de Fisica, Universidade de Sao Paulo, Sao Paulo, Brazil*

25 *Physics Department, Brookhaven National Laboratory, Upton NY, United States of America*

26 [a] *National Institute of Physics and Nuclear Engineering, Bucharest;* [b] *National Institute for Research and Development of Isotopic and Molecular Technologies, Physics Department, Cluj Napoca;* [c] *University Politehnica Bucharest, Bucharest;* [d] *West University in Timisoara, Timisoara, Romania*

27 *Departamento de Física, Universidad de Buenos Aires, Buenos Aires, Argentina*

28 *Cavendish Laboratory, University of Cambridge, Cambridge, United Kingdom*

29 *Department of Physics, Carleton University, Ottawa ON, Canada*

30 *CERN, Geneva, Switzerland*

31 *Enrico Fermi Institute, University of Chicago, Chicago IL, United States of America*

32 [a] *Departamento de Física, Pontificia Universidad Católica de Chile, Santiago;* [b] *Departamento de Física, Universidad Técnica Federico Santa María, Valparaíso, Chile*

33 [a] *Institute of High Energy Physics, Chinese Academy of Sciences, Beijing;* [b] *Department of Modern Physics, University of Science and Technology of China, Anhui;* [c] *Department of Physics, Nanjing University, Jiangsu;* [d] *School of Physics, Shandong University, Shandong;* [e] *Physics Department, Shanghai Jiao Tong University, Shanghai, China*

34 *Laboratoire de Physique Corpusculaire, Clermont Université and Université Blaise Pascal and CNRS/IN2P3, Clermont-Ferrand, France*

35 *Nevis Laboratory, Columbia University, Irvington NY, United States of America*

36 *Niels Bohr Institute, University of Copenhagen, Kobenhavn, Denmark*

37 [a] *INFN Gruppo Collegato di Cosenza, Laboratori Nazionali di Frascati;* [b] *Dipartimento di Fisica, Università della Calabria, Rende, Italy*

38 [a] *AGH University of Science and Technology, Faculty of Physics and Applied Computer Science, Krakow;* [b] *Marian Smoluchowski Institute of Physics, Jagiellonian University, Krakow, Poland*

39 *The Henryk Niewodniczanski Institute of Nuclear Physics, Polish Academy of Sciences, Krakow, Poland*

40 *Physics Department, Southern Methodist University, Dallas TX, United States of America*

41 *Physics Department, University of Texas at Dallas, Richardson TX, United States of America*

42 *DESY, Hamburg and Zeuthen, Germany*

43 *Institut für Experimentelle Physik IV, Technische Universität Dortmund, Dortmund, Germany*

44 *Institut für Kern- und Teilchenphysik, Technische Universität Dresden, Dresden, Germany*

45 *Department of Physics, Duke University, Durham NC, United States of America*

46 *SUPA - School of Physics and Astronomy, University of Edinburgh, Edinburgh, United Kingdom*

47 *INFN Laboratori Nazionali di Frascati, Frascati, Italy*

48 *Fakultät für Mathematik und Physik, Albert-Ludwigs-Universität, Freiburg, Germany*

49 *Section de Physique, Université de Genève, Geneva, Switzerland*

50 [a] *INFN Sezione di Genova;* [b] *Dipartimento di Fisica, Università di Genova, Genova, Italy*

51 [a] *E. Andronikashvili Institute of Physics, Iv. Javakhishvili Tbilisi State University, Tbilisi;* [b] *High Energy Physics Institute, Tbilisi State University, Tbilisi, Georgia*

52 *II Physikalisches Institut, Justus-Liebig-Universität Giessen, Giessen, Germany*

53 *SUPA - School of Physics and Astronomy, University of Glasgow, Glasgow, United Kingdom*

[54] *II Physikalisches Institut, Georg-August-Universität, Göttingen, Germany*

[55] *Laboratoire de Physique Subatomique et de Cosmologie, Université Grenoble-Alpes, CNRS/IN2P3, Grenoble, France*

[56] *Department of Physics, Hampton University, Hampton VA, United States of America*

[57] *Laboratory for Particle Physics and Cosmology, Harvard University, Cambridge MA, United States of America*

[58] [a] *Kirchhoff-Institut für Physik, Ruprecht-Karls-Universität Heidelberg, Heidelberg;* [b] *Physikalisches Institut, Ruprecht-Karls-Universität Heidelberg, Heidelberg;* [c] *ZITI Institut für technische Informatik, Ruprecht-Karls-Universität Heidelberg, Mannheim, Germany*

[59] *Faculty of Applied Information Science, Hiroshima Institute of Technology, Hiroshima, Japan*

[60] *Department of Physics, Indiana University, Bloomington IN, United States of America*

[61] *Institut für Astro- und Teilchenphysik, Leopold-Franzens-Universität, Innsbruck, Austria*

[62] *University of Iowa, Iowa City IA, United States of America*

[63] *Department of Physics and Astronomy, Iowa State University, Ames IA, United States of America*

[64] *Joint Institute for Nuclear Research, JINR Dubna, Dubna, Russia*

[65] *KEK, High Energy Accelerator Research Organization, Tsukuba, Japan*

[66] *Graduate School of Science, Kobe University, Kobe, Japan*

[67] *Faculty of Science, Kyoto University, Kyoto, Japan*

[68] *Kyoto University of Education, Kyoto, Japan*

[69] *Department of Physics, Kyushu University, Fukuoka, Japan*

[70] *Instituto de Física La Plata, Universidad Nacional de La Plata and CONICET, La Plata, Argentina*

[71] *Physics Department, Lancaster University, Lancaster, United Kingdom*

[72] [a] *INFN Sezione di Lecce;* [b] *Dipartimento di Matematica e Fisica, Università del Salento, Lecce, Italy*

[73] *Oliver Lodge Laboratory, University of Liverpool, Liverpool, United Kingdom*

[74] *Department of Physics, Jožef Stefan Institute and University of Ljubljana, Ljubljana, Slovenia*

[75] *School of Physics and Astronomy, Queen Mary University of London, London, United Kingdom*

[76] *Department of Physics, Royal Holloway University of London, Surrey, United Kingdom*

[77] *Department of Physics and Astronomy, University College London, London, United Kingdom*

[78] *Louisiana Tech University, Ruston LA, United States of America*

[79] *Laboratoire de Physique Nucléaire et de Hautes Energies, UPMC and Université Paris-Diderot and CNRS/IN2P3, Paris, France*

[80] *Fysiska institutionen, Lunds universitet, Lund, Sweden*

[81] *Departamento de Fisica Teorica C-15, Universidad Autonoma de Madrid, Madrid, Spain*

[82] *Institut für Physik, Universität Mainz, Mainz, Germany*

[83] *School of Physics and Astronomy, University of Manchester, Manchester, United Kingdom*

[84] *CPPM, Aix-Marseille Université and CNRS/IN2P3, Marseille, France*

[85] *Department of Physics, University of Massachusetts, Amherst MA, United States of America*

[86] *Department of Physics, McGill University, Montreal QC, Canada*

[87] *School of Physics, University of Melbourne, Victoria, Australia*

[88] *Department of Physics, The University of Michigan, Ann Arbor MI, United States of America*

[89] *Department of Physics and Astronomy, Michigan State University, East Lansing MI, United States of America*

[90] [a] *INFN Sezione di Milano;* [b] *Dipartimento di Fisica, Università di Milano, Milano, Italy*

[91] *B.I. Stepanov Institute of Physics, National Academy of Sciences of Belarus, Minsk, Republic of Belarus*

[92] *National Scientific and Educational Centre for Particle and High Energy Physics, Minsk, Republic of Belarus*

[93] *Department of Physics, Massachusetts Institute of Technology, Cambridge MA, United States of America*

[94] *Group of Particle Physics, University of Montreal, Montreal QC, Canada*

[95] *P.N. Lebedev Institute of Physics, Academy of Sciences, Moscow, Russia*

96   *Institute for Theoretical and Experimental Physics (ITEP), Moscow, Russia*
97   *Moscow Engineering and Physics Institute (MEPhI), Moscow, Russia*
98   *D.V.Skobeltsyn Institute of Nuclear Physics, M.V.Lomonosov Moscow State University, Moscow, Russia*
99   *Fakultät für Physik, Ludwig-Maximilians-Universität München, München, Germany*
100 *Max-Planck-Institut für Physik (Werner-Heisenberg-Institut), München, Germany*
101 *Nagasaki Institute of Applied Science, Nagasaki, Japan*
102 *Graduate School of Science and Kobayashi-Maskawa Institute, Nagoya University, Nagoya, Japan*
103 [(a)] *INFN Sezione di Napoli;* [(b)] *Dipartimento di Fisica, Università di Napoli, Napoli, Italy*
104 *Department of Physics and Astronomy, University of New Mexico, Albuquerque NM, United States of America*
105 *Institute for Mathematics, Astrophysics and Particle Physics, Radboud University Nijmegen/Nikhef, Nijmegen, Netherlands*
106 *Nikhef National Institute for Subatomic Physics and University of Amsterdam, Amsterdam, Netherlands*
107 *Department of Physics, Northern Illinois University, DeKalb IL, United States of America*
108 *Budker Institute of Nuclear Physics, SB RAS, Novosibirsk, Russia*
109 *Department of Physics, New York University, New York NY, United States of America*
110 *Ohio State University, Columbus OH, United States of America*
111 *Faculty of Science, Okayama University, Okayama, Japan*
112 *Homer L. Dodge Department of Physics and Astronomy, University of Oklahoma, Norman OK, United States of America*
113 *Department of Physics, Oklahoma State University, Stillwater OK, United States of America*
114 *Palacký University, RCPTM, Olomouc, Czech Republic*
115 *Center for High Energy Physics, University of Oregon, Eugene OR, United States of America*
116 *LAL, Université Paris-Sud and CNRS/IN2P3, Orsay, France*
117 *Graduate School of Science, Osaka University, Osaka, Japan*
118 *Department of Physics, University of Oslo, Oslo, Norway*
119 *Department of Physics, Oxford University, Oxford, United Kingdom*
120 [(a)] *INFN Sezione di Pavia;* [(b)] *Dipartimento di Fisica, Università di Pavia, Pavia, Italy*
121 *Department of Physics, University of Pennsylvania, Philadelphia PA, United States of America*
122 *Petersburg Nuclear Physics Institute, Gatchina, Russia*
123 [(a)] *INFN Sezione di Pisa;* [(b)] *Dipartimento di Fisica E. Fermi, Università di Pisa, Pisa, Italy*
124 *Department of Physics and Astronomy, University of Pittsburgh, Pittsburgh PA, United States of America*
125 [(a)] *Laboratorio de Instrumentacao e Fisica Experimental de Particulas - LIP, Lisboa;* [(b)] *Faculdade de Ciências, Universidade de Lisboa, Lisboa;* [(c)] *Department of Physics, University of Coimbra, Coimbra;* [(d)] *Centro de Física Nuclear da Universidade de Lisboa, Lisboa;* [(e)] *Departamento de Fisica, Universidade do Minho, Braga;* [(f)] *Departamento de Fisica Teorica y del Cosmos and CAFPE, Universidad de Granada, Granada (Spain);* [(g)] *Dep Fisica and CEFITEC of Faculdade de Ciencias e Tecnologia, Universidade Nova de Lisboa, Caparica, Portugal*
126 *Institute of Physics, Academy of Sciences of the Czech Republic, Praha, Czech Republic*
127 *Czech Technical University in Prague, Praha, Czech Republic*
128 *Faculty of Mathematics and Physics, Charles University in Prague, Praha, Czech Republic*
129 *State Research Center Institute for High Energy Physics, Protvino, Russia*
130 *Particle Physics Department, Rutherford Appleton Laboratory, Didcot, United Kingdom*
131 *Physics Department, University of Regina, Regina SK, Canada*
132 *Ritsumeikan University, Kusatsu, Shiga, Japan*
133 [(a)] *INFN Sezione di Roma;* [(b)] *Dipartimento di Fisica, Sapienza Università di Roma, Roma, Italy*
134 [(a)] *INFN Sezione di Roma Tor Vergata;* [(b)] *Dipartimento di Fisica, Università di Roma Tor Vergata, Roma, Italy*
135 [(a)] *INFN Sezione di Roma Tre;* [(b)] *Dipartimento di Matematica e Fisica, Università Roma Tre,*

Roma, Italy

136 [(a)] *Faculté des Sciences Ain Chock, Réseau Universitaire de Physique des Hautes Energies - Université Hassan II, Casablanca;* [(b)] *Centre National de l'Energie des Sciences Techniques Nucleaires, Rabat;* [(c)] *Faculté des Sciences Semlalia, Université Cadi Ayyad, LPHEA-Marrakech;* [(d)] *Faculté des Sciences, Université Mohamed Premier and LPTPM, Oujda;* [(e)] *Faculté des sciences, Université Mohammed V-Agdal, Rabat, Morocco*

137 *DSM/IRFU (Institut de Recherches sur les Lois Fondamentales de l'Univers), CEA Saclay (Commissariat à l'Energie Atomique et aux Energies Alternatives), Gif-sur-Yvette, France*

138 *Santa Cruz Institute for Particle Physics, University of California Santa Cruz, Santa Cruz CA, United States of America*

139 *Department of Physics, University of Washington, Seattle WA, United States of America*

140 *Department of Physics and Astronomy, University of Sheffield, Sheffield, United Kingdom*

141 *Department of Physics, Shinshu University, Nagano, Japan*

142 *Fachbereich Physik, Universität Siegen, Siegen, Germany*

143 *Department of Physics, Simon Fraser University, Burnaby BC, Canada*

144 *SLAC National Accelerator Laboratory, Stanford CA, United States of America*

145 [(a)] *Faculty of Mathematics, Physics & Informatics, Comenius University, Bratislava;* [(b)] *Department of Subnuclear Physics, Institute of Experimental Physics of the Slovak Academy of Sciences, Kosice, Slovak Republic*

146 [(a)] *Department of Physics, University of Cape Town, Cape Town;* [(b)] *Department of Physics, University of Johannesburg, Johannesburg;* [(c)] *School of Physics, University of the Witwatersrand, Johannesburg, South Africa*

147 [(a)] *Department of Physics, Stockholm University;* [(b)] *The Oskar Klein Centre, Stockholm, Sweden*

148 *Physics Department, Royal Institute of Technology, Stockholm, Sweden*

149 *Departments of Physics & Astronomy and Chemistry, Stony Brook University, Stony Brook NY, United States of America*

150 *Department of Physics and Astronomy, University of Sussex, Brighton, United Kingdom*

151 *School of Physics, University of Sydney, Sydney, Australia*

152 *Institute of Physics, Academia Sinica, Taipei, Taiwan*

153 *Department of Physics, Technion: Israel Institute of Technology, Haifa, Israel*

154 *Raymond and Beverly Sackler School of Physics and Astronomy, Tel Aviv University, Tel Aviv, Israel*

155 *Department of Physics, Aristotle University of Thessaloniki, Thessaloniki, Greece*

156 *International Center for Elementary Particle Physics and Department of Physics, The University of Tokyo, Tokyo, Japan*

157 *Graduate School of Science and Technology, Tokyo Metropolitan University, Tokyo, Japan*

158 *Department of Physics, Tokyo Institute of Technology, Tokyo, Japan*

159 *Department of Physics, University of Toronto, Toronto ON, Canada*

160 [(a)] *TRIUMF, Vancouver BC;* [(b)] *Department of Physics and Astronomy, York University, Toronto ON, Canada*

161 *Faculty of Pure and Applied Sciences, University of Tsukuba, Tsukuba, Japan*

162 *Department of Physics and Astronomy, Tufts University, Medford MA, United States of America*

163 *Centro de Investigaciones, Universidad Antonio Narino, Bogota, Colombia*

164 *Department of Physics and Astronomy, University of California Irvine, Irvine CA, United States of America*

165 [(a)] *INFN Gruppo Collegato di Udine, Sezione di Trieste, Udine;* [(b)] *ICTP, Trieste;* [(c)] *Dipartimento di Chimica, Fisica e Ambiente, Università di Udine, Udine, Italy*

166 *Department of Physics, University of Illinois, Urbana IL, United States of America*

167 *Department of Physics and Astronomy, University of Uppsala, Uppsala, Sweden*

168 *Instituto de Física Corpuscular (IFIC) and Departamento de Física Atómica, Molecular y Nuclear and Departamento de Ingeniería Electrónica and Instituto de Microelectrónica de Barcelona (IMB-CNM), University of Valencia and CSIC, Valencia, Spain*

[169] *Department of Physics, University of British Columbia, Vancouver BC, Canada*

[170] *Department of Physics and Astronomy, University of Victoria, Victoria BC, Canada*

[171] *Department of Physics, University of Warwick, Coventry, United Kingdom*

[172] *Waseda University, Tokyo, Japan*

[173] *Department of Particle Physics, The Weizmann Institute of Science, Rehovot, Israel*

[174] *Department of Physics, University of Wisconsin, Madison WI, United States of America*

[175] *Fakultät für Physik und Astronomie, Julius-Maximilians-Universität, Würzburg, Germany*

[176] *Fachbereich C Physik, Bergische Universität Wuppertal, Wuppertal, Germany*

[177] *Department of Physics, Yale University, New Haven CT, United States of America*

[178] *Yerevan Physics Institute, Yerevan, Armenia*

[179] *Centre de Calcul de l'Institut National de Physique Nucléaire et de Physique des Particules (IN2P3), Villeurbanne, France*

[a] *Also at Department of Physics, King's College London, London, United Kingdom*

[b] *Also at Institute of Physics, Azerbaijan Academy of Sciences, Baku, Azerbaijan*

[c] *Also at Particle Physics Department, Rutherford Appleton Laboratory, Didcot, United Kingdom*

[d] *Also at TRIUMF, Vancouver BC, Canada*

[e] *Also at Department of Physics, California State University, Fresno CA, United States of America*

[f] *Also at Tomsk State University, Tomsk, Russia*

[g] *Also at CPPM, Aix-Marseille Université and CNRS/IN2P3, Marseille, France*

[h] *Also at Università di Napoli Parthenope, Napoli, Italy*

[i] *Also at Institute of Particle Physics (IPP), Canada*

[j] *Also at Department of Physics, St. Petersburg State Polytechnical University, St. Petersburg, Russia*

[k] *Also at Chinese University of Hong Kong, China*

[l] *Also at Department of Financial and Management Engineering, University of the Aegean, Chios, Greece*

[m] *Also at Louisiana Tech University, Ruston LA, United States of America*

[n] *Also at Institucio Catalana de Recerca i Estudis Avancats, ICREA, Barcelona, Spain*

[o] *Also at Department of Physics, The University of Texas at Austin, Austin TX, United States of America*

[p] *Also at Institute of Theoretical Physics, Ilia State University, Tbilisi, Georgia*

[q] *Also at CERN, Geneva, Switzerland*

[r] *Also at Ochadai Academic Production, Ochanomizu University, Tokyo, Japan*

[s] *Also at Manhattan College, New York NY, United States of America*

[t] *Also at Novosibirsk State University, Novosibirsk, Russia*

[u] *Also at Institute of Physics, Academia Sinica, Taipei, Taiwan*

[v] *Also at LAL, Université Paris-Sud and CNRS/IN2P3, Orsay, France*

[w] *Also at Academia Sinica Grid Computing, Institute of Physics, Academia Sinica, Taipei, Taiwan*

[x] *Also at Laboratoire de Physique Nucléaire et de Hautes Energies, UPMC and Université Paris-Diderot and CNRS/IN2P3, Paris, France*

[y] *Also at School of Physical Sciences, National Institute of Science Education and Research, Bhubaneswar, India*

[z] *Also at Dipartimento di Fisica, Sapienza Università di Roma, Roma, Italy*

[aa] *Also at Moscow Institute of Physics and Technology State University, Dolgoprudny, Russia*

[ab] *Also at section de Physique, Université de Genève, Geneva, Switzerland*

[ac] *Also at International School for Advanced Studies (SISSA), Trieste, Italy*

[ad] *Also at Department of Physics and Astronomy, University of South Carolina, Columbia SC, United States of America*

[ae] *Also at School of Physics and Engineering, Sun Yat-sen University, Guangzhou, China*

[af] *Also at Faculty of Physics, M.V.Lomonosov Moscow State University, Moscow, Russia*

[ag] *Also at Moscow Engineering and Physics Institute (MEPhI), Moscow, Russia*

[ah] *Also at Institute for Particle and Nuclear Physics, Wigner Research Centre for Physics, Budapest,*

Hungary

^{ai} Also at Department of Physics, Oxford University, Oxford, United Kingdom

^{aj} Also at Department of Physics, Nanjing University, Jiangsu, China

^{ak} Also at Institut für Experimentalphysik, Universität Hamburg, Hamburg, Germany

^{al} Also at Department of Physics, The University of Michigan, Ann Arbor MI, United States of America

^{am} Also at Discipline of Physics, University of KwaZulu-Natal, Durban, South Africa

^{an} Also at University of Malaya, Department of Physics, Kuala Lumpur, Malaysia

[*] Deceased